

A STUDY OF FACTORS AFFECTING THE PRECISION
OF SPAWNING STOCK ESTIMATES USING MARMAP
FISH EGG AND LARVAL SURVEYS

by

Wallace W. Morse¹ and John W. Hauser²

¹Northeast Fisheries Center
Sandy Hook Laboratory
Highlands, New Jersey

²Northeast Fisheries Center
Woods Hole Laboratory
Woods Hole, Massachusetts

June 1985

SUMMARY

Models using assumed and real data are used to quantify and support the following:

1. Increasing the number of surveys within the spawning season of a target species will increase the precision of the estimate of total egg production and the resulting biomass estimate.
2. Decreasing the within survey variance will increase the precision of the estimate of total egg production.
3. Larval mortality estimates from MARMAP surveys will be relatively poor for species with short spawning seasons. The absolute uncertainty of larval mortality estimates does not vary appreciably for various mortality rates; however, this represents a larger fractional change for low mortality rates.
4. The conversion of larval lengths to ages using temperature- dependent growth equations should incorporate a water temperature function to account for the changes in water temperature throughout the life of the larvae.

INTRODUCTION

The implementation of systematic, large scale ichthyoplankton surveys for assessment of spawning stock biomass and recruitment was begun in earnest by the California Cooperative Oceanic Fisheries Investigation (CalCOFI) in 1950. Their successes in describing the rise and fall of fish populations of the California Current ecosystem has led the way to similar studies in the northwest Atlantic, Gulf of Mexico and areas off Alaska (see Sherman et al. 1983). These studies provide information about fish eggs and larvae distribution and abundance as well as invertebrate zooplankton, primary production and hydrographic data as an essential part of the Marine Resources Monitoring Assessment and Prediction (MARMAP) program. The National Marine Fisheries Service began routine MARMAP ichthyoplankton surveys of the northwest Atlantic in 1977 that cover the continental shelf from Cape Hatteras, North Carolina to Nova Scotia. This paper presents an evaluation of the MARMAP sampling methods and the use of the egg and larvae data for spawning stock estimates.

MARMAP ICTHYOPLANKTON SAMPLING

During the past eight years (1977-1984) six to seven surveys were completed annually in the northwest Atlantic. Each survey occupied about 180 stations spaced at between 25-35 km apart. At each station ichthyoplankton is collected using the MARMAP standard 61-cm bongo net array fitted with 0.505- and 0.333-mm mesh nets (Posgay and Marak 1981). All fish eggs and larvae from the 0.505-mm net are sorted, identified to the lowest taxon possible, and enumerated. The larvae are measured to the nearest 0.1mm and the eggs are staged. The abundance of eggs and larvae at a station are standardized to the number under 10m^2 of sea surface. For a detailed explanation of sampling

methods used on MARMAP surveys see Smith and Richardson (1977) and Sibunka and Silverman (1984).

SPAWNING STOCK BIOMASS ESTIMATIONS

Two methods have been applied using the MARMAP data to estimate spawning stock biomass. The first utilizes the staged egg data to determine total egg production for the spawning season. Briefly, the eggs are aged by using a temperature-dependant incubation rate formula and then for each station the number of each egg stage present per 10m^2 per day is determined. Next, for each survey, the mean catch per tow of each stage is calculated and expanded by the survey area to yield the abundance of each stage per day. These means are then multiplied by the number of days represented by each survey to give the abundance of eggs for that time interval of the spawning season. The abundances for each survey in the spawning season are added together to derive the total seasonal production of each egg stage. The next step is to estimate egg mortality and apply this mortality to the youngest egg stage abundance to estimate the total number of eggs spawned during the entire spawning season. This is accomplished by determining a weighted mean age for each stage and calculating the exponential rate of decrease in the season-long abundance from early to later stage eggs. The slope of the exponential regression is an estimate of mortality and is used to back-calculate the egg numbers spawned/ 10m^2 /day at each station. The mean number of eggs spawned/station is then expanded by the total survey area and the days represented by each survey. These expanded totals are added together to give the total eggs spawned for the entire spawning season. Spawning stock biomass is calculated by applying the appropriate length, weight, maturity, fecundity, and sex ratio

information to the total eggs spawned. Examples of the application of the above method for biomass estimation can be found in Pennington (1983), Berrien et al. (1981) and Berrien et al. (1984).

The second method of estimating spawning stock biomass from the MARMAP surveys uses the larval length data. The lengths and abundance of larvae at each station are corrected for net extrusion, net avoidance and shrinkage if appropriate. The length frequencies are converted to age frequencies by applying a temperature-dependent growth function using the temperature at capture as input to the function. The age frequencies from each survey during the spawning season are summed and the slope of the exponential regression line of age verses frequency is used as an estimate of average larval mortality. This mortality is then used to back-calculate from the age frequencies to the number of larvae at age 0 (ie. hatching). Larvae old enough to have been sampled on a previous survey were eliminated before the numbers at hatching were calculated. An estimate of egg mortality and egg incubation time are then used to back-calculate to the number of eggs spawned at each station. The mean catch per 10m^2 of estimated eggs spawned is expanded by the survey area to produce the total number of eggs spawned. Survey totals are summed to give the total eggs spawned for the entire spawning season. Again the appropriate length, weight, fecundity, and sex ratio information is used to determine spawning stock biomass. For detailed explanations of this method see Morse (1984), Zweifel and Smith (1981) and Hewitt and Methot (1982).

The two methods described above attempt to reconstruct the spawning curve and then integrate the area under the curve to estimate the total number of eggs spawned. The methods contain numerous sources of variability and are based on a number of critical assumptions that affect the precision and accuracy of the resulting biomass estimates. Among the most important and the

ones investigated here are:

- 1) Is the MARMAP survey frequency adequate to describe the spawning curve and thus yield "reasonable" results when method one is used?
- 2) What affect does the within survey variability of the mean catch per tow have upon the precision of the biomass estimate using method one?
- 3) Given the non-constant production of eggs and larvae and the MARMAP survey frequency, is it "reasonable" to combine larval age-frequencies to derive a seasonal average mortality rate as in method two?
- 4) How critical are the assumptions about larval growth and the application of the temperature-dependent growth functions?

Computer simulations were used to answer these questions. Questions 3 and 4 were investigated using both artificial data and larval haddock length data collected in 1980.

METHODS

Many temperate and boreal marine fishes have a well defined spawning season with peak spawning occurring once annually. The production of eggs and larvae over time for many species appears to be best characterized by a normal

curve. Though some variations obviously occur, the normal curve was chosen as the generalized model of the spawning curve for most species in the MARMAP sampling area. The duration of spawning from 2-10 months long was used to evaluate the effects of survey frequency and timing on estimated total egg and larval production. In forming the spawning curve a value of three standard deviations was used. For example, for a two months spawning curve there would be two months between -3 standard deviations and +3 standard deviations. The mean (ie.peak) production was held constant at 180 Julian days or at about June 29th. Survey timing and frequency for simulation purposes were determined from an evaluation of the 1977-1981 MARMAP surveys (Table 1). A total of six or seven surveys were completed each year with a minimum of 17 days and a maximum of 88 days between surveys.

Using the information in Table 1, points on the normal spawning curve were selected at random to represent survey dates. The area under straight lines connecting the sampling points was compared to the area under the normal curve (Figure 1). The normal spawning curves ranged from 2 to 10 months long by 1 month increments. This represents species with a short spawning season (2 mon.) to species with protracted spawning (10 mon.). For each of the 9 spawning curves 100 survey schedules were simulated and the area under the connected points for each was calculated. The difference between the area of the normal curve and the area under the connected points indicates the variability associated with the MARMAP survey frequency.

The points selected on the normal curve represent the mean number of eggs spawned/ $10m^2/day$ in the context of method 1 described above. To account for the variability about the mean number of eggs a random variance component was added to each sample point on the normal curve (Figure 2). A logarithmic standard error term was introduced and incremented from 1.25 to 2.0 by 0.25.

This represents a coefficient of variability of between 25% to 100%. Again 100 runs per spawning curve for 2 to 10 months long by 1 month increment were made and the calculated areas compared to the actual areas under the curves. With this simulation the variability associated with both the MARMAP survey timing and the mean catch-per-tow were evaluated.

The next step in the study was to investigate the effects of MARMAP survey schedules on estimates of larval mortality. Again a normal spawning curve was assumed. Duration of the spawning curve ranged from 2 to 10 months as before. Larvae were subjected to input mortality rates from 0.05 to 0.20 which translates to a death rate of 4.9 to 18.1% per day. Random samples were taken from the larval population according to the empirical MARMAP survey schedule (Table 1). Each survey sample is a calculated age frequency of the larval population. The survey samples were summed to yield an annual age frequency for which an exponential regression line was calculated. The slope of the regression line was compared to the input mortality. Differences in the values are attributed to the limited number of surveys per year and survey timing. A total of 100 annual survey schedules were processed per spawning curve.

The relationship of the duration of spawning and mortality to the expected age frequencies was examined graphically. Normal spawning curves with standard deviations of 10, 30 and 50 days were subjected to mortality rates of 0.05, 0.10 and 0.20. From each of the nine larval populations ten samples were taken and age frequencies constructed. These age frequencies should be equivalent to the observed MARMAP samples. The question then is, given the age frequencies from field caught samples, can the spawning curve which produced the samples be defined by manipulation of mortality rates? To try to answer this question we analyzed the larval haddock age frequencies from three

survey and the abundance of each age class within the survey. By changing the mortality rates and back-calculating to the number at age 0, various spawning curves were produced. Mortality rates were changed to reflect day-dependent, age-dependent or constant mortality. The spawning curves calculated by altering the mortality were examined for reasonableness. A reasonable curve would not show contradictions to known biological information. The various surveys would join together smoothly. While the spawning curve would not necessarily be of any particular form, a curve showing irregularities only at survey joining points would not be regarded as reasonable.

One of the critical factors in converting field caught larval length frequencies to age frequencies is the application of temperature-dependent growth functions. Morse (1984) used the surface water temperature at the time of capture as the input temperature to the growth functions. Since haddock larvae persist in the plankton for about two months and water temperatures are, in general, rising during the life of a larva (April, May and June) then the use of the temperature at the time of capture will convert a given length to the minimum age. The result of this is that mortality will be overestimated. To evaluate this bias a temperature algorithm was calculated which represents the average daily sea water temperature to 50m deep on Georges Bank. The algorithm was used to convert the larval lengths of the 1980 haddock catch to ages such that the temperature for each day of the larva's life was input into the growth functions. This then permitted a direct comparison of the two aging methods.

As mentioned above, the evaluation of field caught larval age frequencies in relation to the spawning that produced them will be affected by the adequacy of the input age frequencies. Therefore, the age frequencies using the temperature algorithm were back-calculated to the number at age 0 and the resulting spawning curves were again examined.

RESULTS AND DISCUSSION

SPAWNING CURVES

The ability to reconstruct adequate spawning curves from egg data, as outlined above, for spawning stock biomass estimation is obviously dependent upon the number of data points, i.e. surveys, available during the spawning season. If only one point is available then no curve can be reconstructed. As more data points become available along the curve then more precise approximations of the spawning curve can be made. Table 2 shows that as the length of spawning increases from 2 to 10 months, thereby increasing the number of surveys within the spawning season, the precision increases dramatically. The standard deviation of the mean ratio of the estimated to the input spawning curve decreases from 62% to 3% of the mean for spawning curves from 2 to 10 months. The mean number of days between surveys ranges from about 35-60 days (Table 1). On average then a spawning season of two months will at most have only two observations to reconstruct the spawning curve. The number of observations will increase to 4 to 6 for spawners with a 10 months season. Thus increasing the number of surveys within a spawning season will have very significant effects on the precision of the estimate of total egg production and the resulting biomass estimate.

When the within survey variance component is included in the analysis the precision of the estimate decreases as the variance increases (Tables 3-6). The highest variability occurs for 2 months spawning curves and decreases as the spawning time increases. There is also a trend towards overestimating the mean ratio of input to estimated spawning curves as the variance component increases.

The relationship of the duration of spawning, the within survey variance,

and the input to estimated ratios is shown in Figure 3. The coefficient of variation decreases rapidly from the 2 to the 4 months curves. It then trends lower but at a much slower rate. While the five curves in Figure 3 show the same general trends, it should be noted that changing the spawning period results in a much greater fractional change in the coefficient of variation for the lower (small within cruise variation) curves.

Two results are evident from this analysis of the duration of spawning and within survey variability. First, by decreasing the within survey variance there is a concomitant increase in the precision of the estimate of the spawning curve and the estimate of total egg production. Secondly, increasing the number of surveys within a spawning season will further increase the precision of the estimate of egg production.

LARVAL MORTALITY

The conversion of larval lengths to ages and the estimation of mortality from age frequencies are critical steps in estimating spawning biomass. Larval mortality, when used to back-calculate numbers at spawning, has an exponential relationship to the estimated biomass. Thus relatively small changes in larval mortality will have significant effects on the estimates. The first question we addressed is, given various normal spawning curves and larval mortality from 0.05 to 0.20, what are the expected age frequencies of samples taken at varying intervals throughout the spawning season? Samples taken during the ascending limb of the spawning curve are expected to overestimate mortality and underestimate on the descending limb. Figures 4-12 show that this is true regardless of the duration of spawning or mortality rate.

An examination of Figures 4-12 reveals two trends in the shape of the age frequencies. First, as the duration of spawning decreases, the logarithmic age

frequencies become more curvilinear until, at a spawning duration of two months, the curve is rather dome shaped. This indicates that the age samples from spawners with a short season will be highly variable and not easily interpreted for mortality calculations. The second observation is that as larval mortality decreases, regardless of the spawning curve, there is an increase in the curvilinearity in the logarithmic age frequencies. The least variability between the slopes of age frequencies of samples collected at various times during the spawning seasons occurs for species with long spawning seasons and high mortality rates.

The relationship described above of the duration of spawning and mortality to the shape of the age frequency curves has an obvious impact on the calculation of larval mortality from MARMAP samples. The method presently used to estimate larval mortality is to combine the age frequencies from all surveys made during the spawning season of a species and then determine the slope of the exponential regression line of the combined age frequency. The variability of the input age frequencies into this calculation will account for much of the uncertainty of the mortality estimation. To illustrate this point, the larvae produced from a normal spawning curve were subjected to a 0.10 mortality rate and then sampled according to a MARMAP sampling schedule. Age frequencies of the sampled larvae were calculated for each survey, then summed for all surveys in the spawning season (Figures 13-15). The slope of the regression line was compared to the 0.10 input mortality. For the spawning curve with two months duration the ratio of calculated to input mortality was 1.45 (Figure 13), for 4 months spawners the ratio was 1.20 (Figure 14) and for an 8 months spawner the ratio decreased to only 1.06 (Figure 15).

The above relationship was investigated for spawning curves from 2-10 months long and for input mortalities from 0.05 to 0.20. The results for 100

annual survey schedules per month and mortality are shown in Tables 7-10. The highest ratios of calculated to input mortality were for 2 months spawners with 0.05 mortality rate. The ratios approach 1 as the spawning season increases from 2 to 10 months and as the mortality rate increases (Figure 16). This indicates that mortality estimates will be relatively poor for species with short spawning seasons and low mortality rates. Note, however, that when mortality rather than mortality ratio is considered, the standard deviation is relatively independent of the mortality rate (Figure 17).

LARVAL HADDOCK DATA -- MORTALITY

The following is the results of an analysis of MARMAP catches of larval haddock from the Georges Bank area in 1980. Larvae were captured during three surveys in the spring (Feb.-Jun.). Age frequencies were calculated for each survey according to the method in Morse (1984) and plotted using the estimated date of spawning as the X-axis. Various mortality rates were applied to the age frequencies to reconstruct the spawning curves. Mortality rates were changed in an effort to produce a "reasonable" spawning curve. Peak spawning should occur in the March-April time span for the curve to be considered biologically reasonable.

It was evident from the age frequency plot for the 1980 haddock data that a constant mortality, ie. an average annual mortality, would produce an unreasonable spawning curve. This can be seen by examining the age frequencies; examples are shown in Figures 18-21. We therefore applied various time-dependent mortality rates and evaluated the spawning curves. The results of various input mortalities are shown in Figures 22-31. The input mortality rates used to produce Figures 22-31 formed normal curves wherein the larval mortality was low at the beginning of spawning and increased to 0.10 at

between 100 and 150 Julian days. After peaking at 0.10 the mortality rate decreased to near zero on the descending limb of the normal curve. Some of the spawning curves appear quite "reasonable", however, the use of a normal input mortality function has little support either theoretically or biologically. It would take a rather complex mortality mechanism to account for the mortality rate manipulations used to produce the spawning curves in Figures 22-31.

LARVAL HADDOCK DATA -- AGING

An alternative to changing the mortality rates is to reevaluate the methodology and results of the larval aging techniques as given in Morse (1984). The length frequencies of haddock larvae from three surveys on Georges Bank were used in the analysis (Table 11). The length frequencies in survey 1 and 2 were truncated at 7 and 9-mm lengths, respectively, to simplify the output for evaluating temperature-dependent growth and larval aging methods. The 1980 haddock larvae are used merely as an example and the truncation of the length frequencies does not affect the conclusions from the analysis.

We initially converted lengths to ages utilizing an estimate of the mean water temperature during each survey as the input temperature into the temperature-dependent growth function. The age frequencies were back-calculated to numbers at spawning using mortality rates between 0.025 to 0.20 (Figures 32-39). The shape of the spawning curves produced by this method did not conform well to our criteria for reasonableness. This is not surprising given that water temperatures are changing during the spring warming trend on Georges Bank. Temperature changes are continuously altering the age-length relationship under the influence of temperature-dependent growth. We incorporated the instantaneous change in the growth parameters throughout the life of the larvae to reflect the changes in average daily water temperature

from the surface to 50m deep on Georges Bank. The length frequencies were again aged and back-calculated to number at spawning for input mortalities from 0.025 to 0.20 (Figures 40-47). The spawning curves produced by using the average water temperature algorithm are both "reasonable" and consistent, for input mortalities near 0.10. An approximately normal curve can be drawn through all except one point which represents low numbers of young larvae early in the spawning season. That point must be rejected in any case since it implies a peak in the spawning curve earlier in the year than is biologically reasonable. This lends some support to our original assumption, at least for haddock, that the spawning curve can be represented by a normal curve. In addition, the results indicate that, when calculating larval age from length data using temperature-dependent growth equations, the method of calculating should utilize an average daily temperature algorithm. This method incorporates in a realistic way the effects of temperature on larval growth.

When the input mortalities are increased from 0.025 to 0.20, the area under the estimated spawning curve increased exponentially. The area of the spawning curves shown in Figures 32-47 were calculated and plotted in Figure 48. For survey sample temperatures the area increased from 9.9×10^4 for mortality 0.025 to 1.6×10^8 for 0.20 mortality and for the daily temperature algorithm the increase for the same mortalities was from 1.2×10^5 to 1.3×10^9 . Thus the increase of one order of magnitude in mortality resulted in 4 orders of magnitude change in the area under the spawning curve, regardless of the aging method.

The results presented in this paper use survey frequency and timing statistics based on actual MARMAP cruises. Future models could consider other cruise schedules of different frequency and regularity. It would then be

possible to investigate the tradeoff between a large number of cruises and a large number of samples per cruise (reduced within cruise uncertainty). This would be most valuable if done in concert with a study of the actual within cruise uncertainty due to the spatial sampling scheme; the nonrandom distribution of eggs and larvae could be exploited in developing an estimate of total eggs and larvae. The effects of uncertain mortality estimates on the final estimate of spawning biomass and the effects of uncertainty in growth rates could be further investigated in a more comprehensive model.

While some of the computer programs developed for this paper were specifically intended to produce the published results, other programs have a wider future use. Programs are available to convert lengths to ages and ages to lengths using various assumptions concerning temperature dependent growth. Another program is available to convert age frequencies to graphically represented spawning curves using a chosen constant or variable mortality rate. These programs should be useful as routine interactive tools in the interpretation of sampled frequencies. The latter program is especially useful when used with more than one cruise during a spawning period. It enables the user to quickly test hypotheses concerning mortality rates and spawning curves.

The inclusion of egg data and temperature-dependent egg development rates would enhance the usefulness of the procedures. While the mortality rate can often be determined with reasonable accuracy, its logarithmic relation to the area under the spawning curve (Figure 48) caused a major problem. The egg data being less sensitive to mortality rates would moderate this problem and the larval data would serve to fill the spaces between surveys.

LITERATURE CITED

- Berrien, P. L., N. A. Naplan and M. R. Pennington. 1981. Atlantic mackerel, *Scomber scombrus*, egg production and spawning population estimates for 1977 in the Gulf of Maine, Georges Bank, and Middle Atlantic Bight. Rapp. P.-v. Reun. Cons. int. Explor. Mer. 178: 279-288.
- Berrien, P., W. Morse and M. Pennington. 1984. Recent estimates of adult spawning stock biomass off the northeastern United States from MARMAP ichthyoplankton surveys. NOAA TECH. MEM. NMFS-F/NEC-30: 111p.
- Hewitt, R. P. and R. D. Methot, Jr. 1982. Distribution and mortality of Northern Anchovy larvae in 1978 and 1979. CalCOFI Rep.23: 226-245.
- Morse, W. 1984. An assessment of the Georges Bank haddock stock based on larvae collected on MARMAP plankton surveys, 1977-1982. MARMAP Contr. No. MED/NEFC 84-09: 20p.
- Pennington, M. 1983. Efficient estimators of abundance for fish and plankton surveys. Biometrics,39: 281-286.
- Sherman, K., R. Lasker, W. Richards and A. W. Kendall, Jr. 1983. Ichthyoplankton and fish recruitment studies in large marine ecosystems. Mar Fish. Rev.45(10-12): 1-25.
- Sibunka, J. D. and M. J. Silverman. 1984. MARMAP surveys of the continental shelf from Cape Hatteras, North Carolina, to Cape Sable, Nova Scotia (1977-1983) Atlas No. 1. Summary of operations. NOAA TECH. MEM. NMFS-F/NEC-33: 306p.

Smith, P. E. and S. Richardson. 1977. Standard techniques for pelagic fish eggs and larval surveys. FAO Fish. Tech Pap. 175: 100p.

Zweifel, J. R. and P. E. Smith. 1981. Estimates of abundance and mortality of larval anchovies (1951-75): application of a new method. Rapp. P.-v. Reun. Cons. int. Explor. Mer, 178: 248-259.

TABLE 1. Survey timing and frequency from the 1977-1981 MARMAP surveys

From - to (survey)(survey)	Range of days between surveys	Average days between surveys	Std. Dev. in days
Jan. 1 - 1	49 - 87	68	12
1 - 2	17 - 67	42	15
2 - 3	23 - 65	42	14
3 - 4	27 - 54	44	8
4 - 5	38 - 79	61	13
5 - 6	26 - 88	55	18
6 - 7	18 - 59	34	14
7 - Dec. 31	13 - 41	31	10

Table 2. The ratios of the area under the actual spawning curve (R) to the area estimated from MARMAP sampling (E) with no variability. Means are from 100 samples.

Duration of spawning (months)	Mean ratio of E/R	Std. Dev. of E/R	Minimum ratio	Maximum ratio
2	1.010	0.654	0.069	2.407
3	1.079	0.340	0.217	1.769
4	1.052	0.176	0.514	1.389
5	1.035	0.122	0.587	1.319
6	1.033	0.061	0.885	1.180
7	0.999	0.070	0.611	1.177
8	1.003	0.041	0.857	1.098
9	0.989	0.032	0.869	1.058
10	0.976	0.028	0.833	1.031

Table 3. The ratios of the area under the actual spawning curve (R) to the area estimated from MARMAP sampling (E) with logarithmic standard error factor of 1.25. Means are from 100 samples.

Duration of spawning (months)	Mean ratio of E/R	Std. Dev. of E/R	Minimum ratio	Maximum ratio
2	1.124	0.728	0.019	3.264
3	1.173	0.424	0.086	2.348
4	1.073	0.277	0.420	2.213
5	1.085	0.210	0.558	1.674
6	1.062	0.160	0.680	1.480
7	1.012	0.163	0.611	1.768
8	0.996	0.139	0.673	1.429
9	1.023	0.145	0.749	1.460
10	1.019	0.120	0.762	1.352

Table 4. The ratios of the area under the actual spawning curve (R) to the area estimated from MARMAP sampling (E) with logarithmic standard error factor of 1.50. Means are from 100 samples.

Duration of spawning (months)	Mean ratio of E/R	Std. Dev. of E/R	Minimum ratio	Maximum ratio
2	1.134	0.679	0.022	3.112
3	1.184	0.558	0.306	3.034
4	1.115	0.554	0.399	4.197
5	1.127	0.359	0.442	2.282
6	1.109	0.352	0.504	2.286
7	1.028	0.278	0.530	2.126
8	1.106	0.274	0.601	1.794
9	1.067	0.258	0.534	1.942
10	1.029	0.219	0.585	1.723

Table 5. The ratios of the area under the actual spawning curve (R) to the area estimated from MARMAP sampling (E) with logarithmic standard error factor of 1.75. Means are from 100 samples.

Duration of spawning (months)	Mean ratio of E/R	Std. Dev. of E/R	Minimum ratio	Maximum ratio
2	1.367	1.540	0.010	10.184
3	1.145	0.714	0.172	4.110
4	1.257	0.613	0.308	3.591
5	1.212	0.517	0.471	2.606
6	1.183	0.460	0.343	2.994
7	1.163	0.438	0.508	2.494
8	1.189	0.415	0.603	2.966
9	1.137	0.376	0.495	3.107
10	1.144	0.380	0.540	2.514

Table 5. The ratios of the area under the actual spawning curve (R) to the area estimated from MARMAP sampling (E) with logarithmic standard error factor of 1.75. Means are from 100 samples.

Duration of spawning (months)	Mean ratio of E/R	Std. Dev. of E/R	Minimum ratio	Maximum ratio
2	1.367	1.540	0.010	10.184
3	1.145	0.714	0.172	4.110
4	1.257	0.613	0.308	3.591
5	1.212	0.517	0.471	2.606
6	1.183	0.460	0.343	2.994
7	1.163	0.438	0.508	2.494
8	1.189	0.415	0.603	2.966
9	1.137	0.376	0.495	3.107
10	1.144	0.380	0.540	2.514

Table 6. The ratios of the area under the actual spawning curve (R) to the area estimated from MARMAP sampling (E) with logarithmic standard error factor of 2.00. Means are from 100 samples.

Duration of spawning (months)	Mean ratio of E/R	Std. Dev. of E/R	Minimum ratio	Maximum ratio
2	1.410	1.694 *	0.001	9.349
3	1.472	1.158	0.093	5.378
4	1.393	0.897	0.235	4.590
5	1.349	0.788	0.404	4.836
6	1.286	0.453	0.453	2.915
7	1.365	0.806	0.326	5.306
8	1.206	0.464	0.486	2.546
9	1.292	0.602	0.421	3.651
10	1.189	0.651	0.511	6.017

Table 7. The ratios of the input mortality (I) to mortality estimated from MARMAP sampling (E). Input mortality equals 0.05. Means are from 100 samples.

Duration of spawning (months)	Mean ratio of E/I	Std. Dev. of E/I	Minimum ratio	Maximum ratio
2	1.250	1.067	-1.041	4.239
3	1.223	0.391	0.400	2.257
4	1.115	0.217	0.658	1.698
5	1.078	0.143	0.725	1.466
6	1.063	0.110	0.763	1.400
7	1.053	0.078	0.862	1.305
8	1.050	0.059	0.871	1.197
9	1.027	0.051	0.883	1.160
10	1.028	0.044	0.935	1.117

Table 8. The ratios of the input mortality (I) to mortality estimated from MARMAP sampling (E). Input mortality equals 0.10. Means are from 100 samples.

Duration of spawning (months)	Mean ratio of E/I	Std. Dev. of E/I	Minimum ratio	Maximum ratio
2	1.114	0.477	-0.296	2.308
3	1.064	0.178	0.630	1.617
4	1.043	0.103	0.672	1.328
5	1.050	0.067	0.916	1.249
6	1.035	0.056	0.853	1.162
7	1.028	0.040	0.941	1.122
8	1.017	0.034	0.911	1.099
9	1.015	0.026	0.940	1.091
10	1.014	0.020	0.971	1.069

Table 9. The ratios of the input mortality (I) to mortality estimated from MARMAP sampling (E). Input mortality equals 0.15. Means are from 100 samples.

Duration of spawning (months)	Mean ratio of E/I	Std. Dev. of E/I	Minimum ratio	Maximum ratio
2	1.056	0.295	0.082	1.866
3	1.031	0.159	0.592	1.463
4	1.053	0.088	0.822	1.378
5	1.029	0.045	0.928	1.173
6	1.019	0.029	0.955	1.092
7	1.015	0.024	0.949	1.101
8	1.016	0.019	0.966	1.059
9	1.012	0.016	0.972	1.047
10	1.010	0.013	0.983	1.042

Table 10. The ratios of the input mortality (I) to mortality estimated from MARMAP sampling (E). Input mortality equals 0.20. Means are from 100 samples.

Duration of spawning (months)	Mean ratio of E/I	Std. Dev. of E/I	Minimum ratio	Maximum ratio
2	1.066	0.234	0.581	1.611
3	1.043	0.106	0.783	1.503
4	1.030	0.056	0.863	1.191
5	1.017	0.030	0.936	1.110
6	1.017	0.028	0.925	1.083
7	1.009	0.020	0.972	1.058
8	1.013	0.014	0.975	1.049
9	1.009	0.012	0.981	1.035
10	1.008	0.010	0.983	1.037

Table 11. Length frequencies of haddock larvae from the spring MARMAP surveys on Georges Bank used for analysis of temperature-dependent growth.

Length (mm)	Surveys		
	1	2	3
4	397	712	
5	475	1379	6
6	37	817	9
7	6	937	15
8		313	16
9		66	41
10			32
11			43
12			23
13			18
14			17

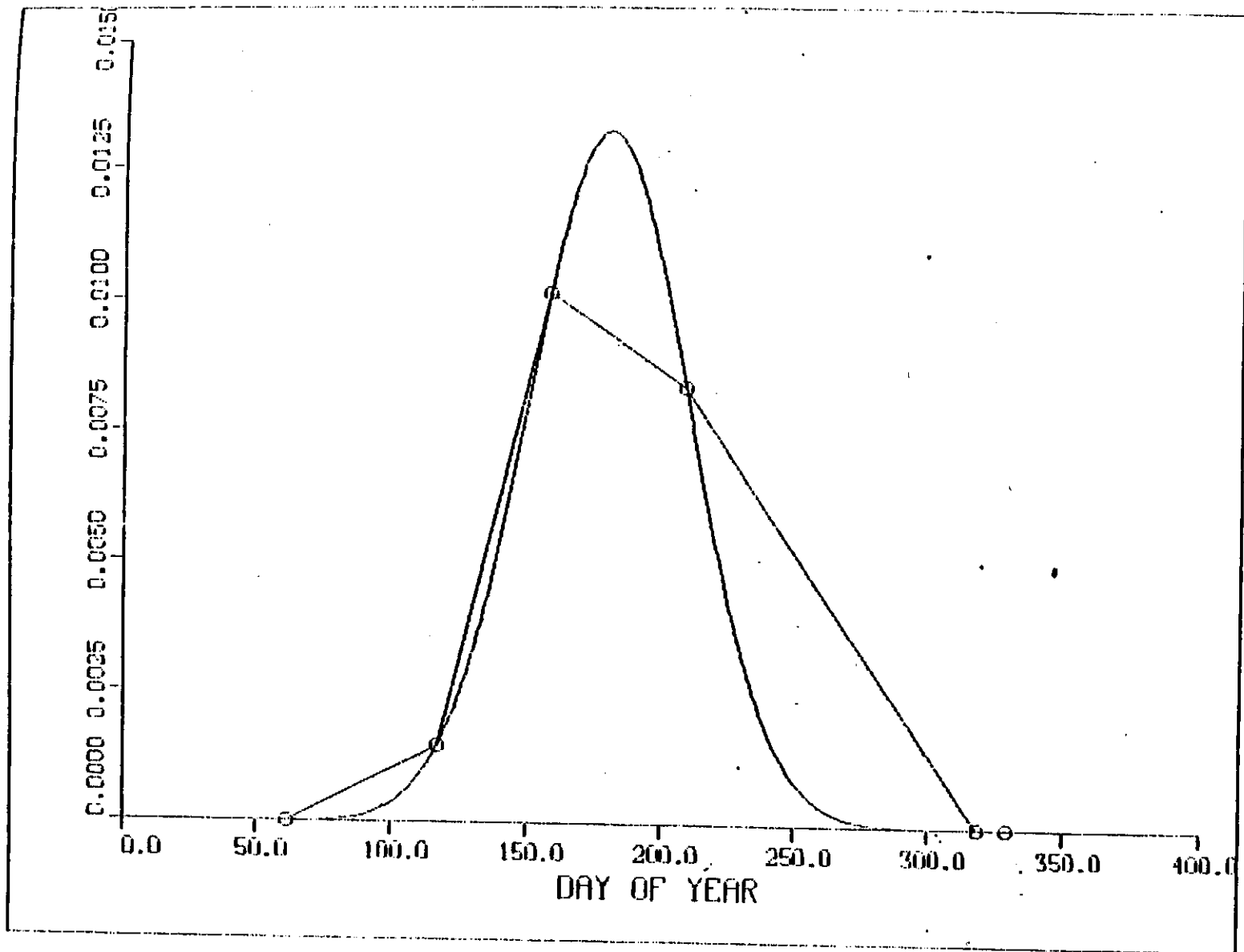


Figure 1. An example of estimating the area of a normal spawning curve by connecting the sampling points with straight lines.

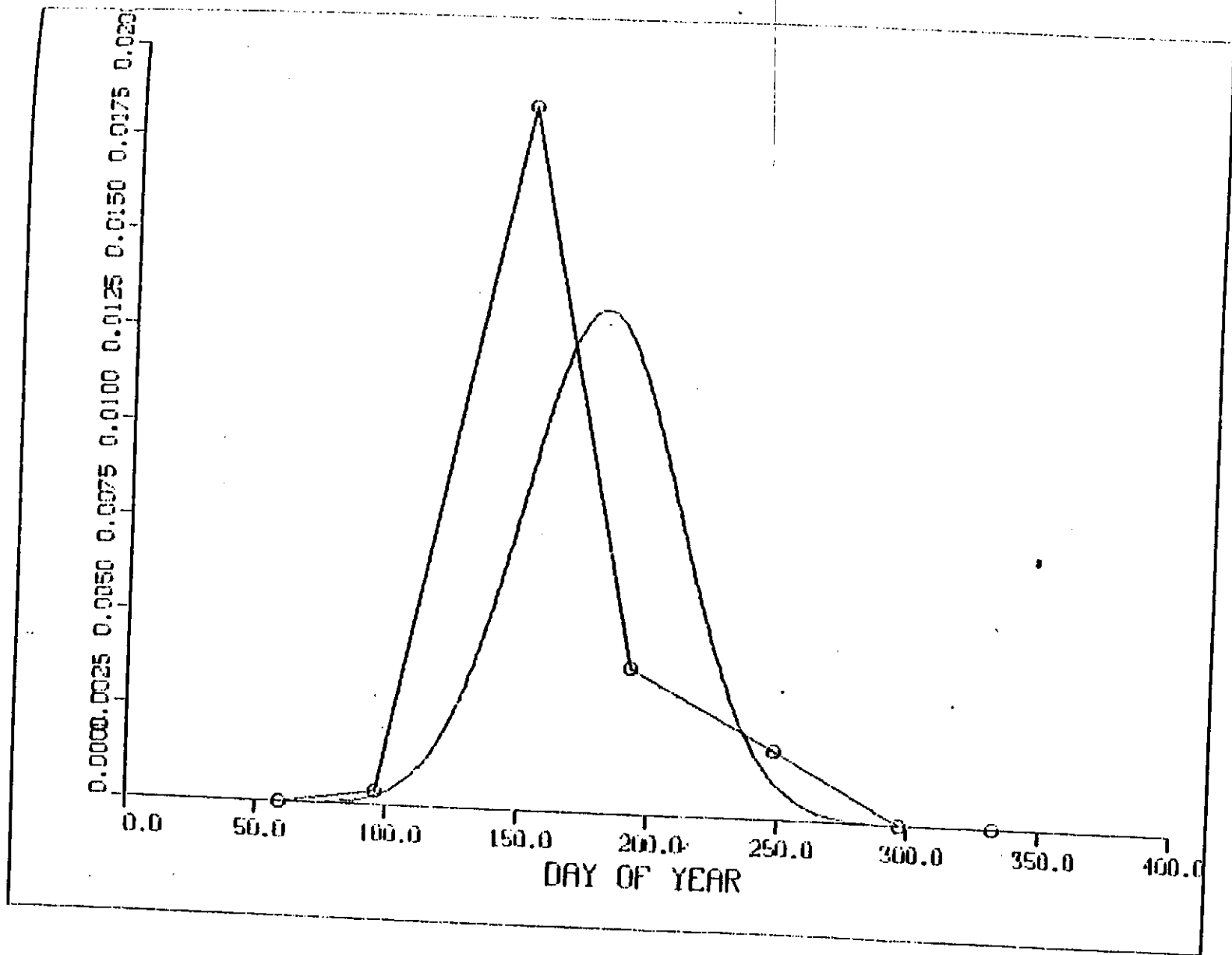


Figure 2. An example of estimating the area of a normal spawning curve by connecting the sampling points that contain a random variance component.

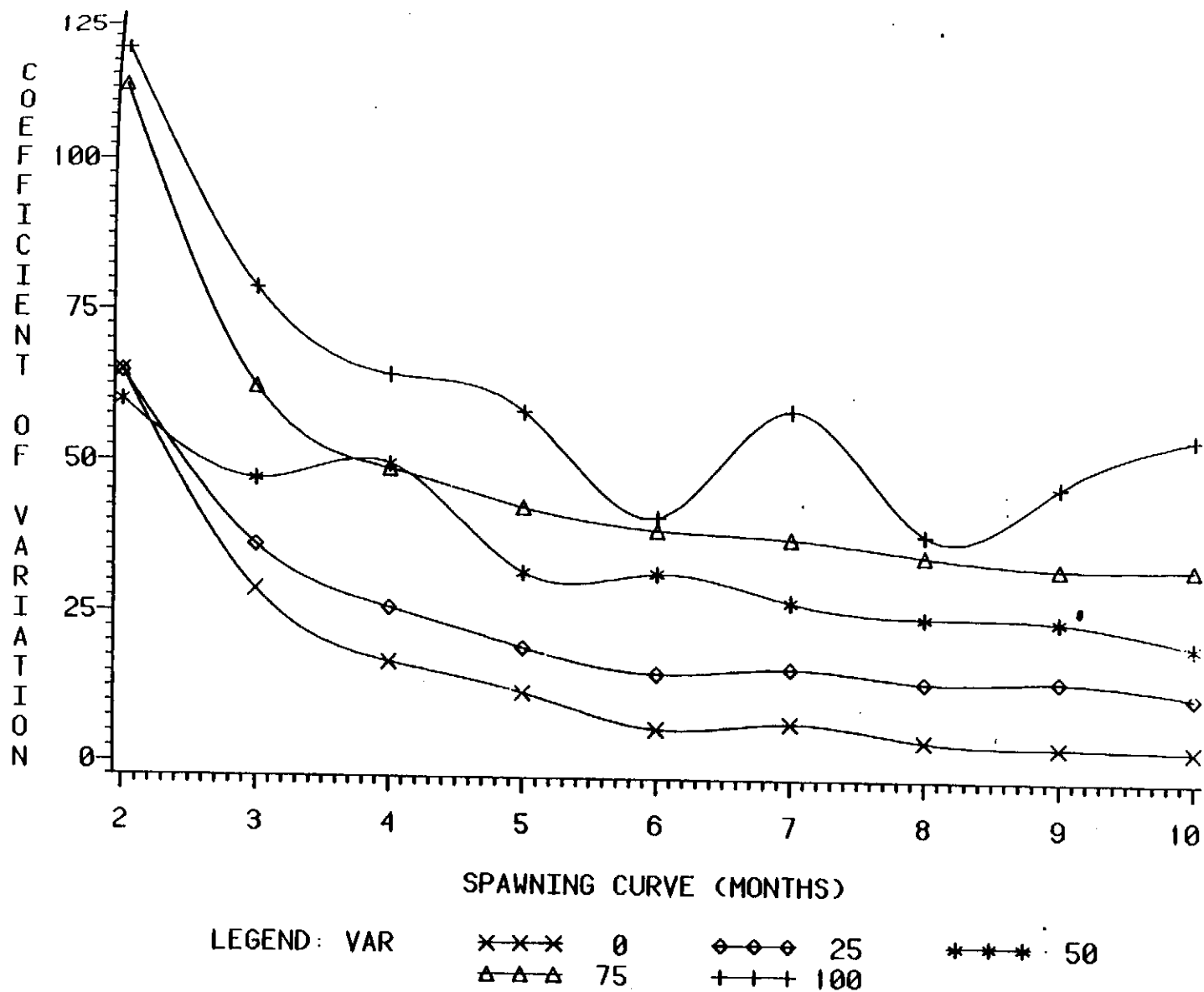


Figure 3. The relationship of the duration of spawning (months), the within survey logarithmic standard error factor (var.= 0 to 100% of the mean) and the coefficient of variation of the ratios of input to estimated spawning curves from MARMAP sampling.

STANDARD DEVIATION IS 10.000
MORTALITY RATE IS 0.050

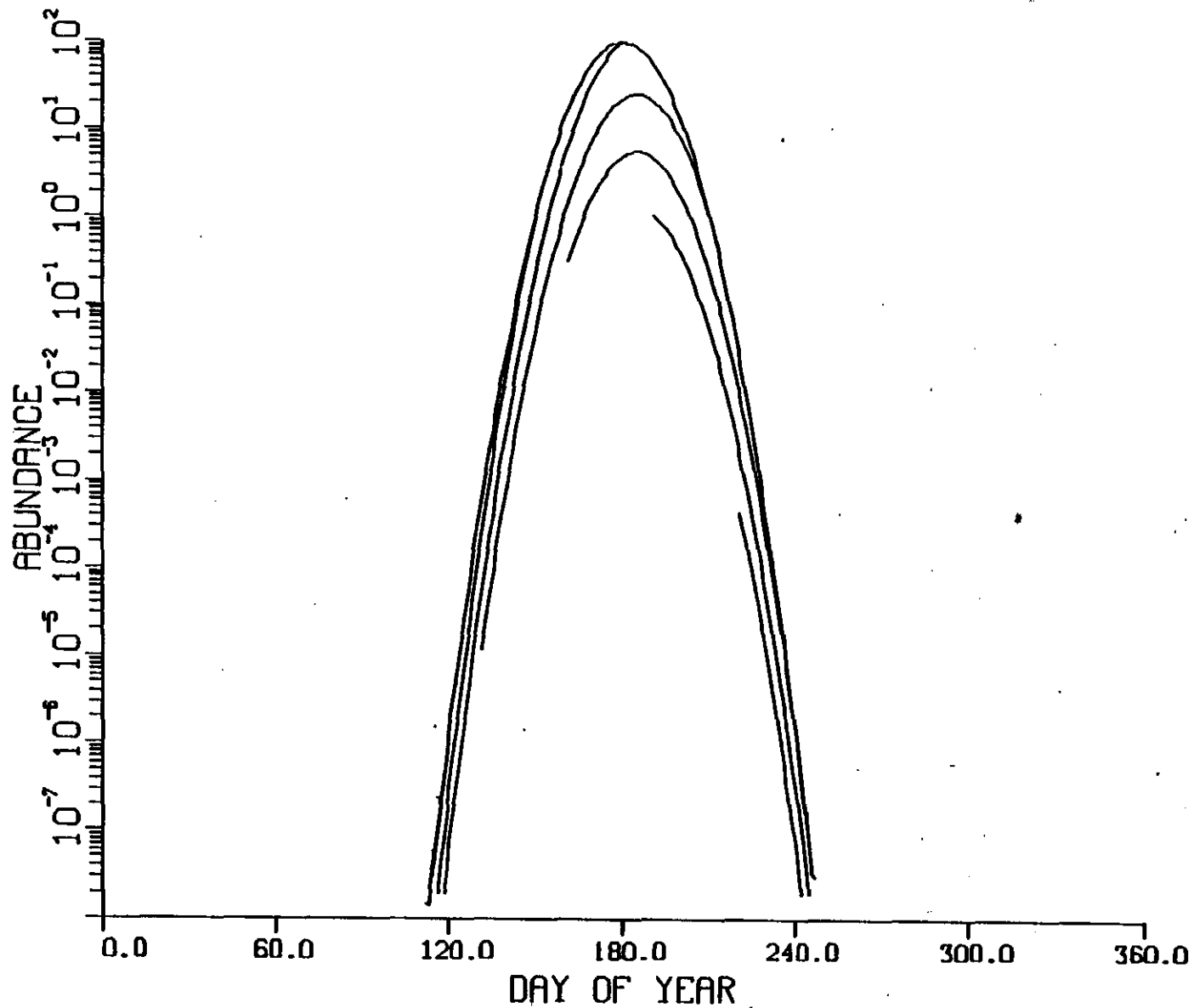


Figure 4. Age frequency samples from a normal spawning curve of 2 months duration (SD= 10 days) and mortality = 0.05.

STANDARD DEVIATION IS 10.000
MORTALITY RATE IS 0.100

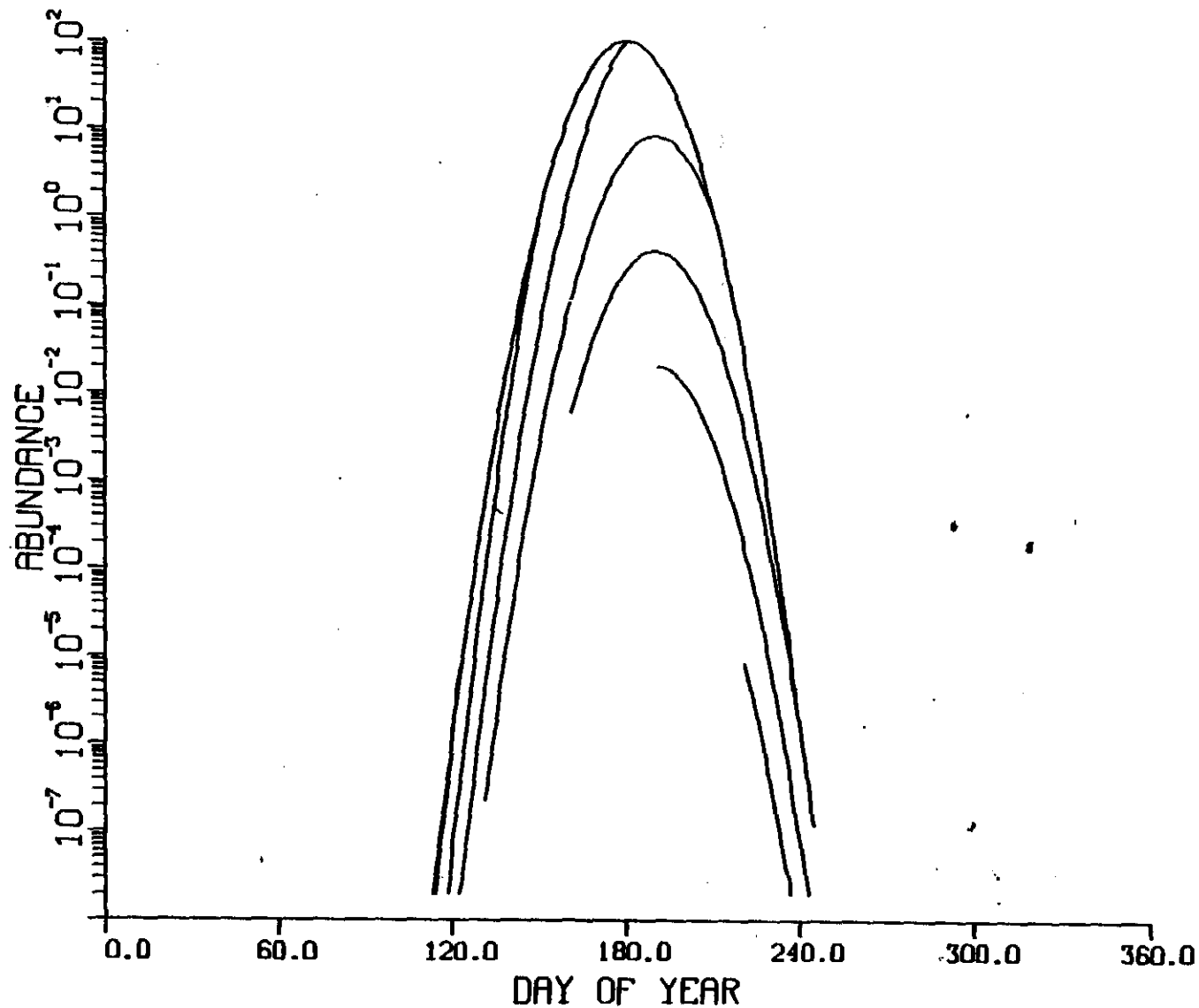


Figure 5. Age frequency samples from a normal spawning curve of 2 months duration (SD= 10 days) and mortality = 0.10.

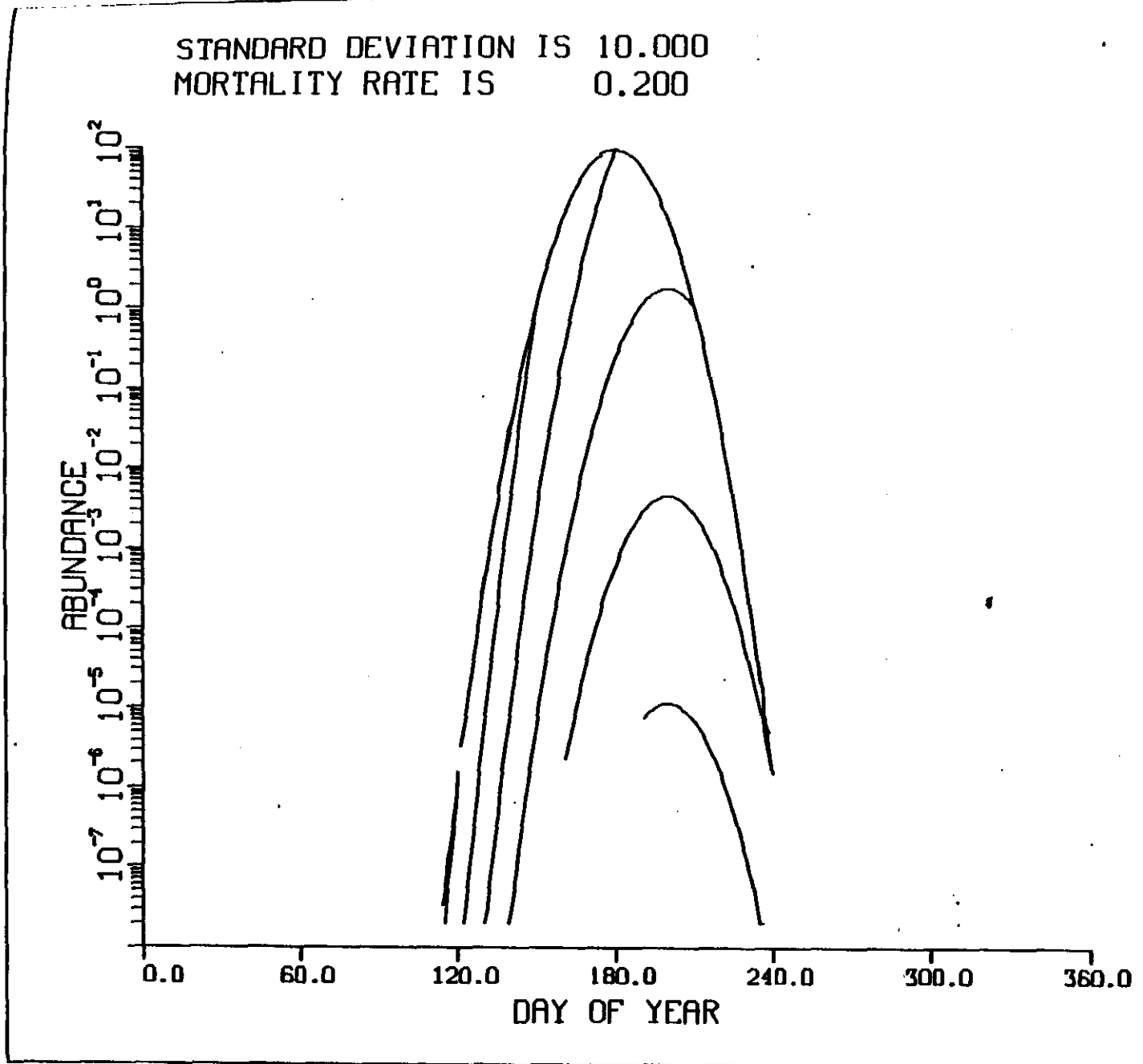


Figure 6. Age frequency samples from a normal spawning curve of 2 months duration (SD= 10 days) and mortality = 0.20.

STANDARD DEVIATION IS 30.000
MORTALITY RATE IS 0.050

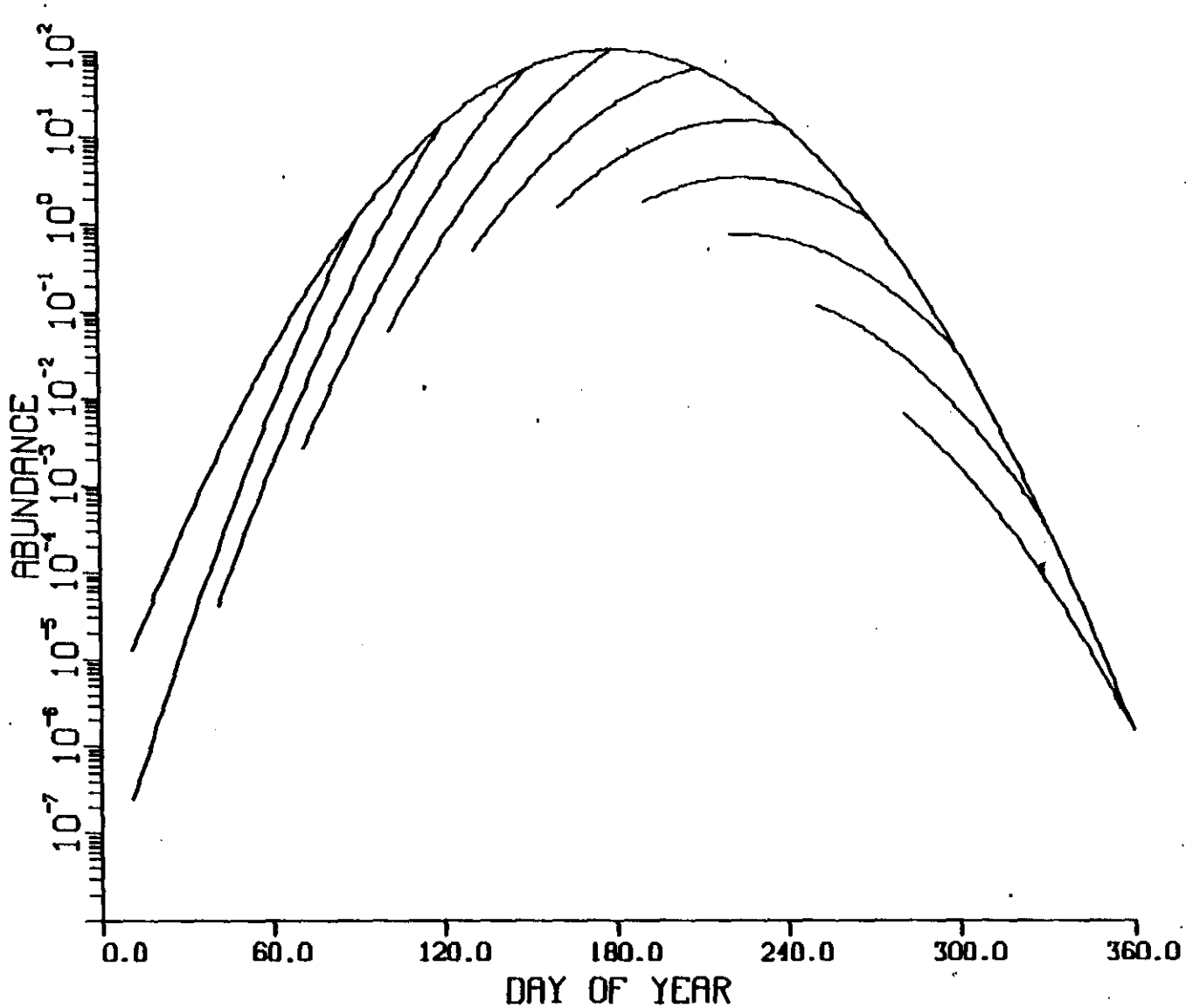


Figure 7. Age frequency samples from a normal spawning curve of 6 months duration (SD= 30 days) and mortality = 0.05.

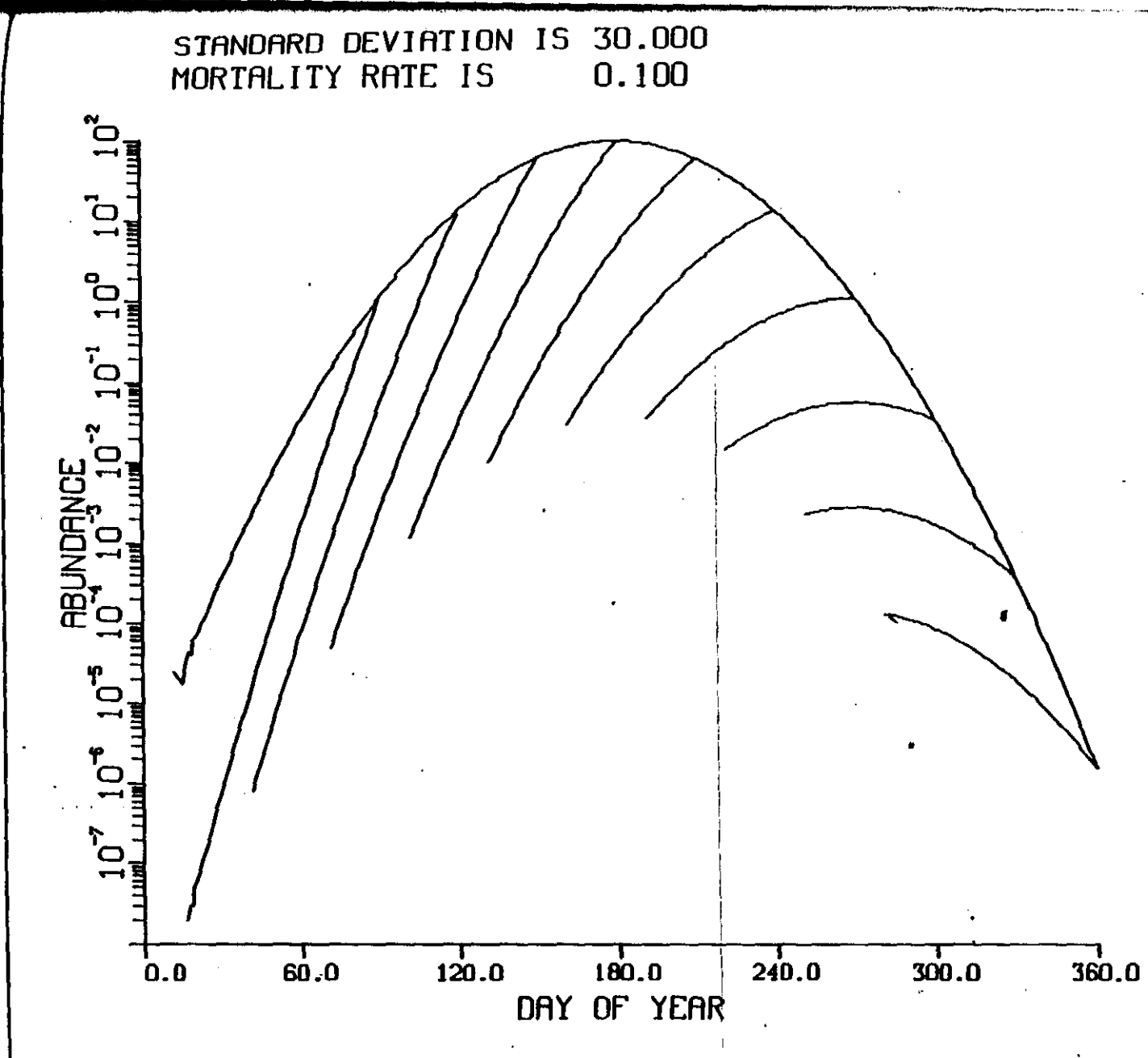


Figure 8. Age frequency samples from a normal spawning curve of 6 months duration (SD= 30 days) and mortality = 0.10.

STANDARD DEVIATION IS 30.000
MORTALITY RATE IS 0.200

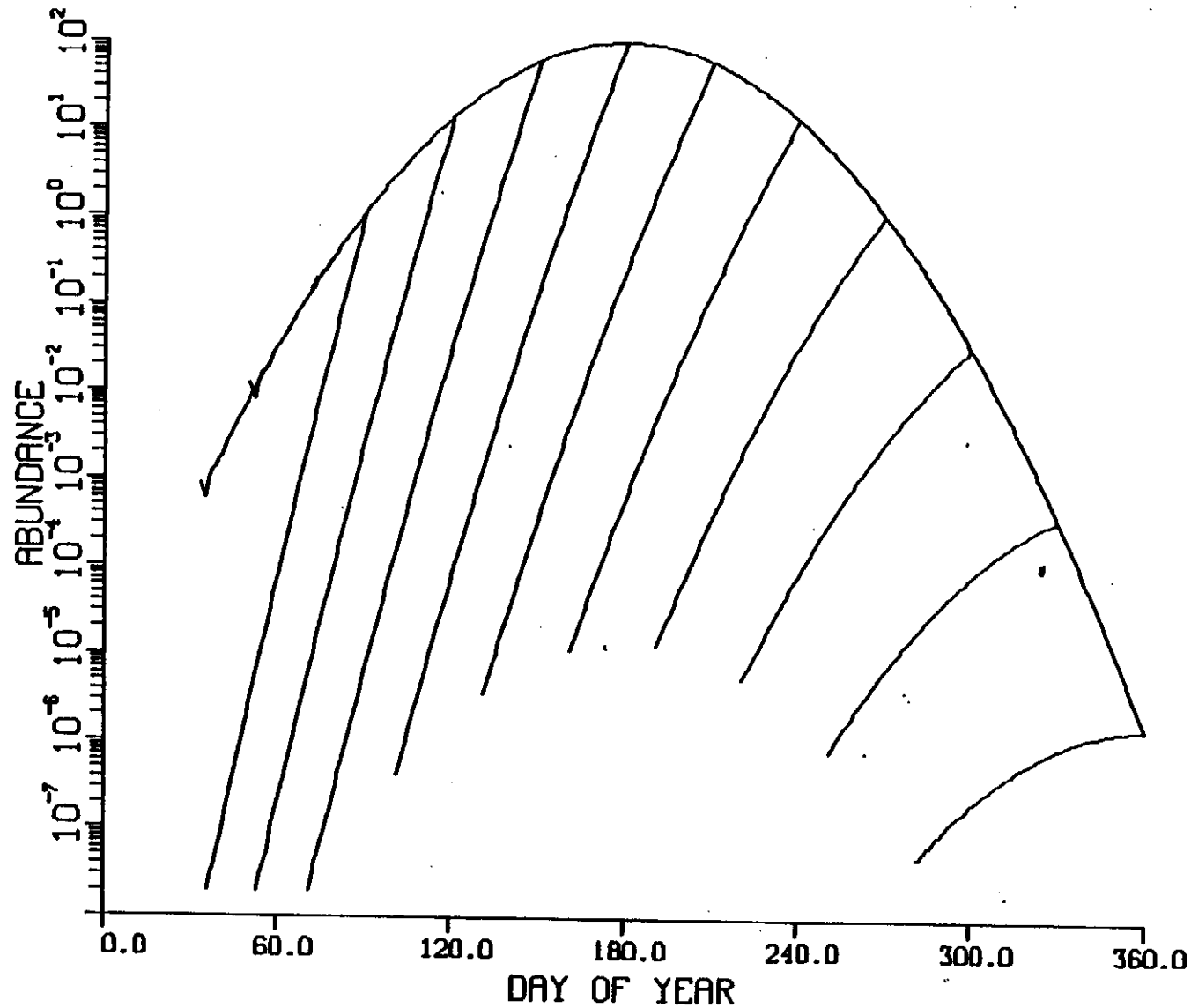


Figure 9. Age frequency samples from a normal spawning curve of 6 months duration (SD= 30 days) and mortality = 0.20.

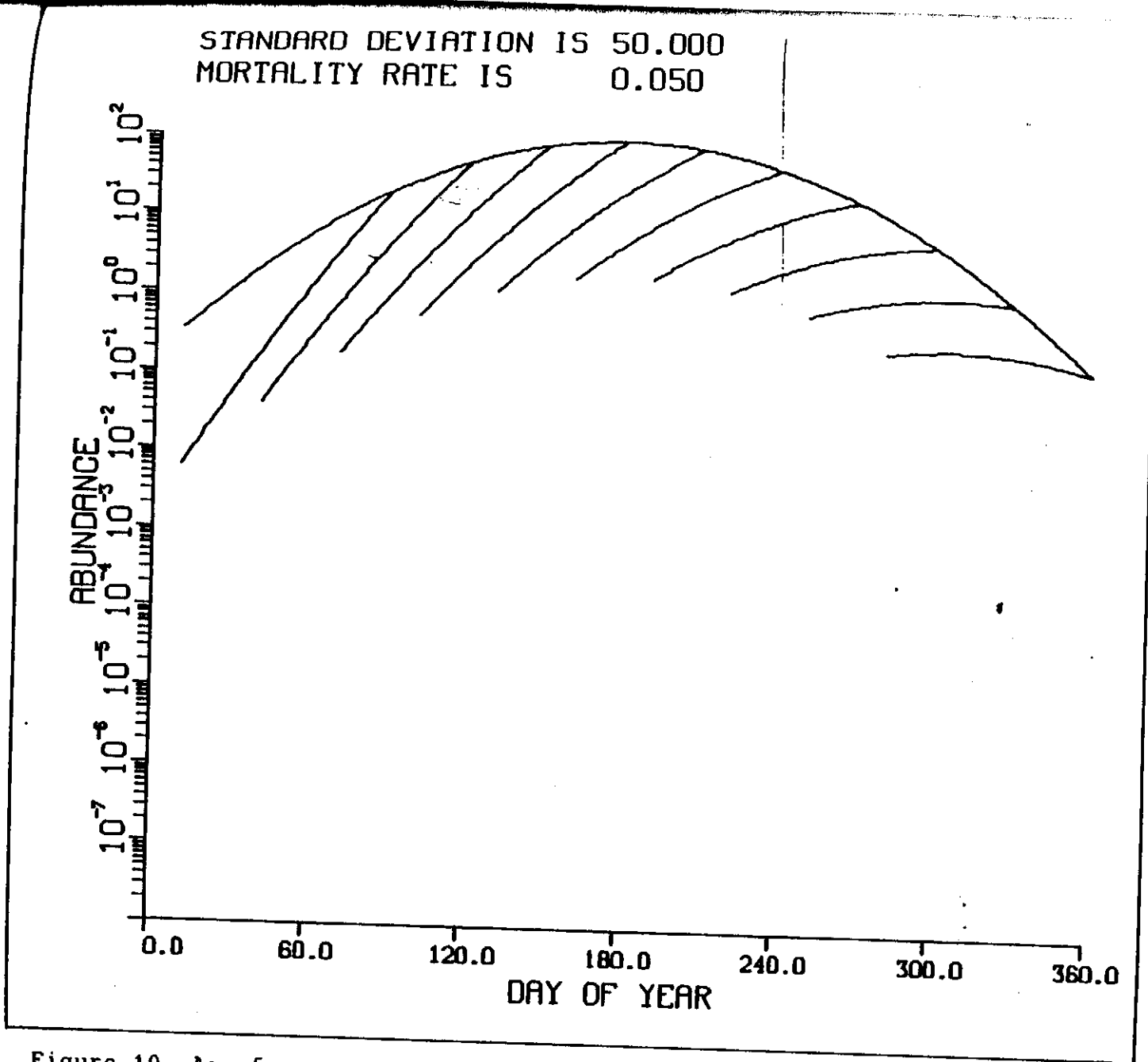


Figure 10. Age frequency samples from a normal spawning curve of 10 months duration (SD= 50 days) and mortality = 0.05.

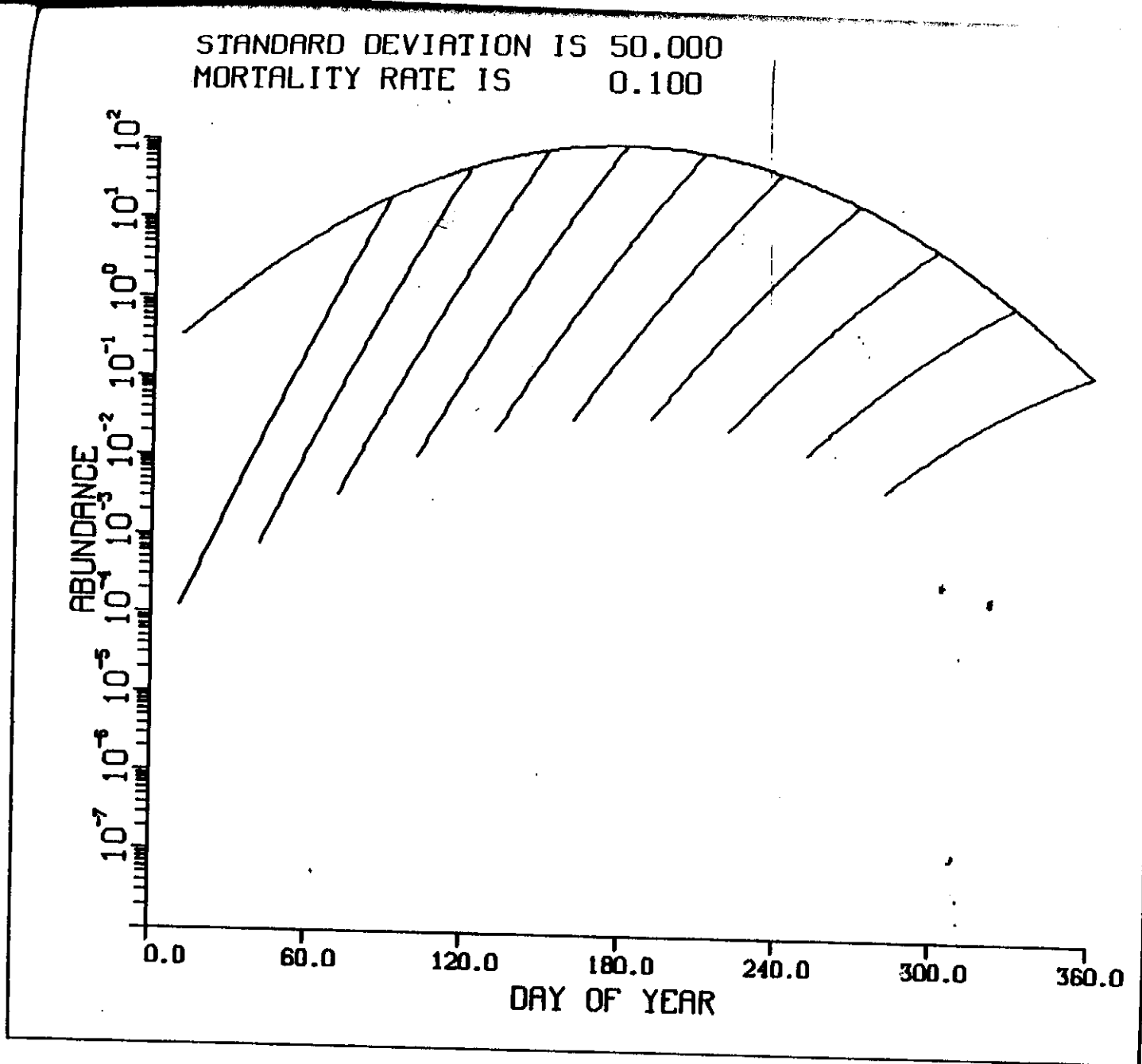


Figure 11. Age frequency samples from a normal spawning curve of 10 months duration (SD= 50 days) and mortality = 0.10.

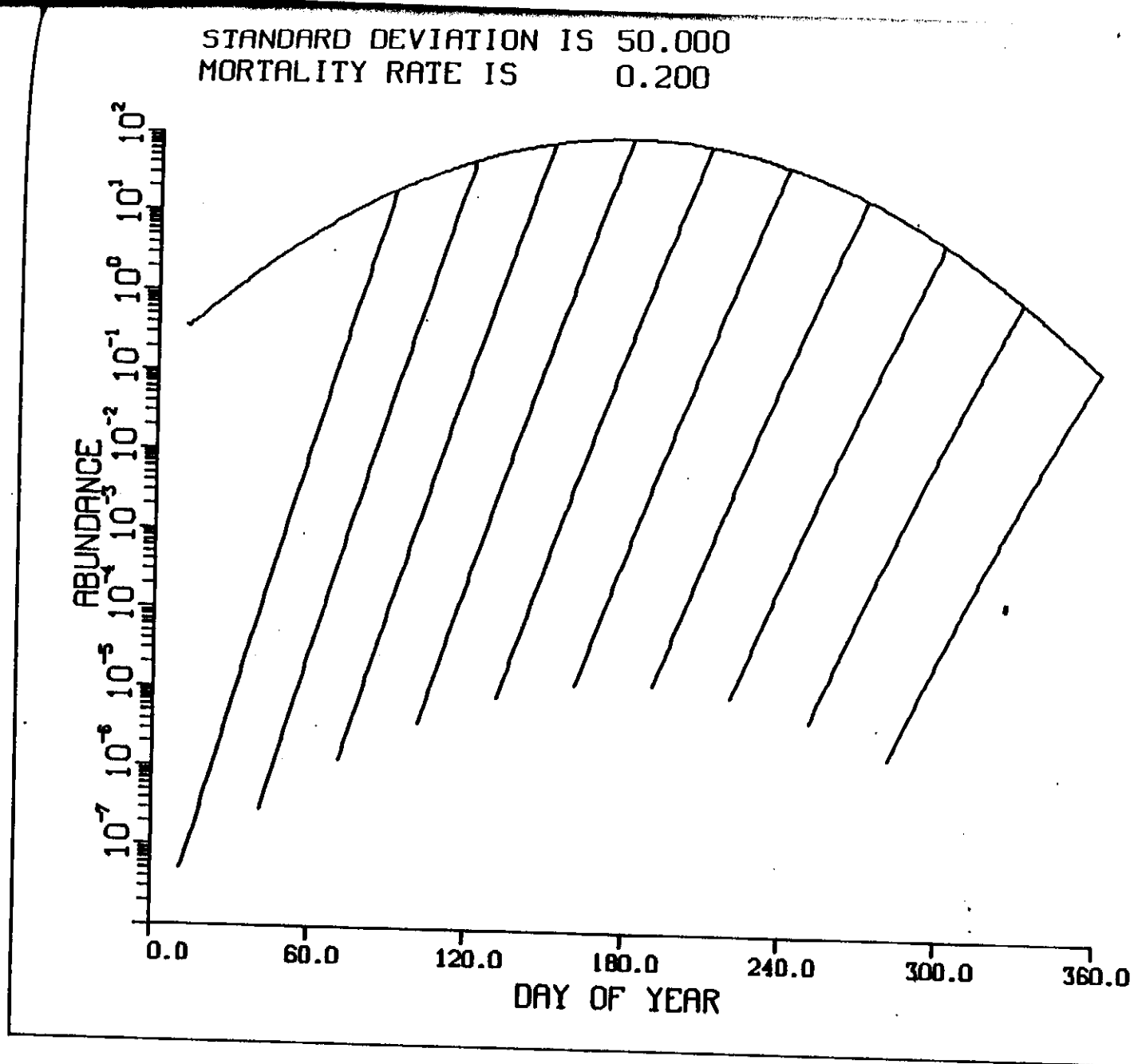


Figure 12. Age frequency samples from a normal spawning curve of 10 months duration (SD= 50 days) and mortality \neq 0.20.

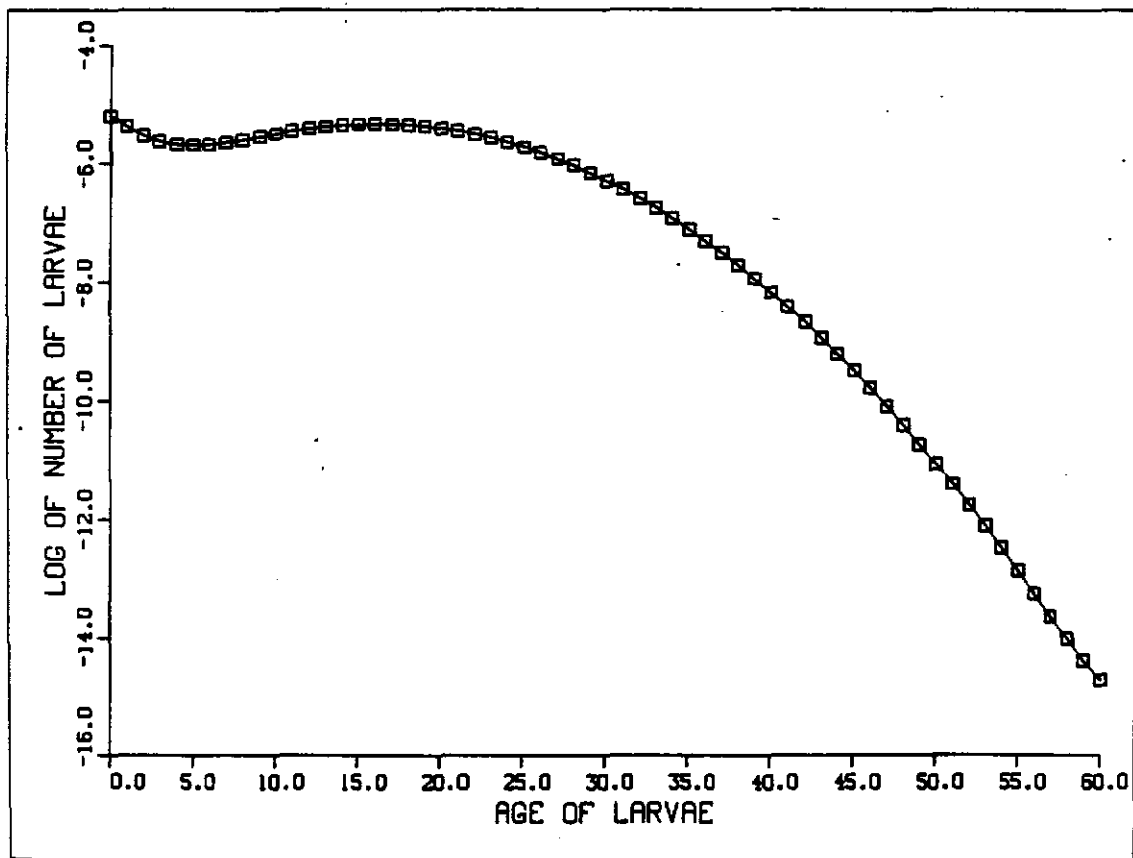
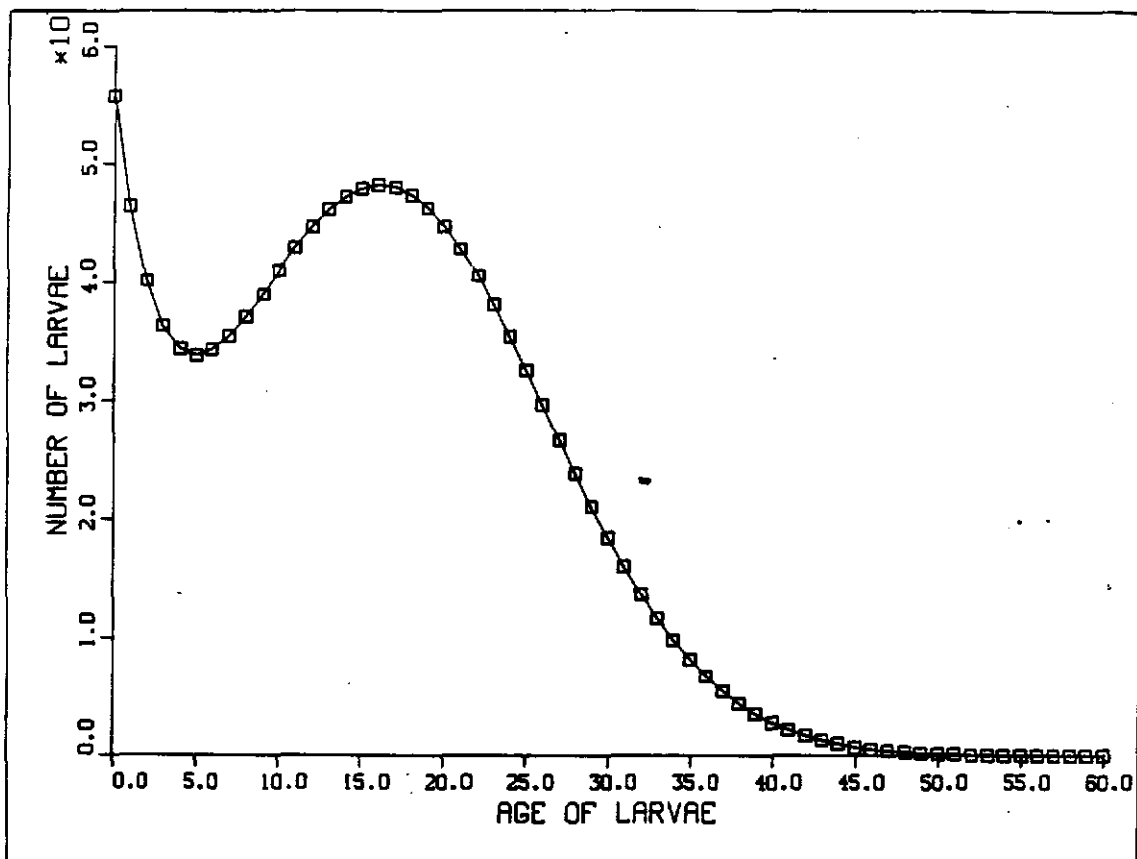


Figure 13. A combined age frequency from MARMAP sampling of a 2 months normal spawning curve with a 0.10 mortality (upper) and the logarithmic plot (bottom). The ratio of the calculated mortality (slope of log plot) to 0.10 is 1.45.

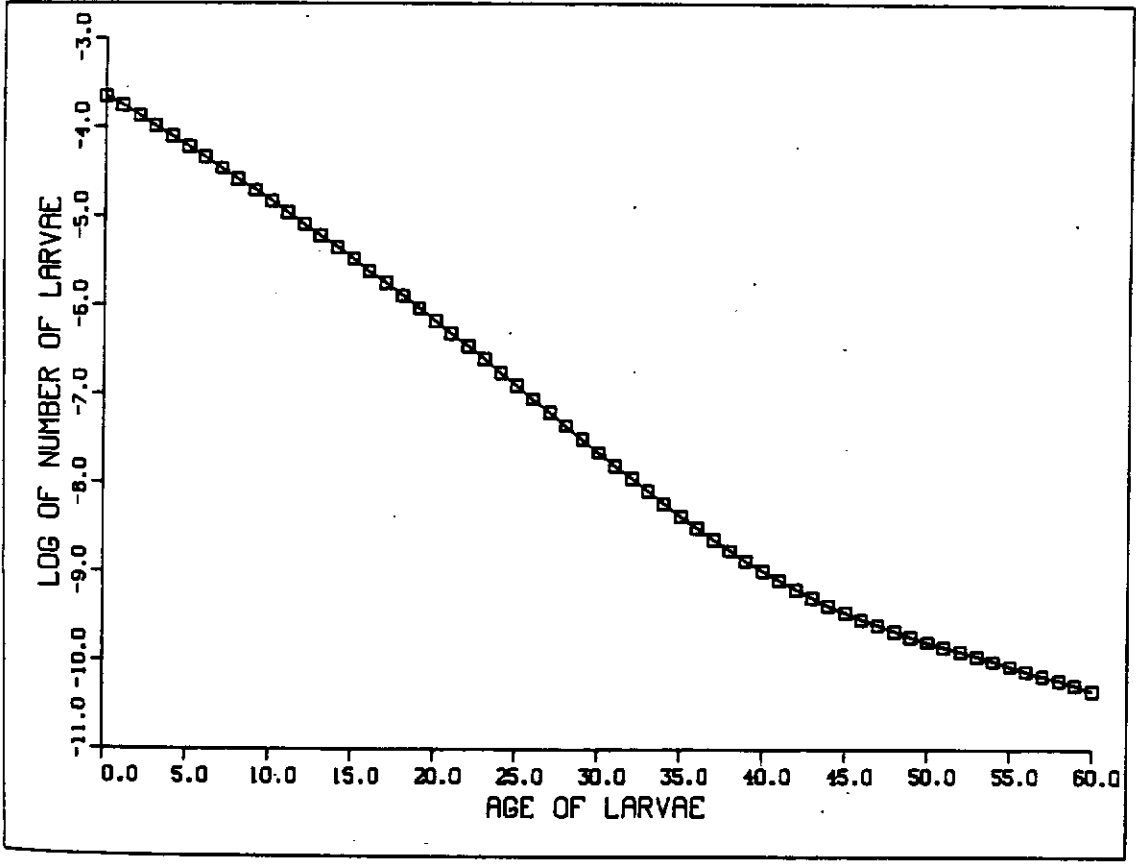
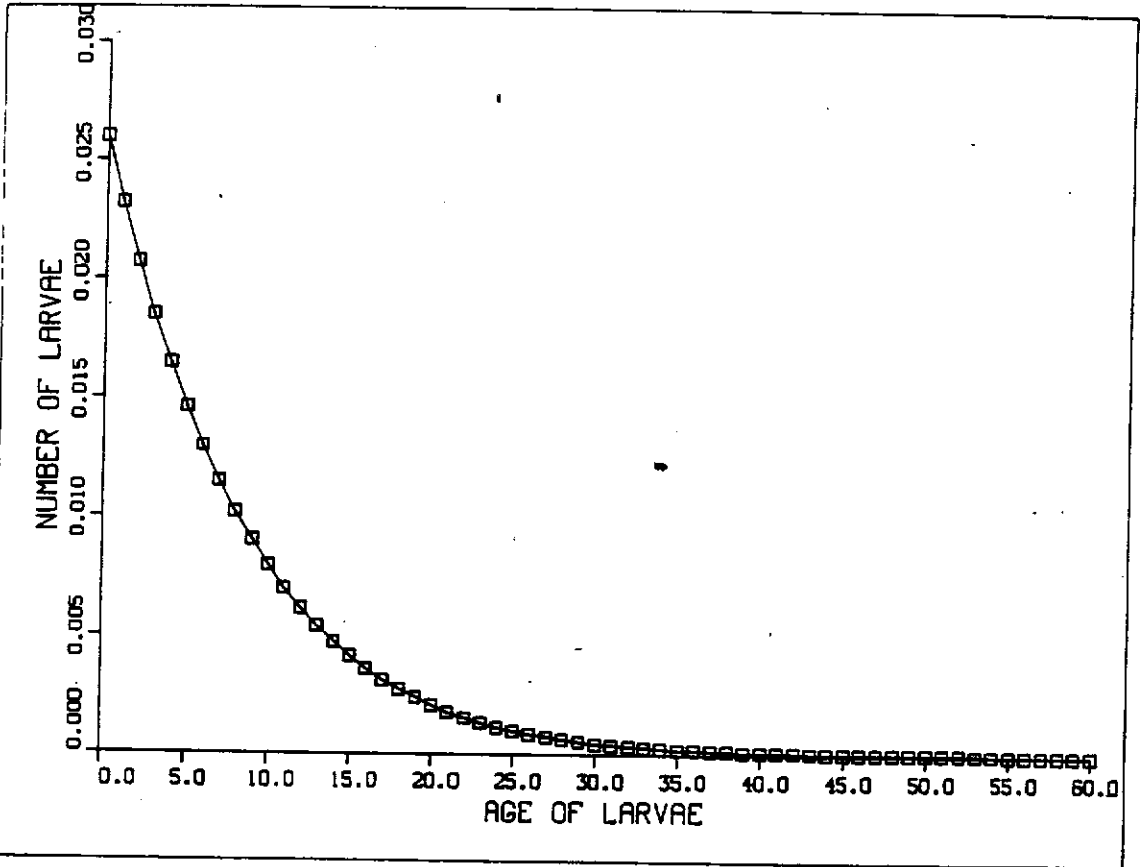


Figure 14. A combined age frequency from MARMAP sampling of a 4 months normal spawning curve with a 0.10 mortality (upper) and the logarithmic plot (bottom). The ratio of the calculated mortality (slope of log plot) to 0.10 is 1.20.

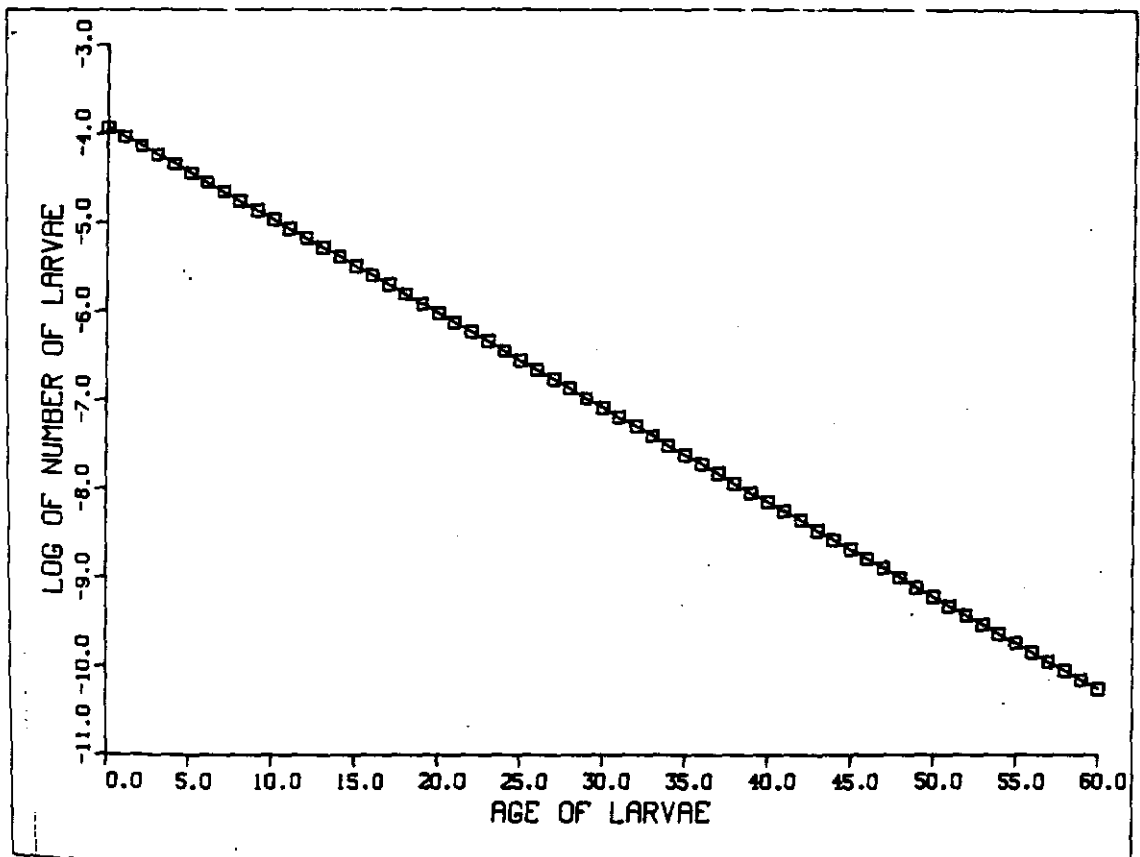
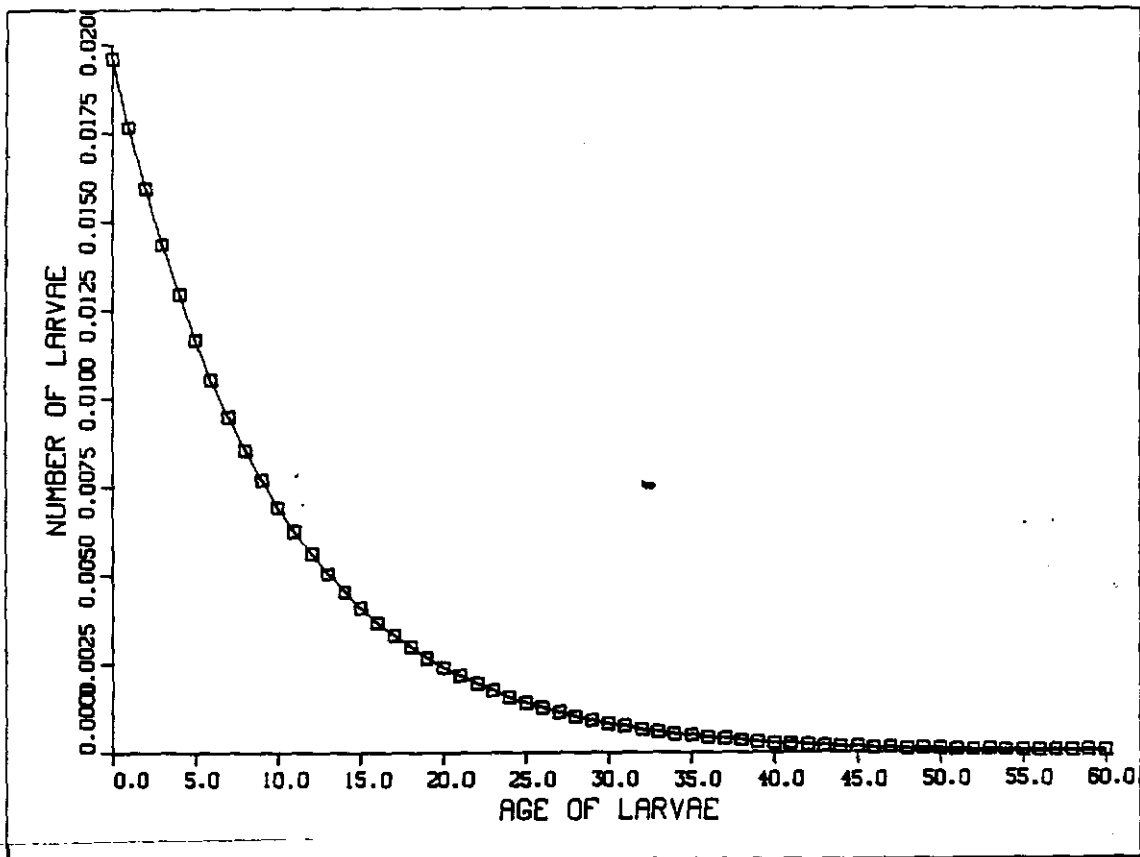


Figure 15. A combined age frequency from MARMAP sampling of an 8 months normal spawning curve with a 0.10 mortality (upper) and the logarithmic plot (bottom). The ratio of the calculated mortality (slope of log plot) to 0.10 is 1.06.

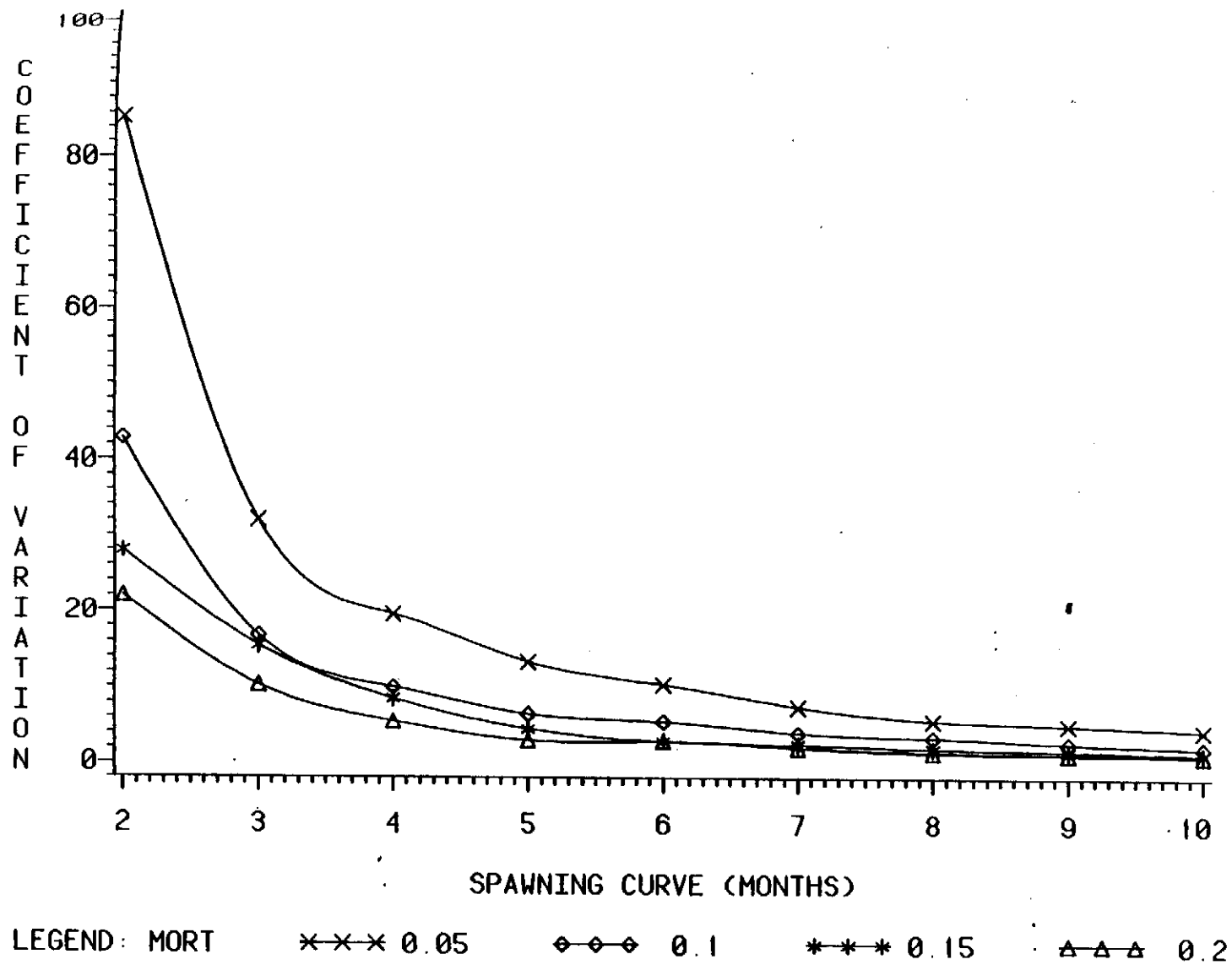


Figure 16. The relationship of the duration of spawning (months), the larval mortality rate (0.05-0.20) and the coefficient of variation of the ratios of input to estimated mortality rates from MARMAP sampling.

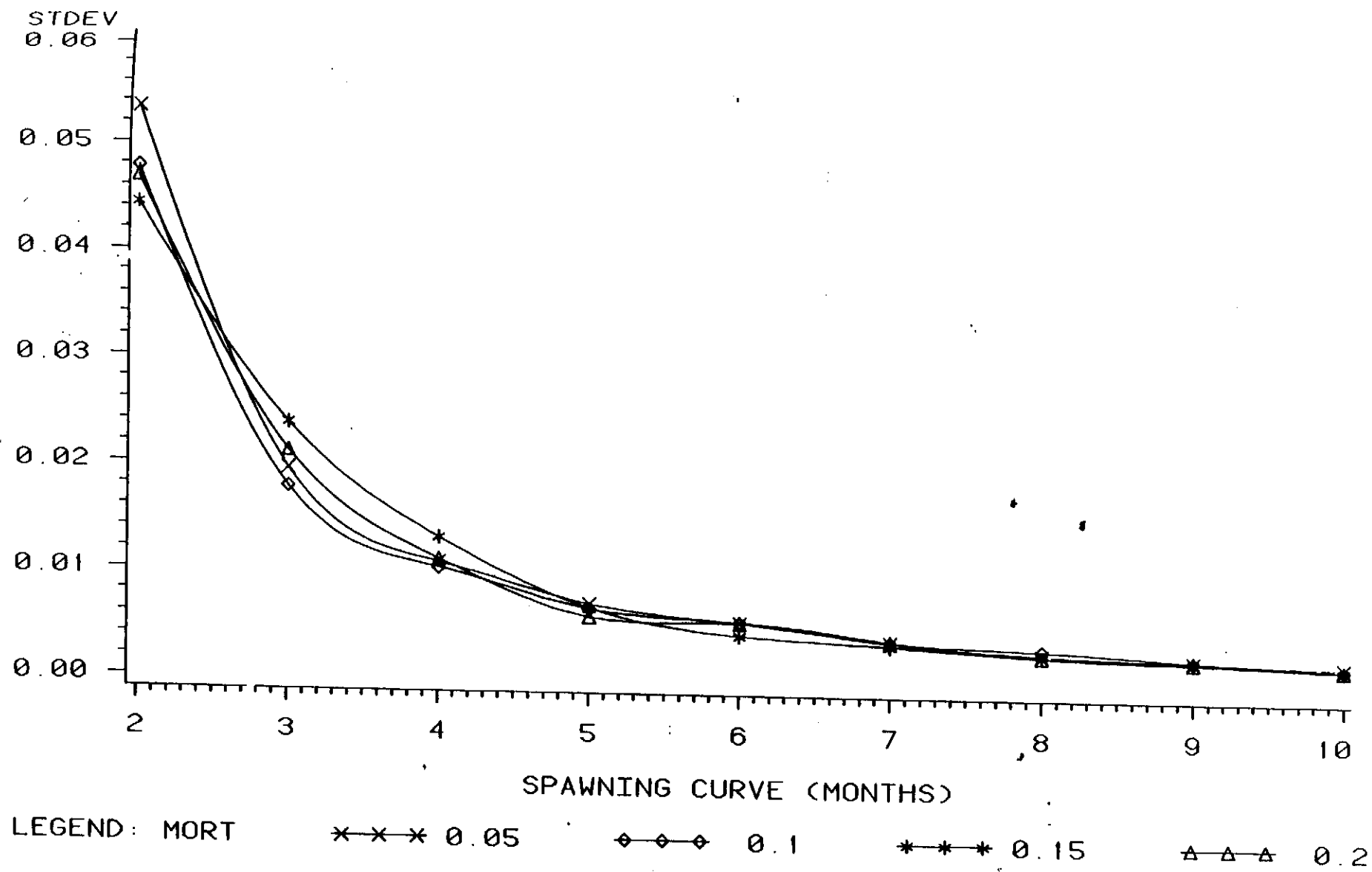


Figure 17. The standard deviation of the estimated mortality rate as a function of spawning period and mortality rate.

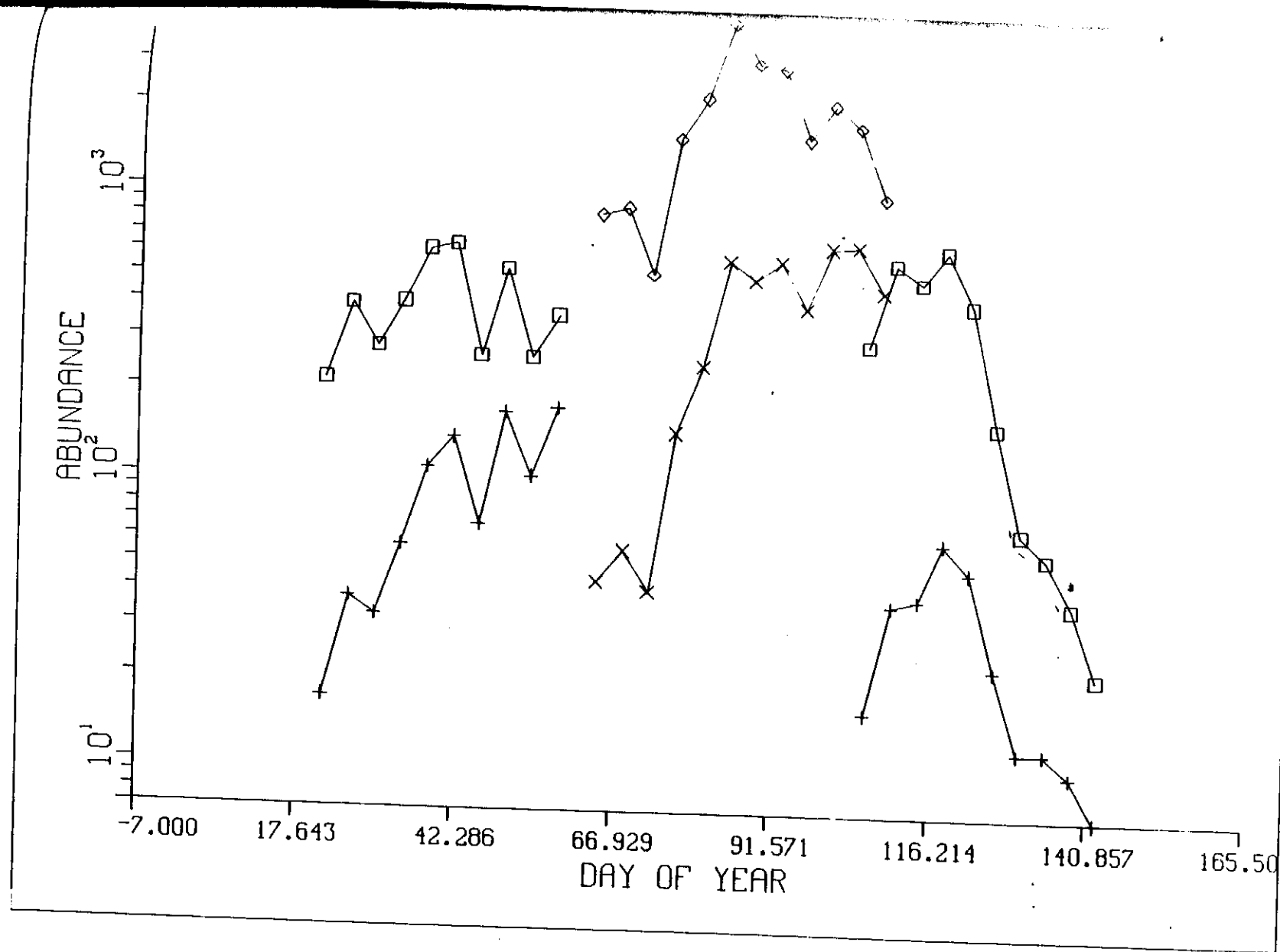


Figure 18. The age frequencies of Georges Bank haddock larvae for 1980 (X) were back-calculated to numbers at spawning (□) using a 0.05 mortality rate.

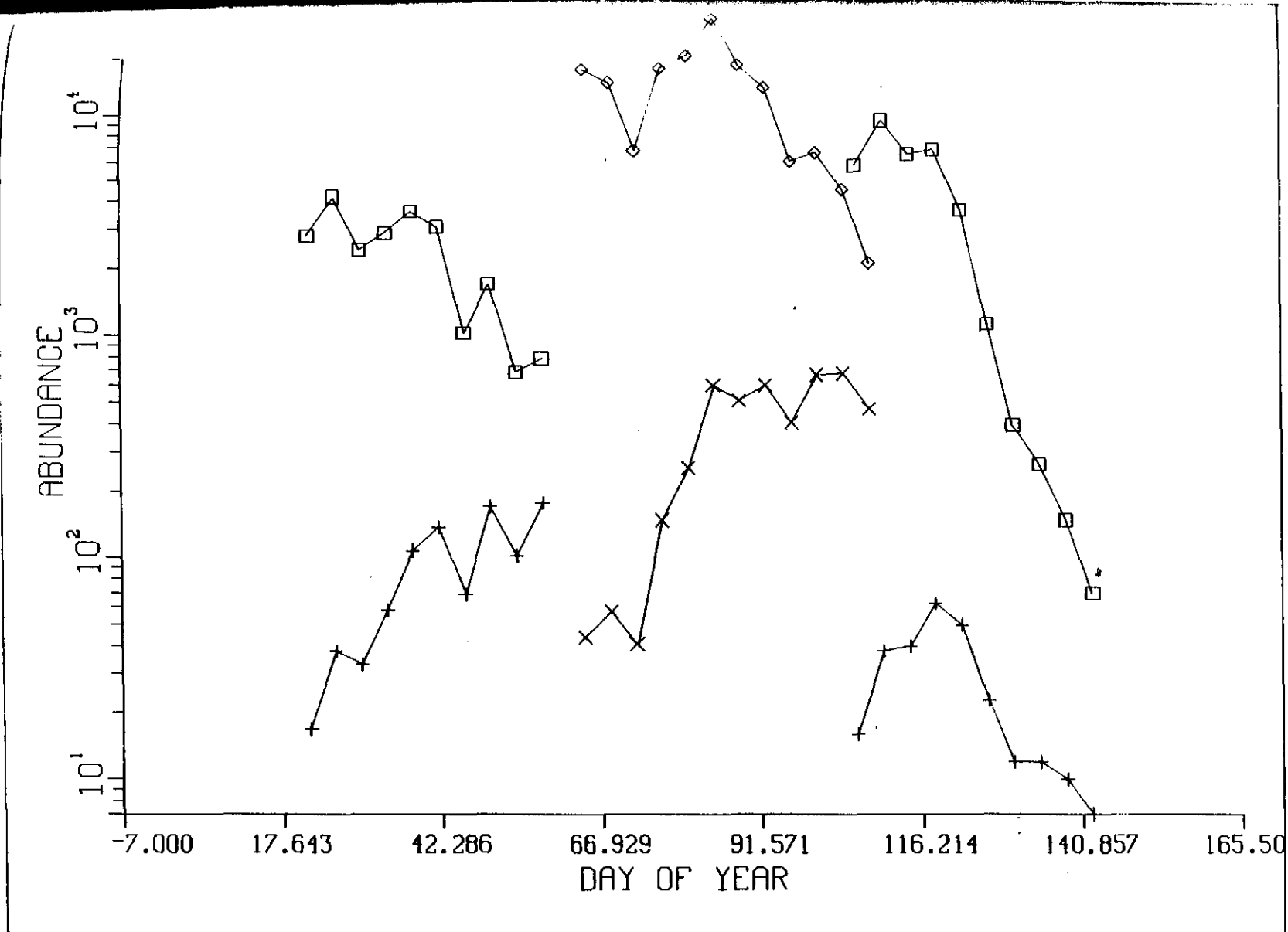


Figure 19. The age frequencies of Georges Bank haddock larvae for 1980 (X) were back-calculated to numbers at spawning (□) using a 0.10 mortality rate.

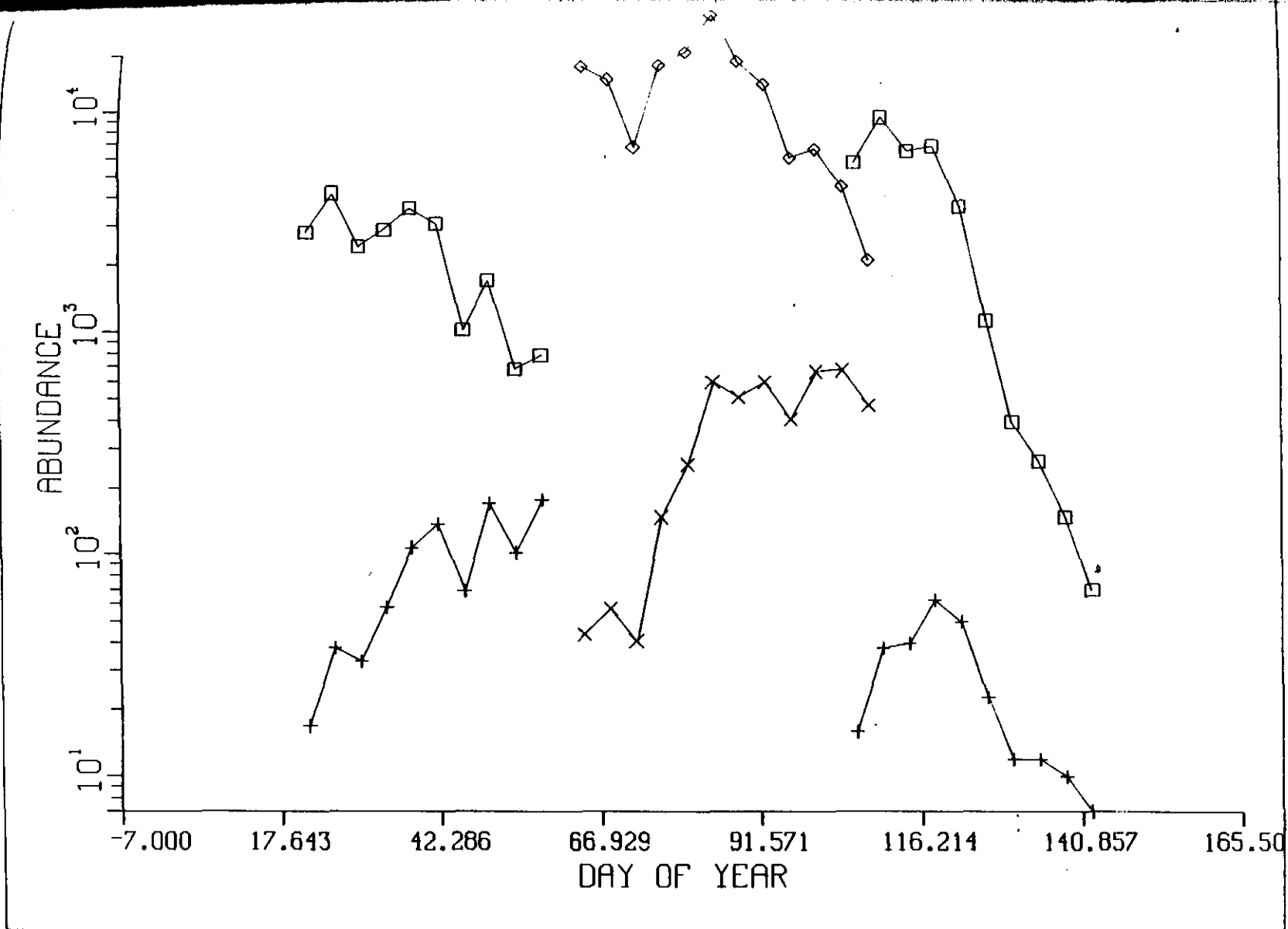


Figure 19. The age frequencies of Georges Bank haddock larvae for 1980 (X) were back-calculated to numbers at spawning (\square) using a 0.10 mortality rate.

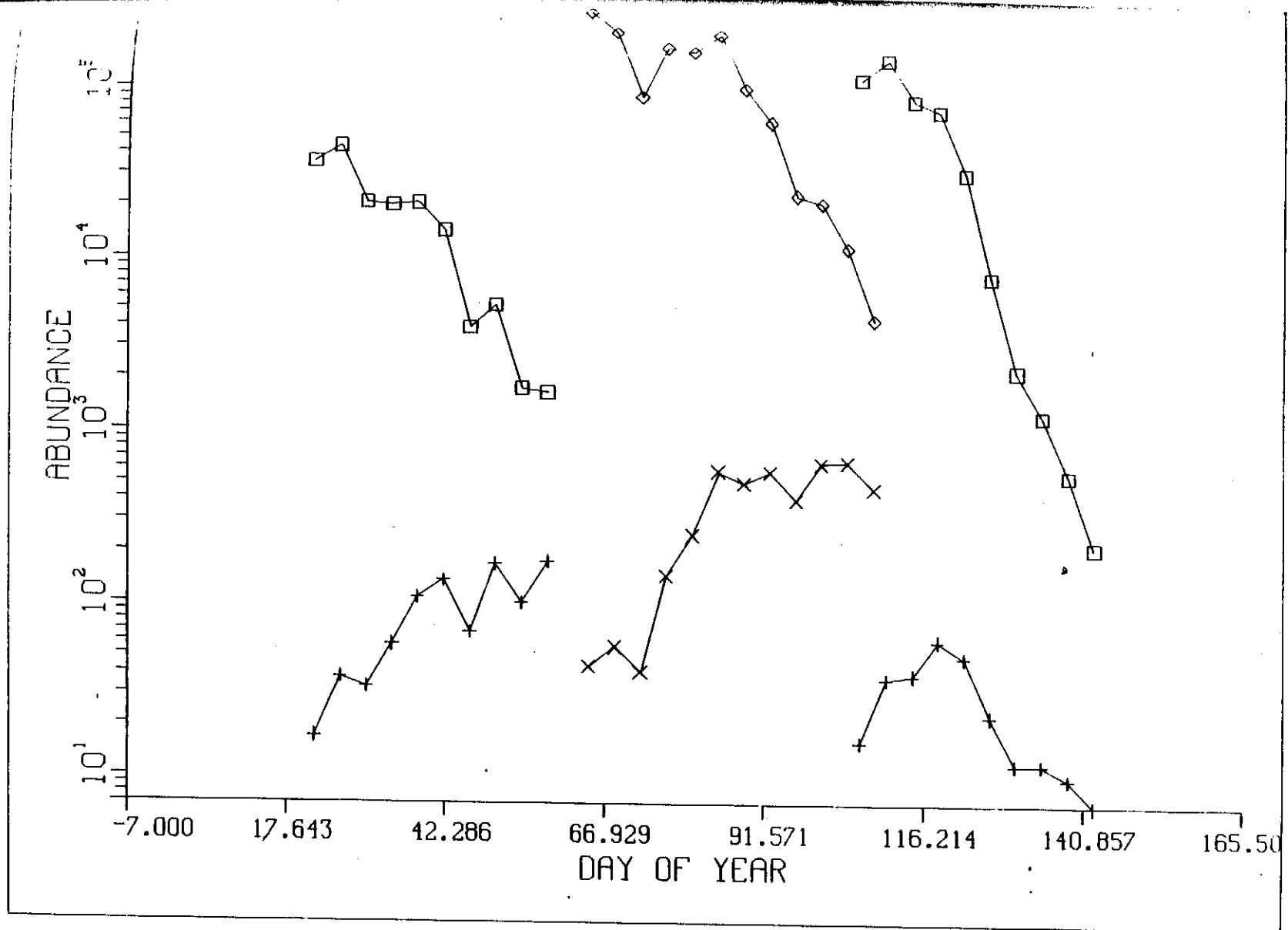


Figure 20. The age frequencies of Georges Bank haddock larvae for 1980 (X) were back-calculated to numbers at spawning (\square) using a 0.15 mortality rate.

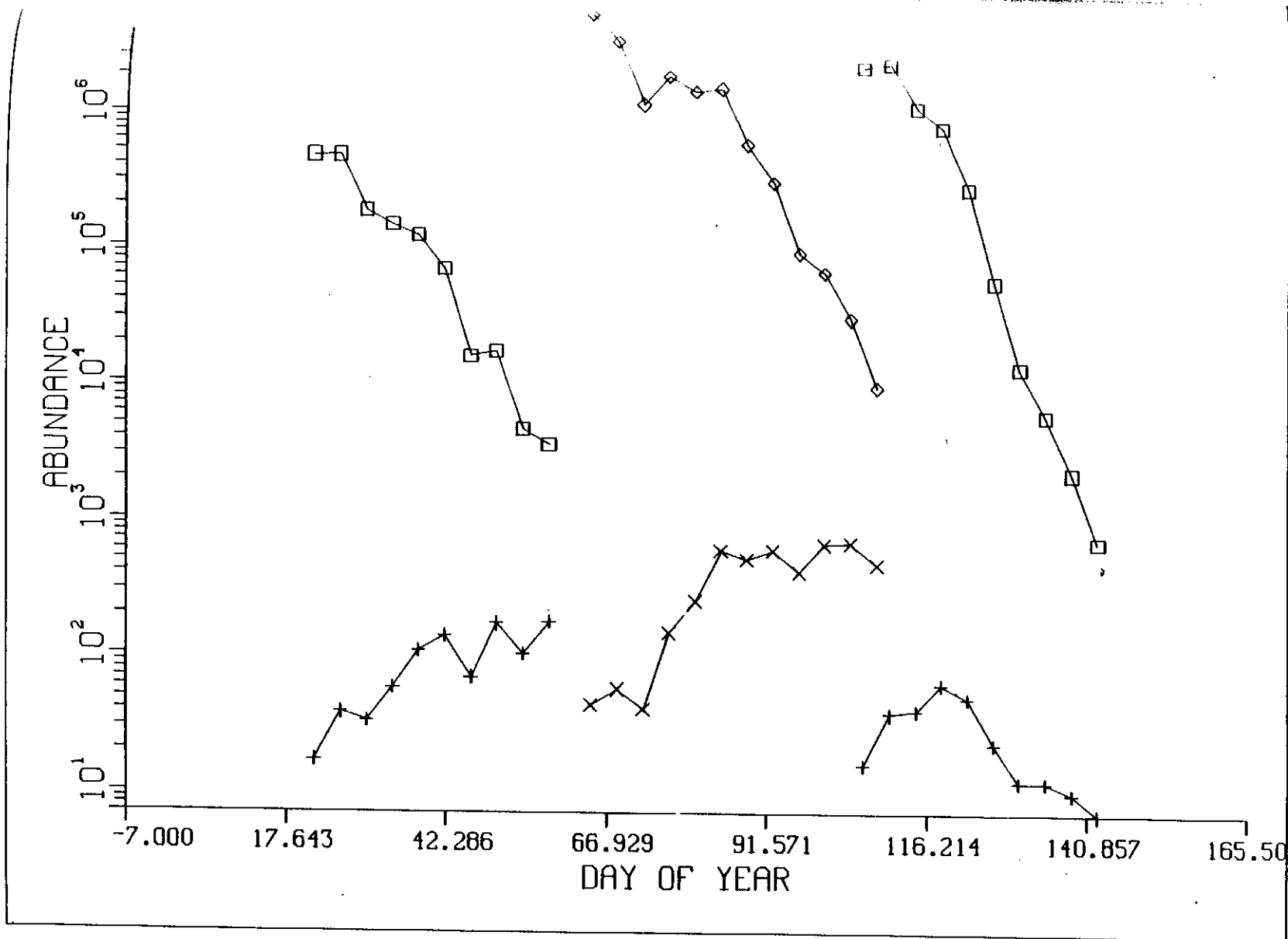


Figure 21. The age frequencies of Georges Bank haddock larvae for 1980 (X) were back-calculated to numbers at spawning (□) using a 0.20 mortality rate.

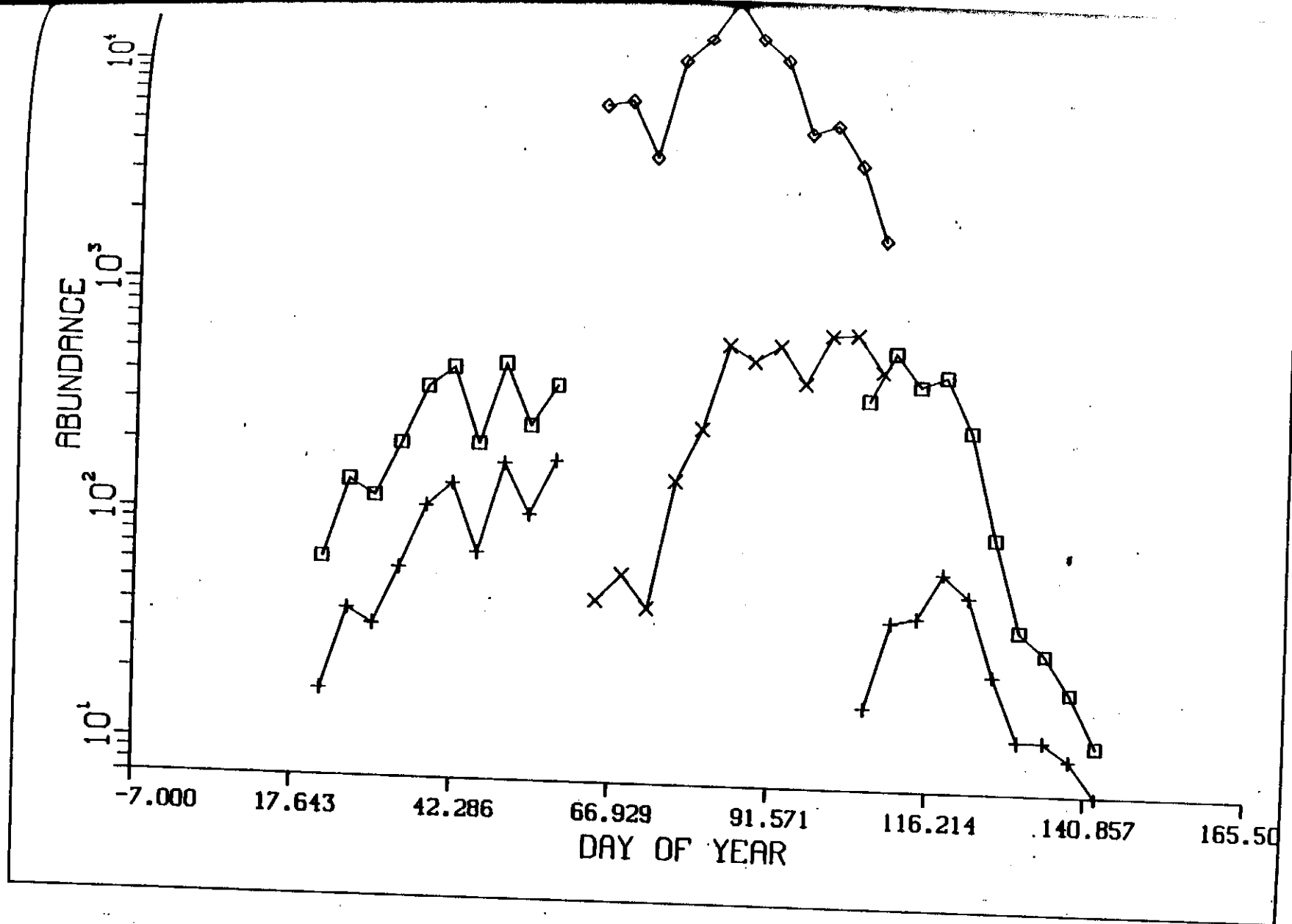


Figure 22. The age frequencies of Georges Bank haddock larvae for 1980 (X) were back-calculated to numbers at spawning (□). The mortality function was a normal curve with a maximum value of 0.10 at 100 Julian days and a standard deviation of 30 days.

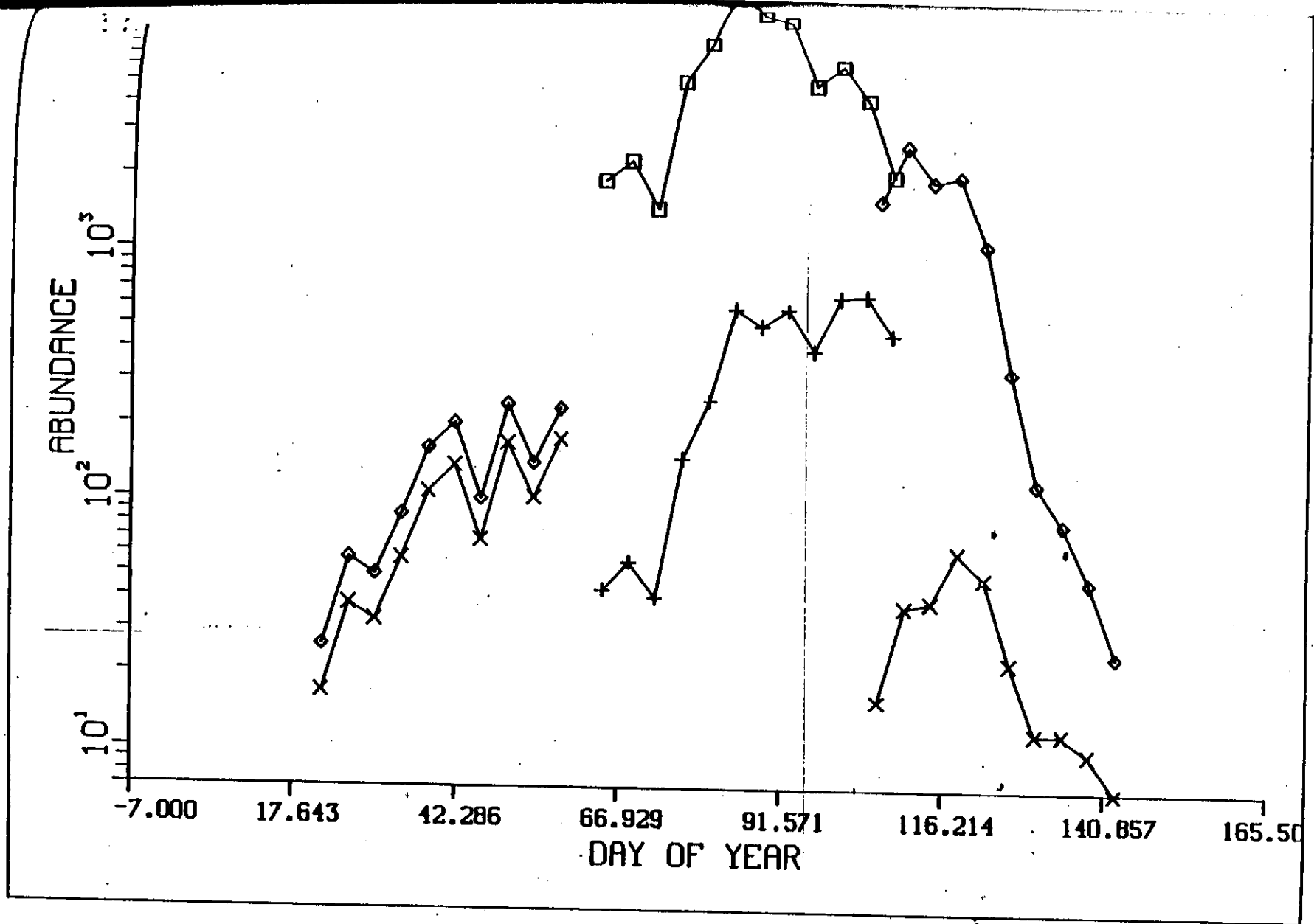


Figure 23. The age frequencies of Georges Bank haddock larvae for 1980 (X) were back-calculated to numbers at spawning (□). The mortality function was a normal curve with a maximum value of 0.10 at 120 Julian days and a standard deviation of 30 days.

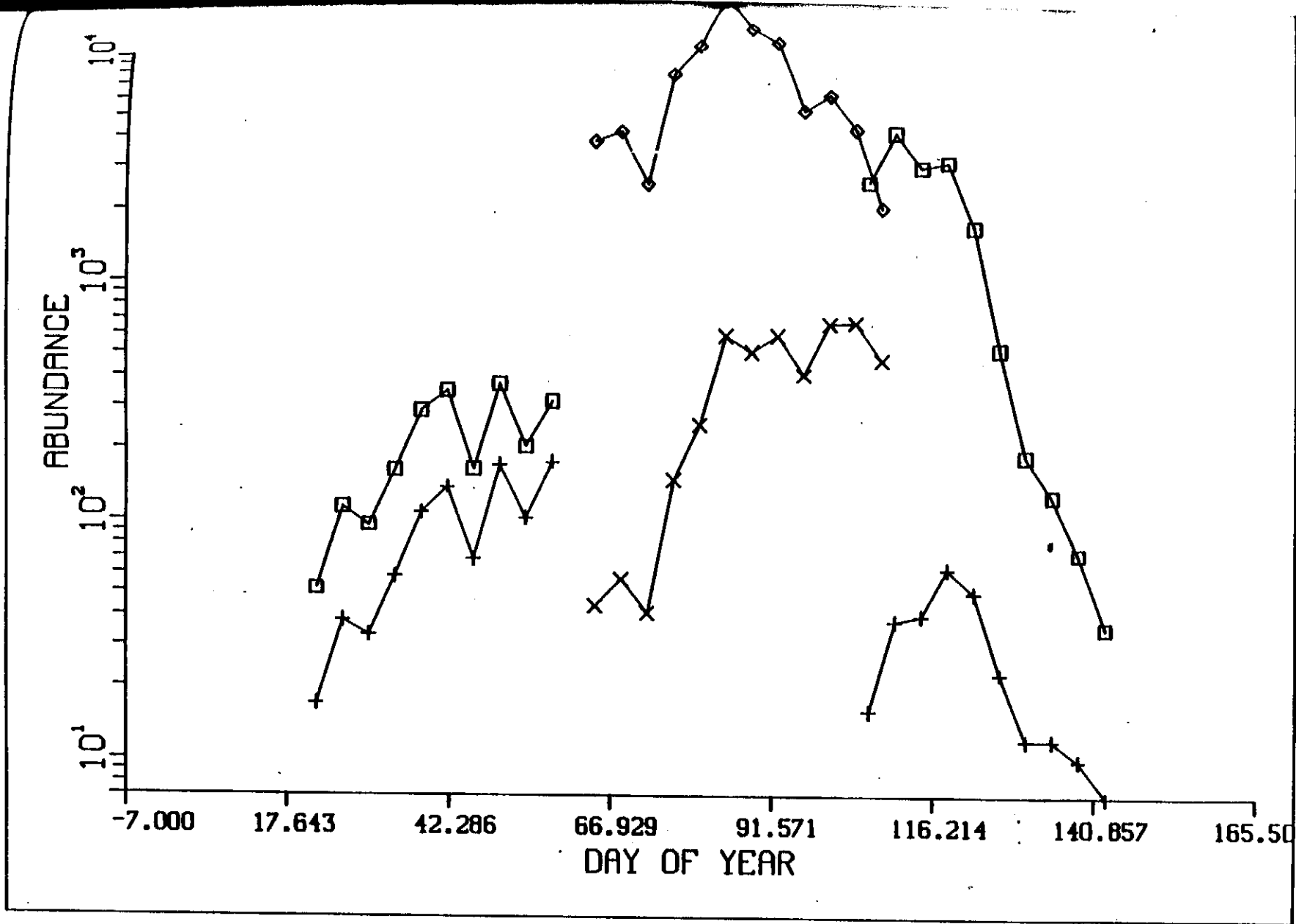


Figure 24. The age frequencies of Georges Bank haddock larvae for 1980 (X) were back-calculated to numbers at spawning (□). The mortality function was a normal curve with a maximum value of 0.10 at 120 Julian days and a standard deviation of 40 days.

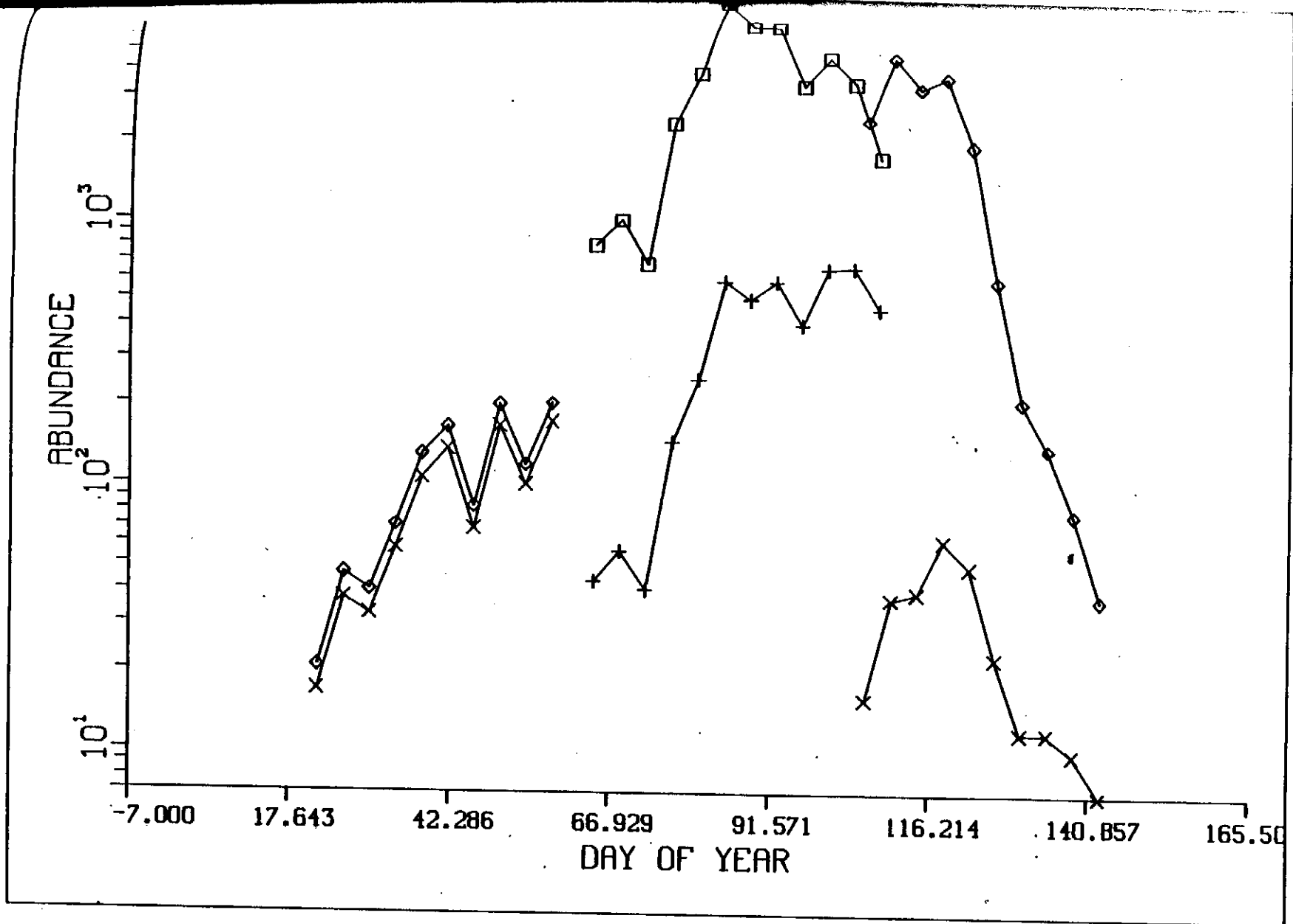


Figure 25. The age frequencies of Georges Bank haddock larvae for 1980 (X) were back-calculated to numbers at spawning (□). The mortality function was a normal curve with a maximum value of 0.10 at 130 Julian days and a standard deviation of 30 days.

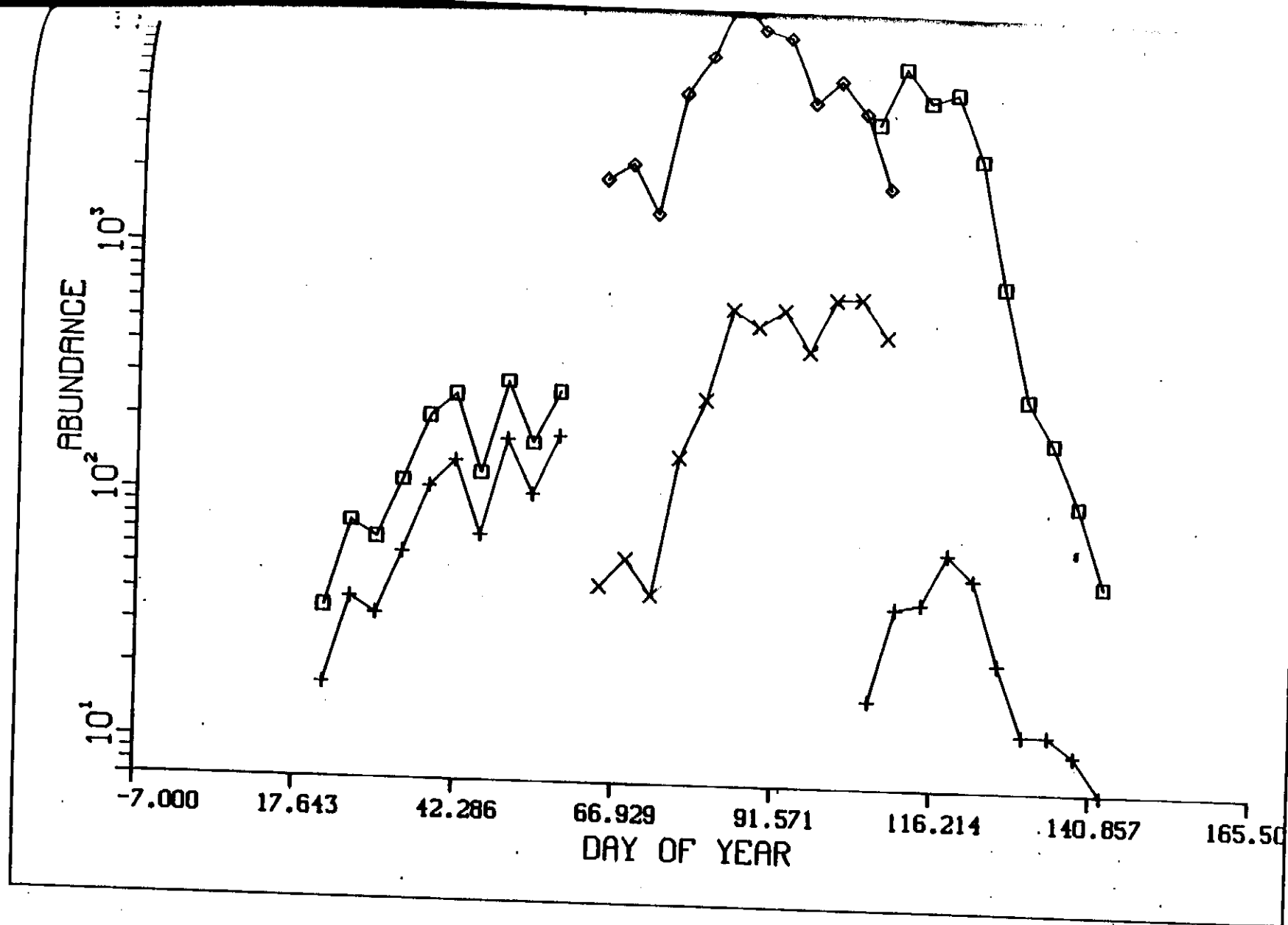


Figure 26. The age frequencies of Georges Bank haddock larvae for 1980 (X) were back-calculated to numbers at spawning (□). The mortality function was a normal curve with a maximum value of 0.10 at 130 Julian days and a standard deviation of 40 days.

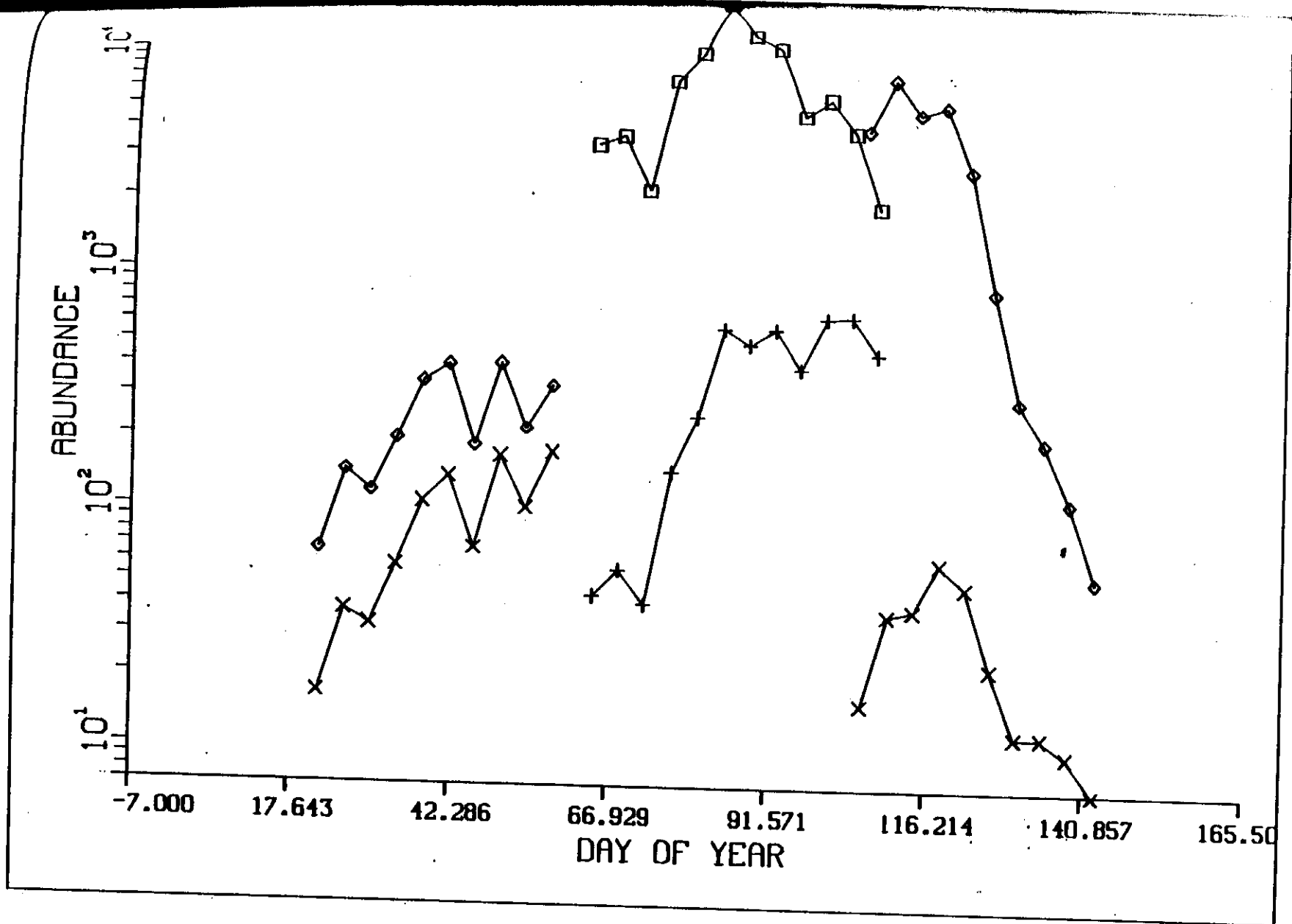


Figure 27. The age frequencies of Georges Bank haddock larvae for 1980 (X) were back-calculated to numbers at spawning (\square). The mortality function was a normal curve with a maximum value of 0.10 at 130 Julian days and a standard deviation of 50 days.

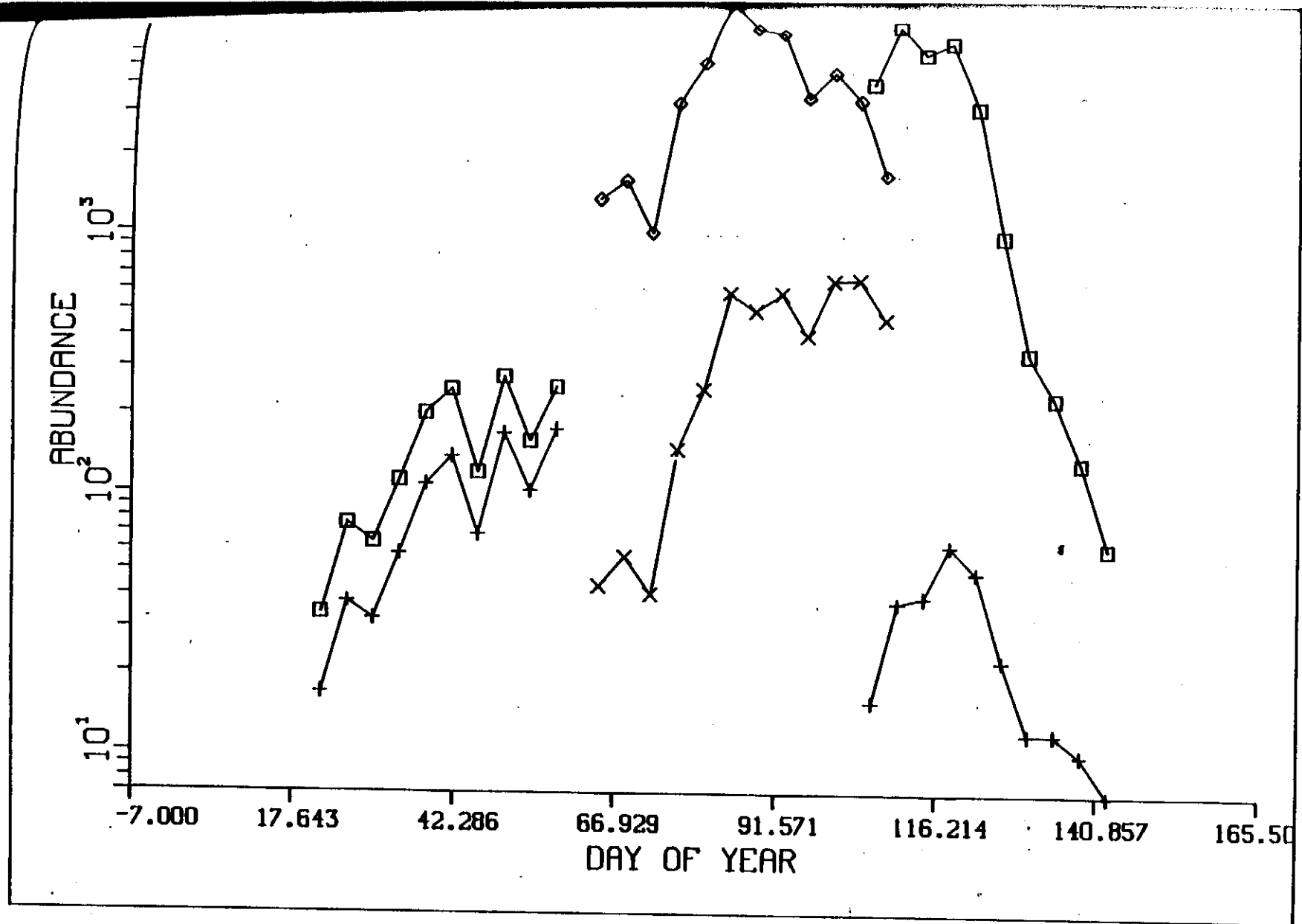


Figure 28. The age frequencies of Georges Bank haddock larvae for 1980 (X) were back-calculated to numbers at spawning (□). The mortality function was a normal curve with a maximum value of 0.10 at 140 Julian days and a standard deviation of 45 days.

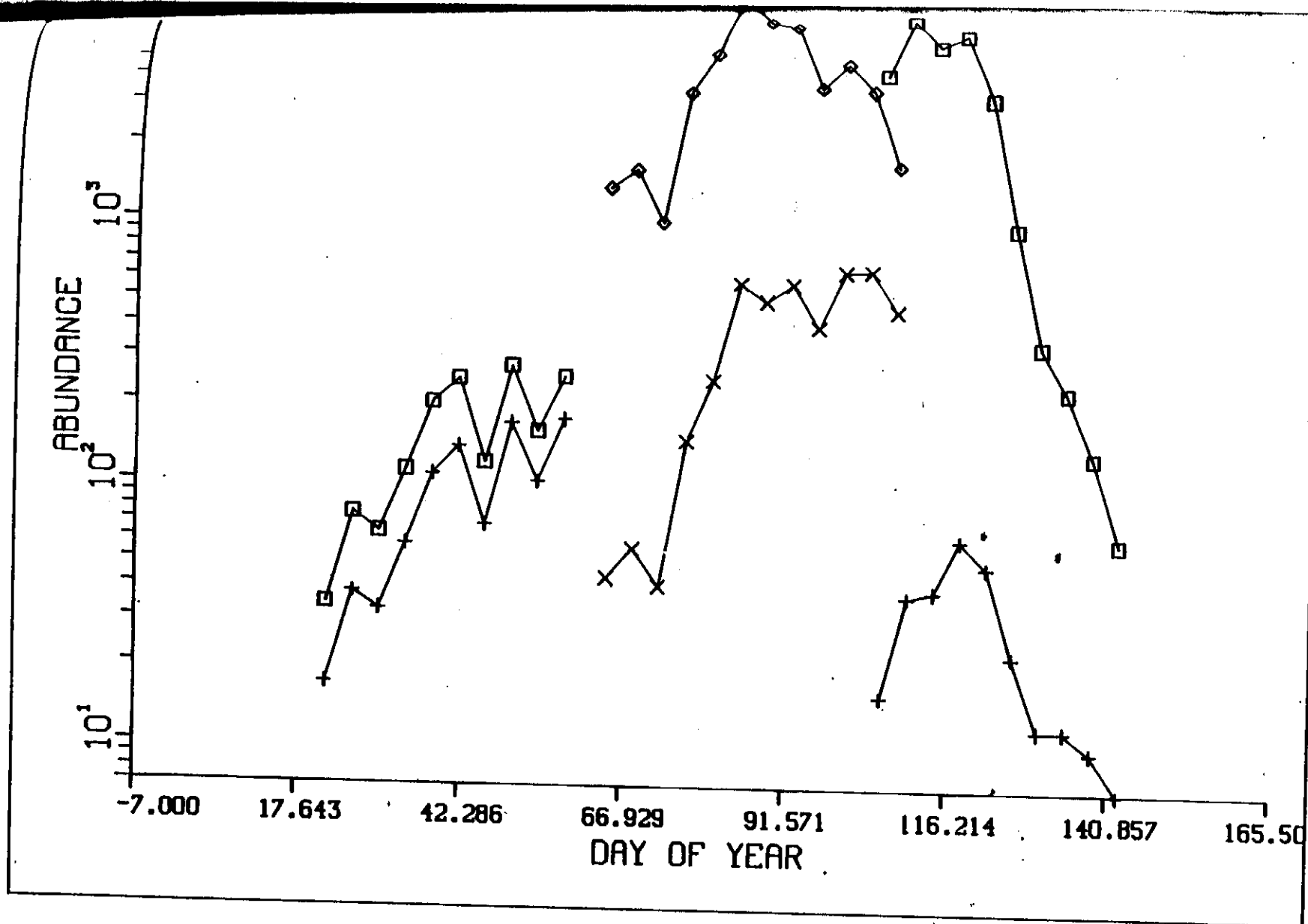


Figure 29. The age frequencies of Georges Bank haddock larvae for 1980 (X) were back-calculated to numbers at spawning (□). The mortality function was a normal curve with a maximum value of 0.10 at 150 Julian days and a standard deviation of 30 days.

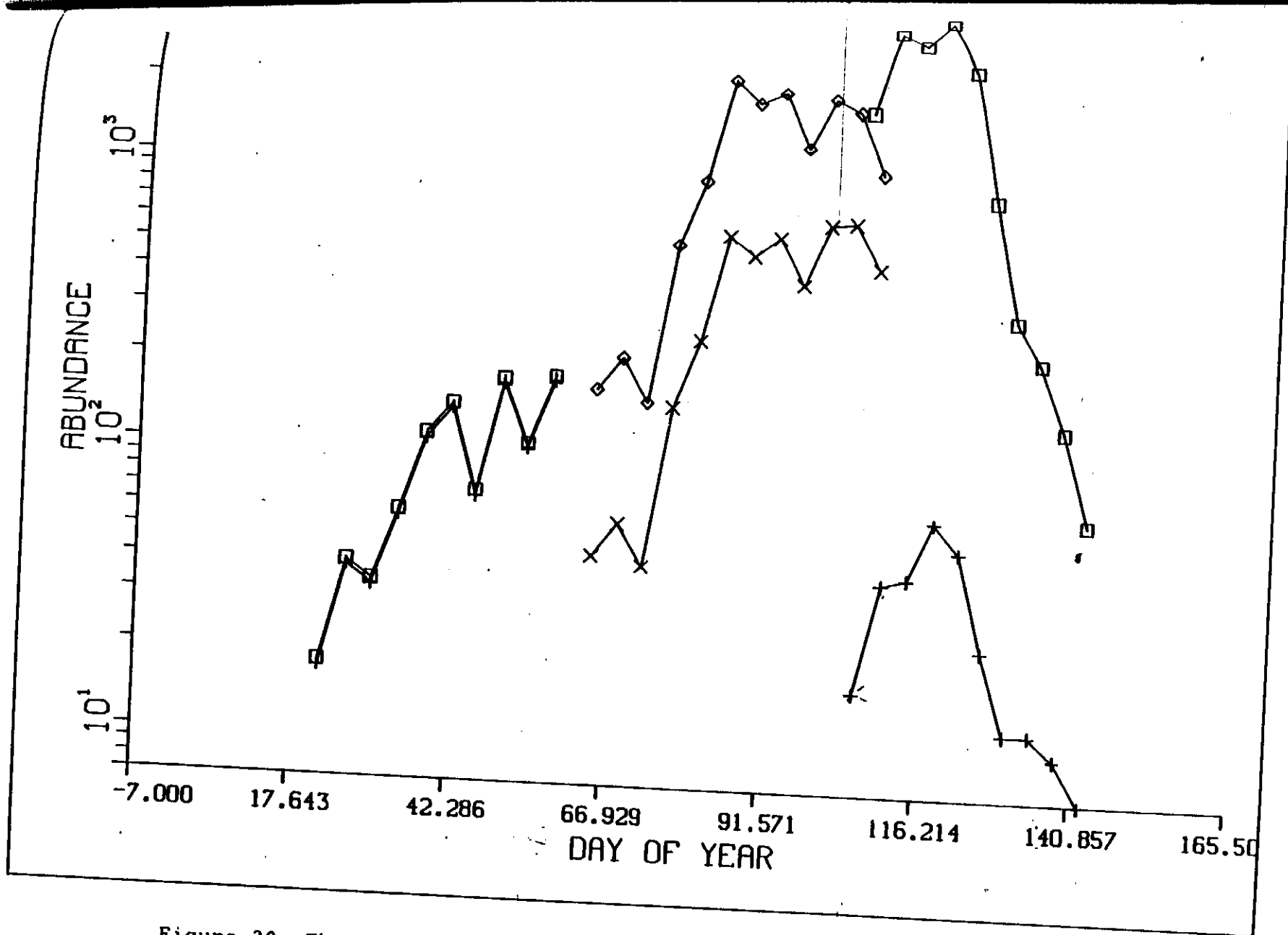


Figure 30. The age frequencies of Georges Bank haddock larvae for 1980 (X) were back-calculated to numbers at spawning (\square). The mortality function was a normal curve with a maximum value of 0.10 at 150 Julian days and a standard deviation of 40 days.

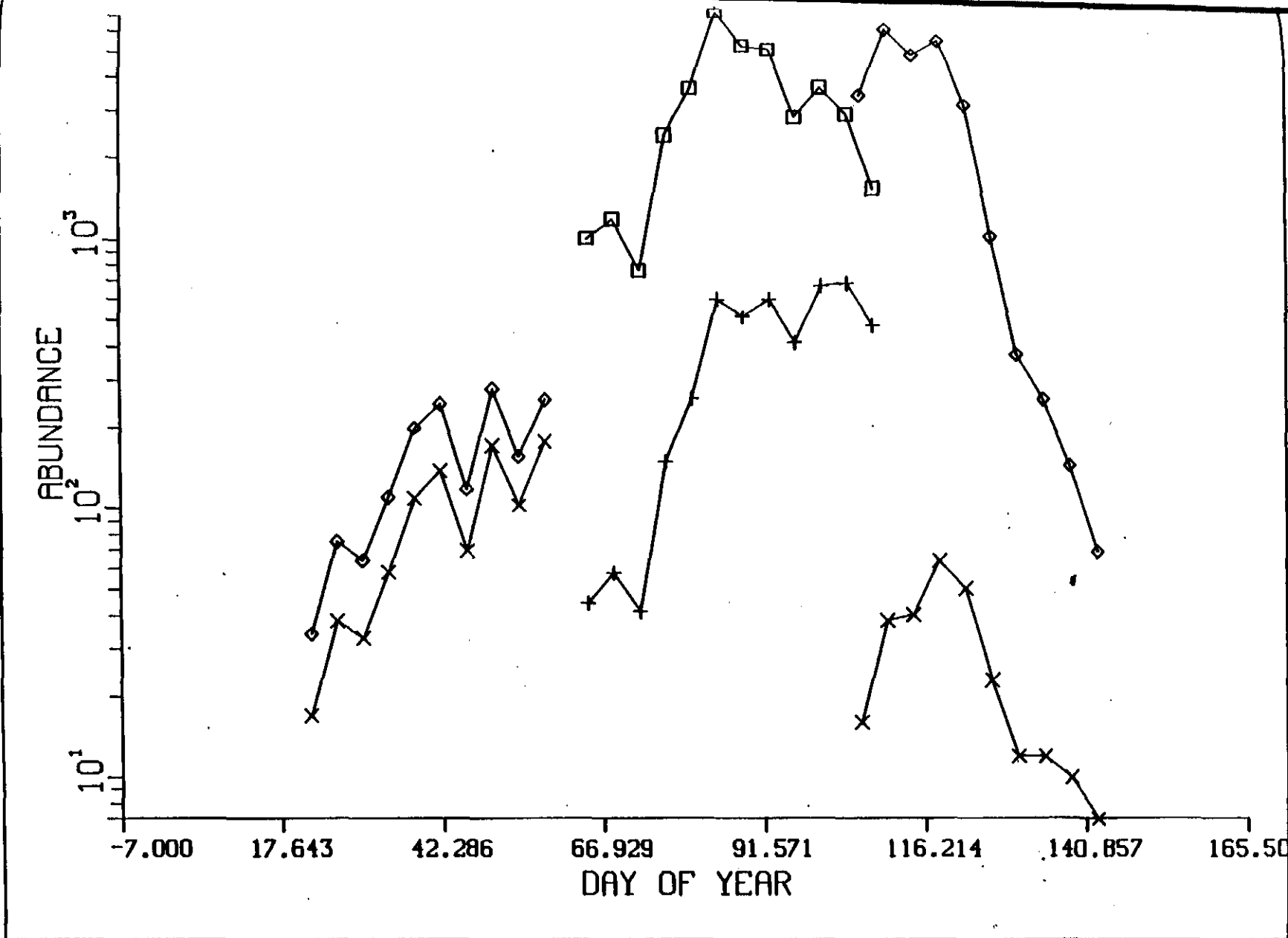


Figure 31. The age frequencies of Georges Bank haddock larvae for 1980 (X) were back-calculated to numbers at spawning (□). The mortality function was a normal curve with a maximum value of 0.10 at 150 Julian days and a standard deviation of 50 days.

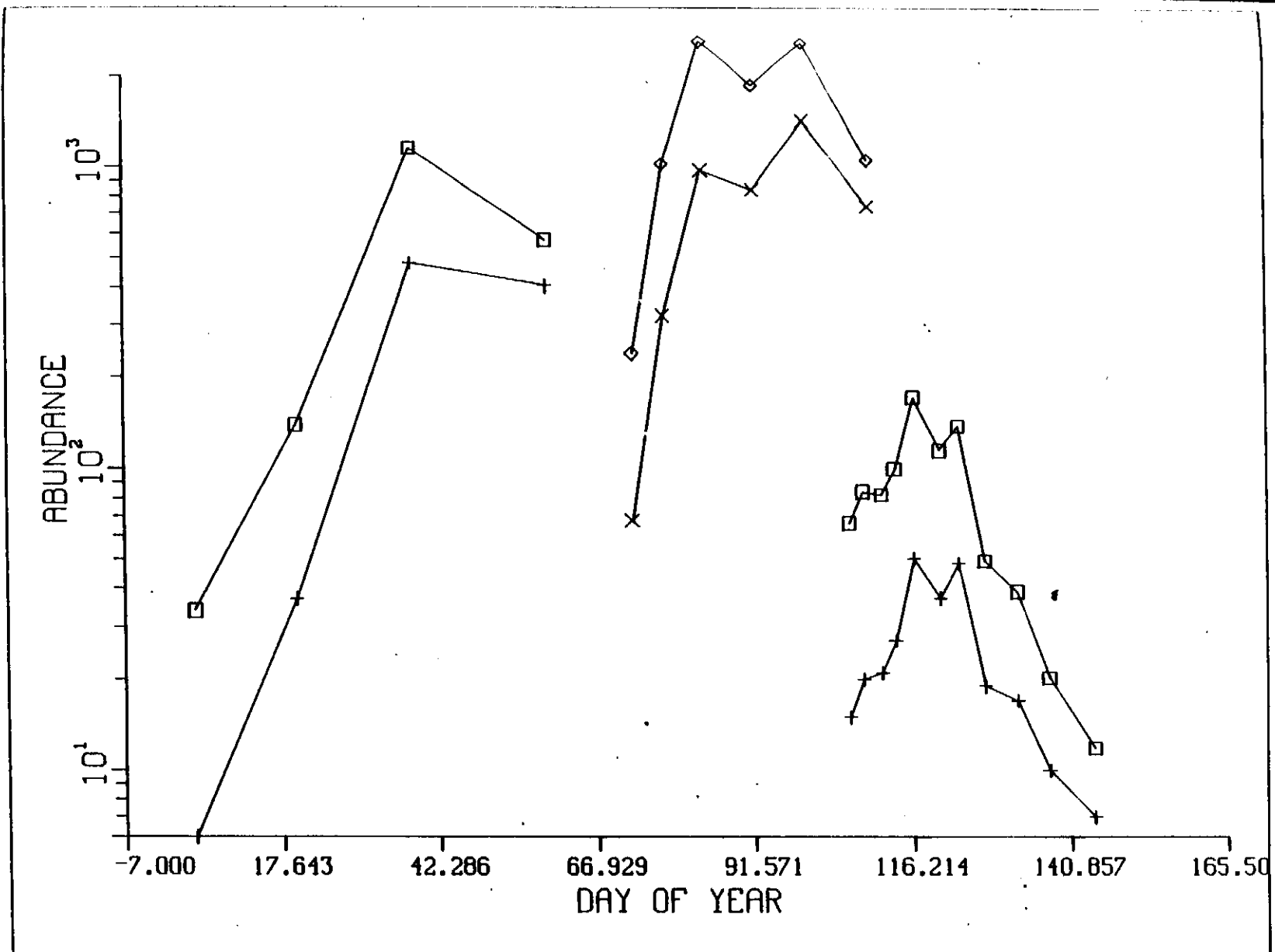


Figure 32. Length frequencies of Georges Bank haddock larvae for 1980 were converted to ages using an average water temperature for each of the three surveys (X). The ages were back-calculated to numbers at spawning (□) using a 0.025 mortality rate.

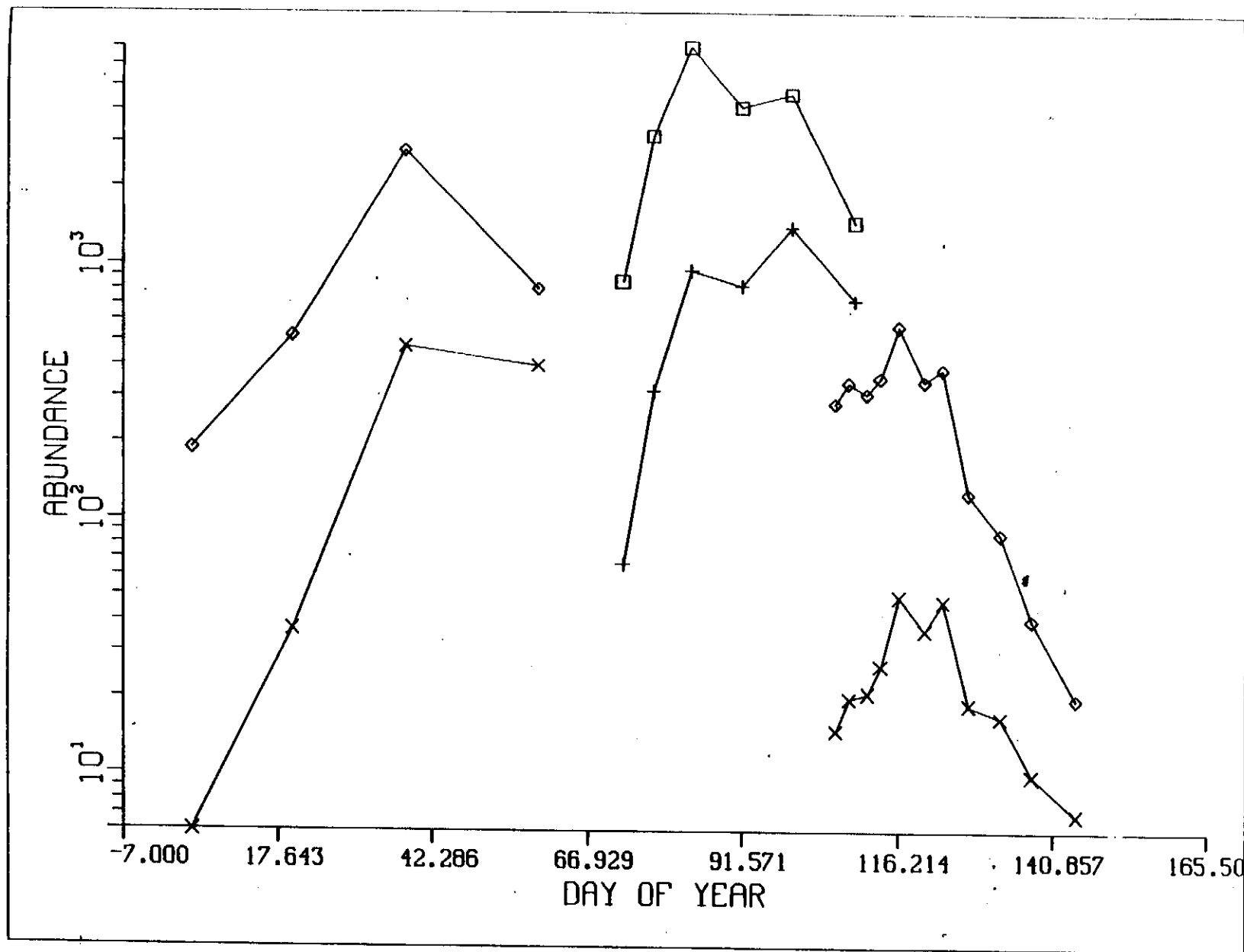


Figure 33. Length frequencies of Georges Bank haddock larvae for 1980 were converted to ages using an average water temperature for each of the three surveys (X). The ages were back-calculated to numbers at spawning (\square) using a 0.05 mortality rate.

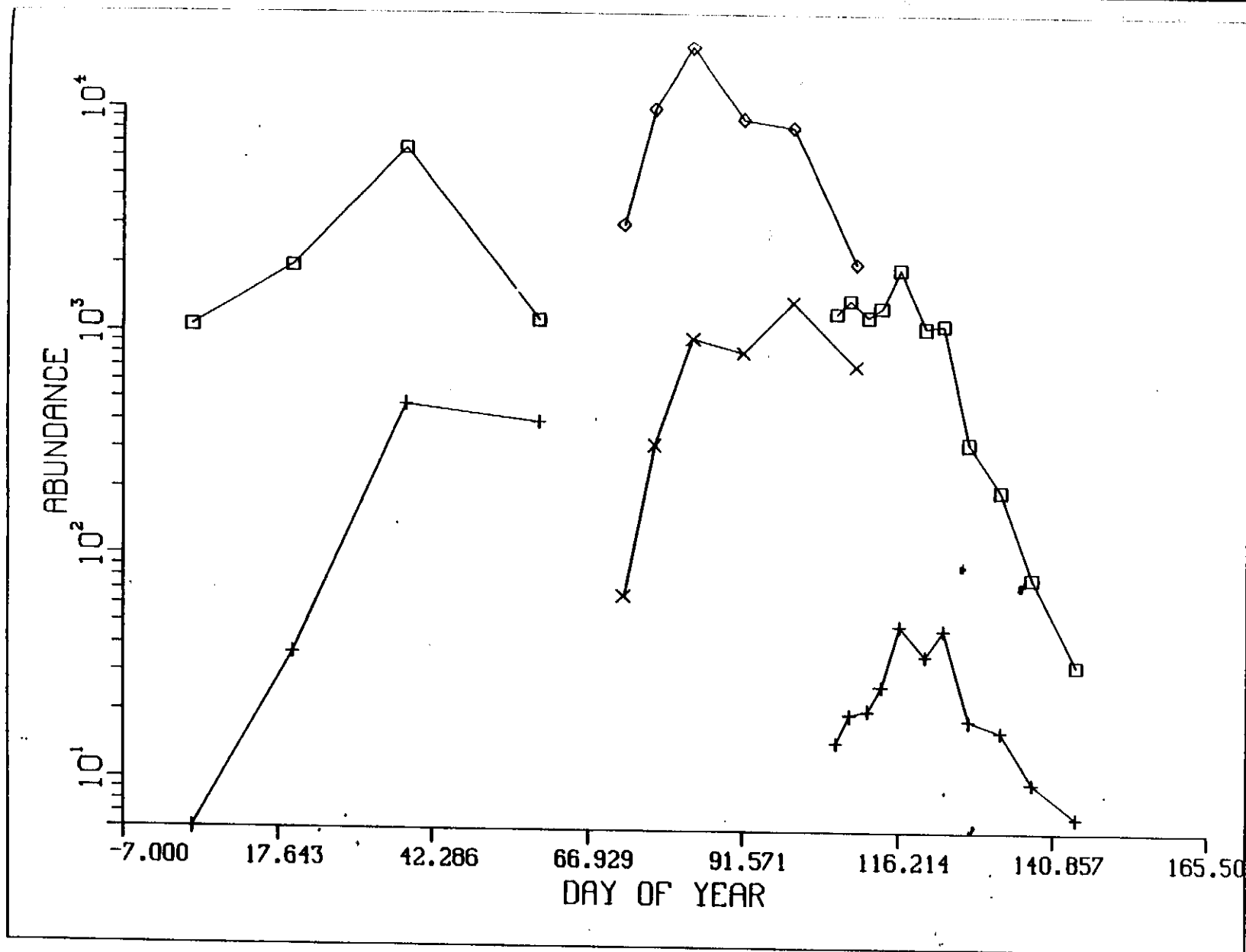


Figure 34. Length frequencies of Georges Bank haddock larvae for 1980 were converted to ages using an average water temperature for each of the three surveys (X). The ages were back-calculated to numbers at spawning (\square) using a 0.075 mortality rate.

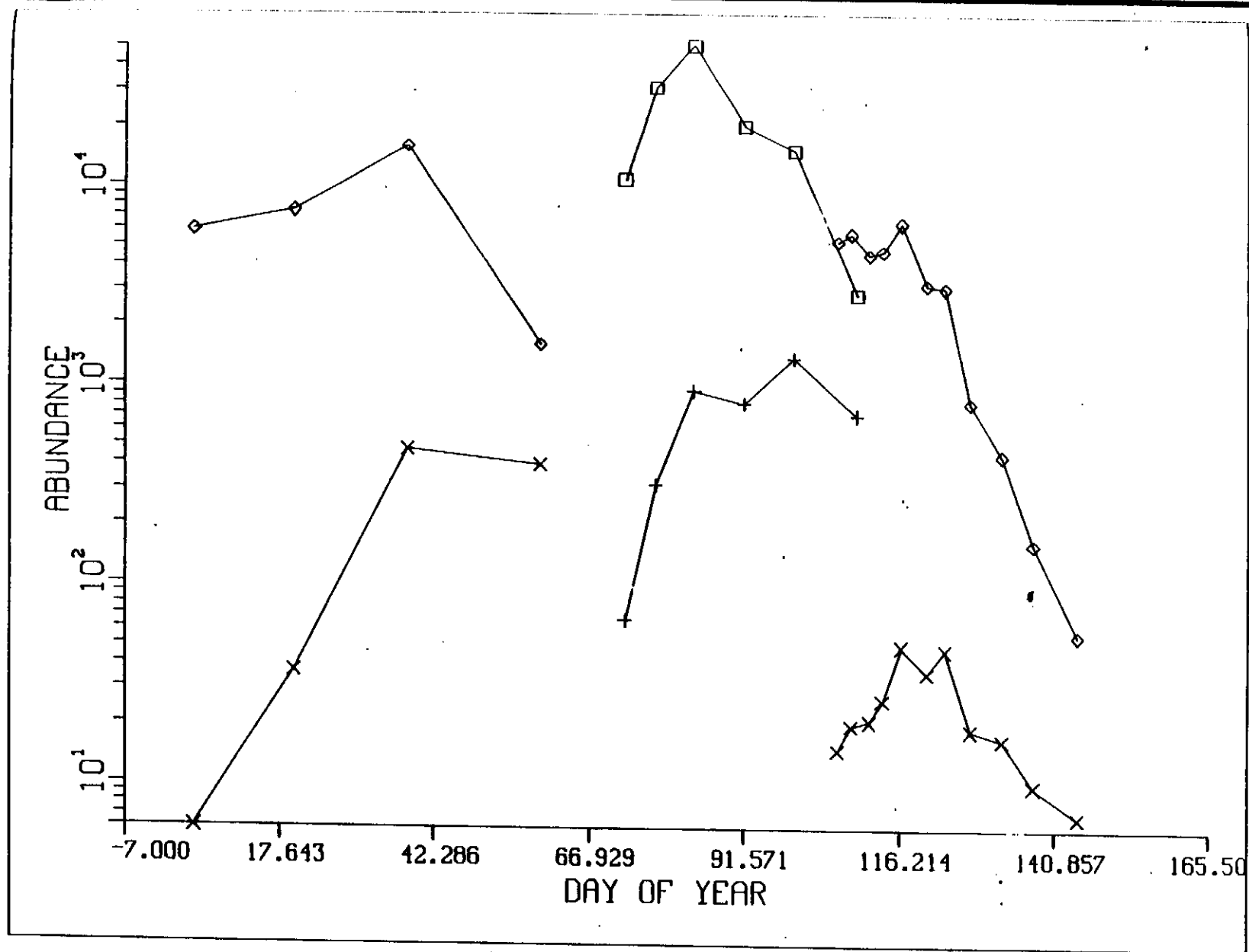


Figure 35. Length frequencies of Georges Bank haddock larvae for 1980 were converted to ages using an average water temperature for each of the three surveys (X). The ages were back-calculated to numbers at spawning (□) using a 0.10 mortality rate.

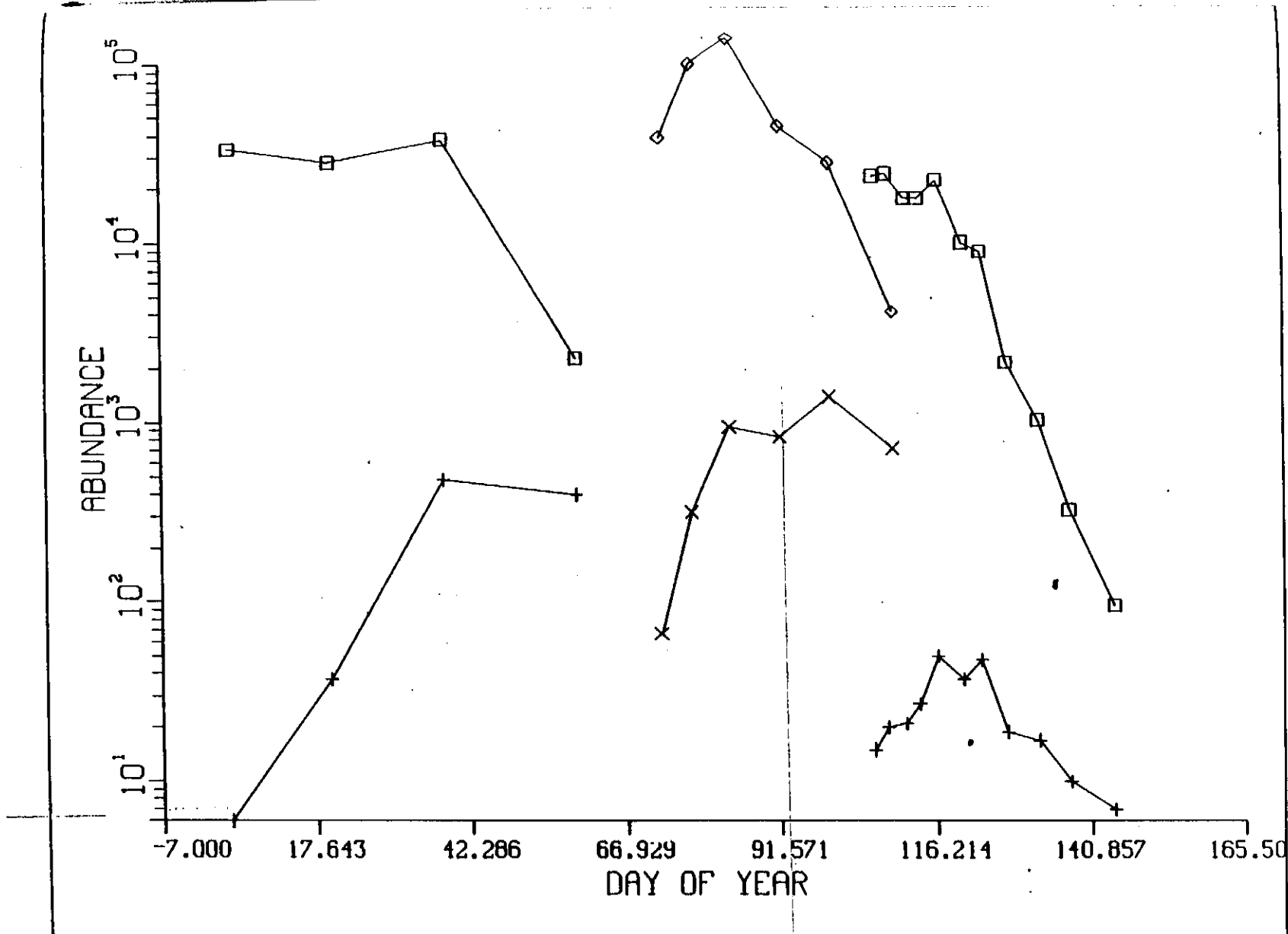


Figure 36. Length frequencies of Georges Bank haddock larvae for 1980 were converted to ages using an average water temperature for each of the three surveys (X). The ages were back-calculated to numbers at spawning (\square) using a 0.125 mortality rate.

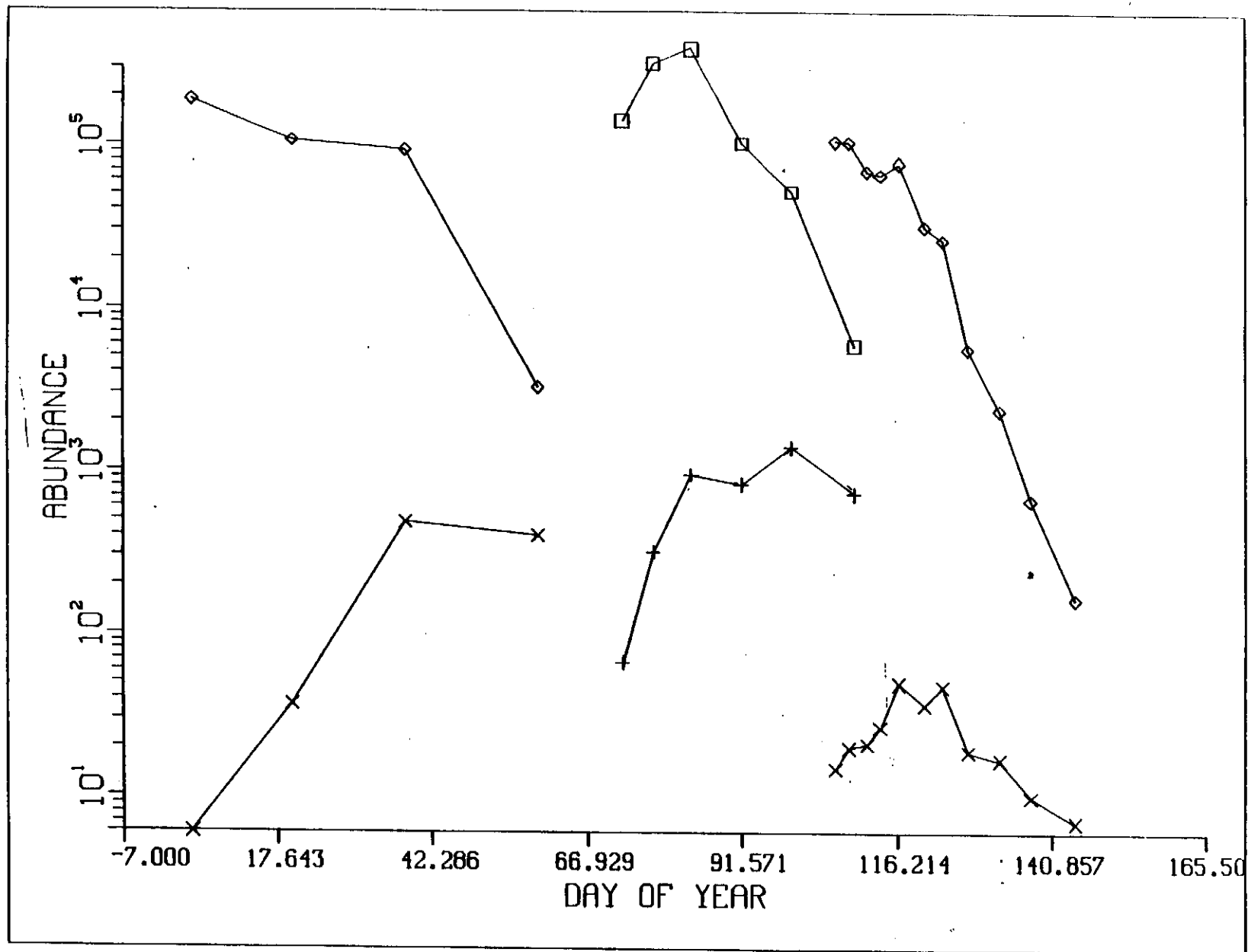


Figure 37. Length frequencies of Georges Bank haddock larvae for 1980 were converted to ages using an average water temperature for each of the three surveys (X). The ages were back-calculated to numbers at spawning (□) using a 0.15 mortality rate.

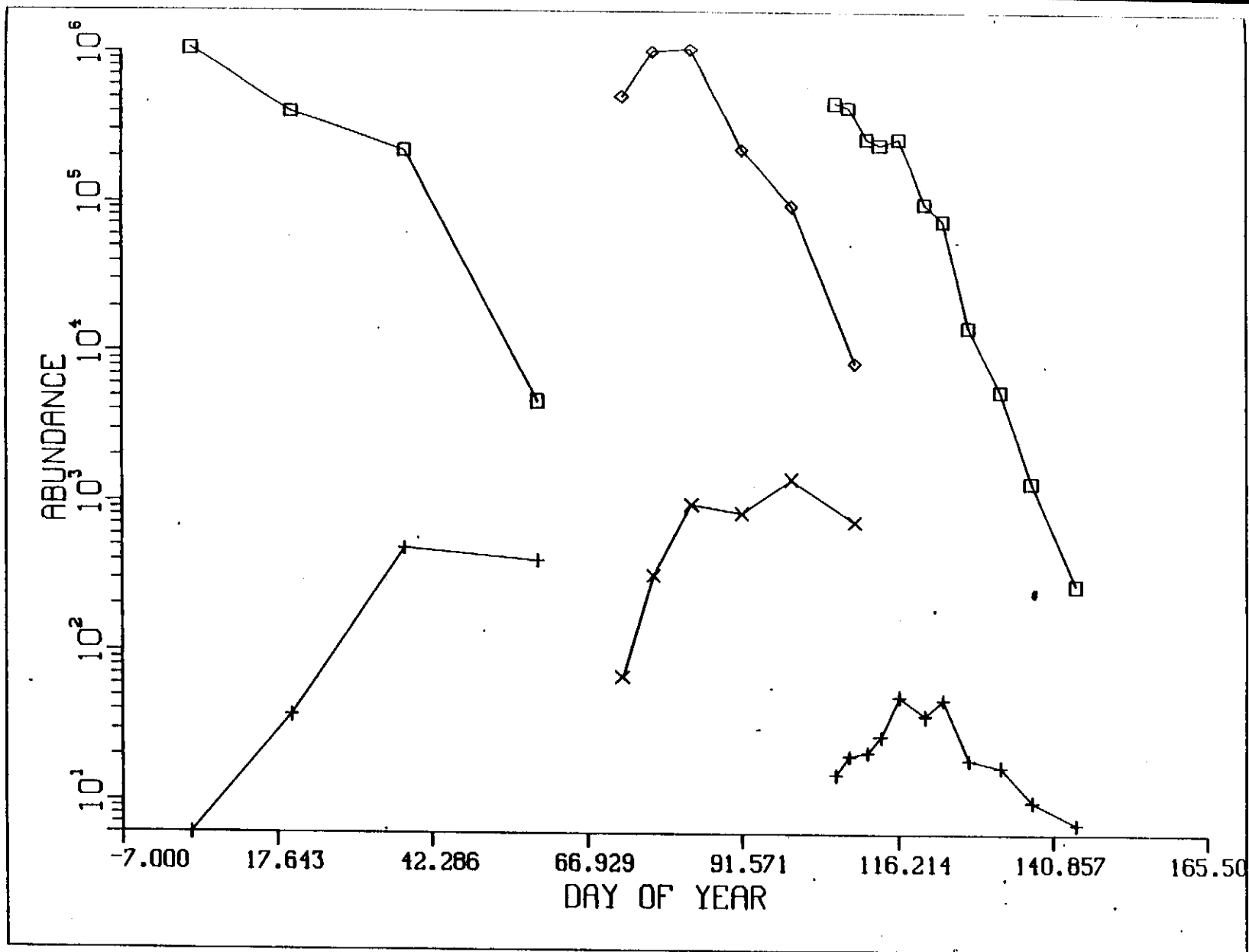


Figure 38. Length frequencies of Georges Bank haddock larvae for 1980 were converted to ages using an average water temperature for each of the three surveys (X). The ages were back-calculated to numbers at spawning (□) using a 0.175 mortality rate.

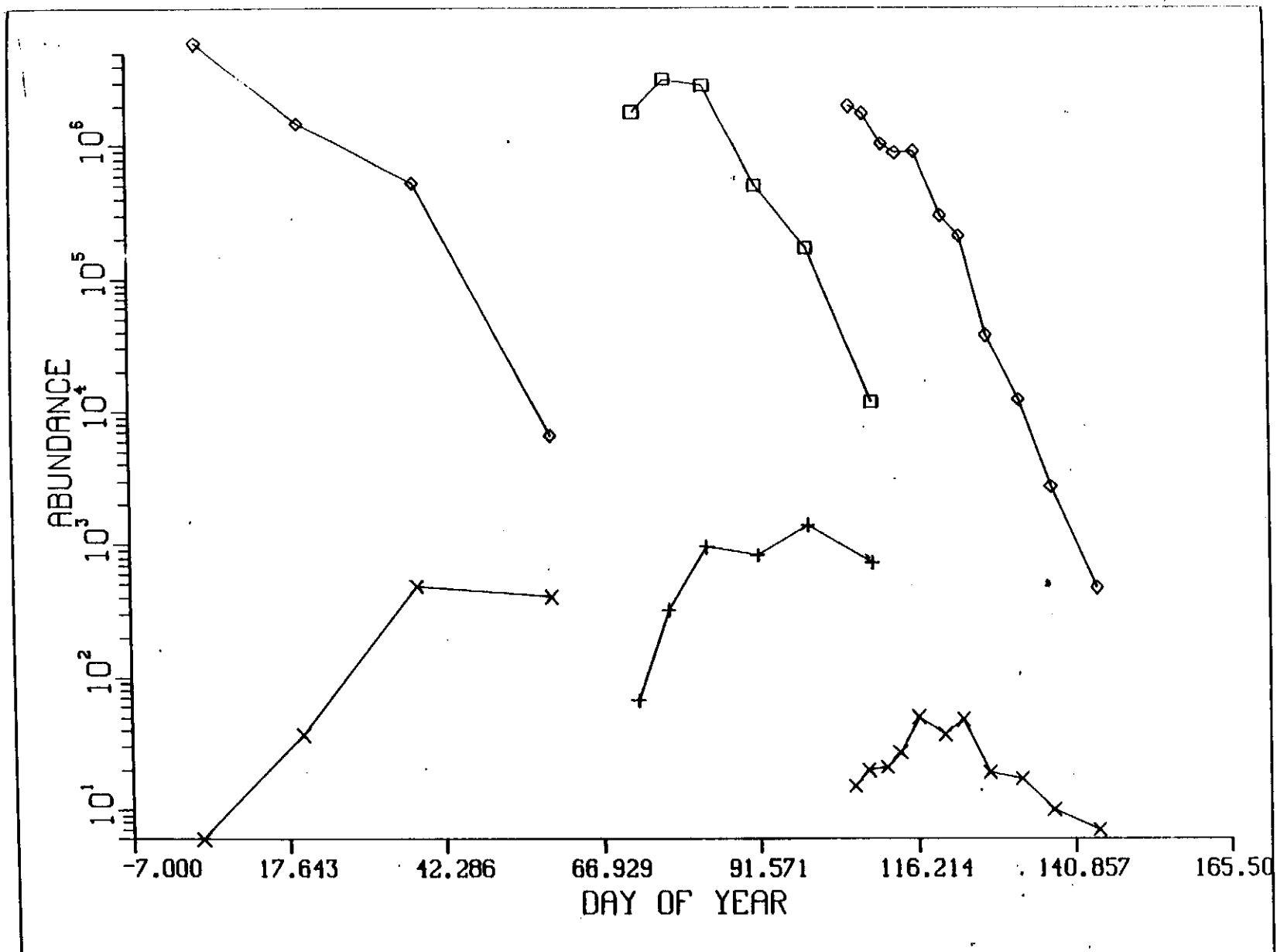


Figure 39. Length frequencies of Georges Bank haddock larvae for 1980 were converted to ages using an average water temperature for each of the three surveys (X). The ages were back-calculated to numbers at spawning (□) using a 0.20 mortality rate.

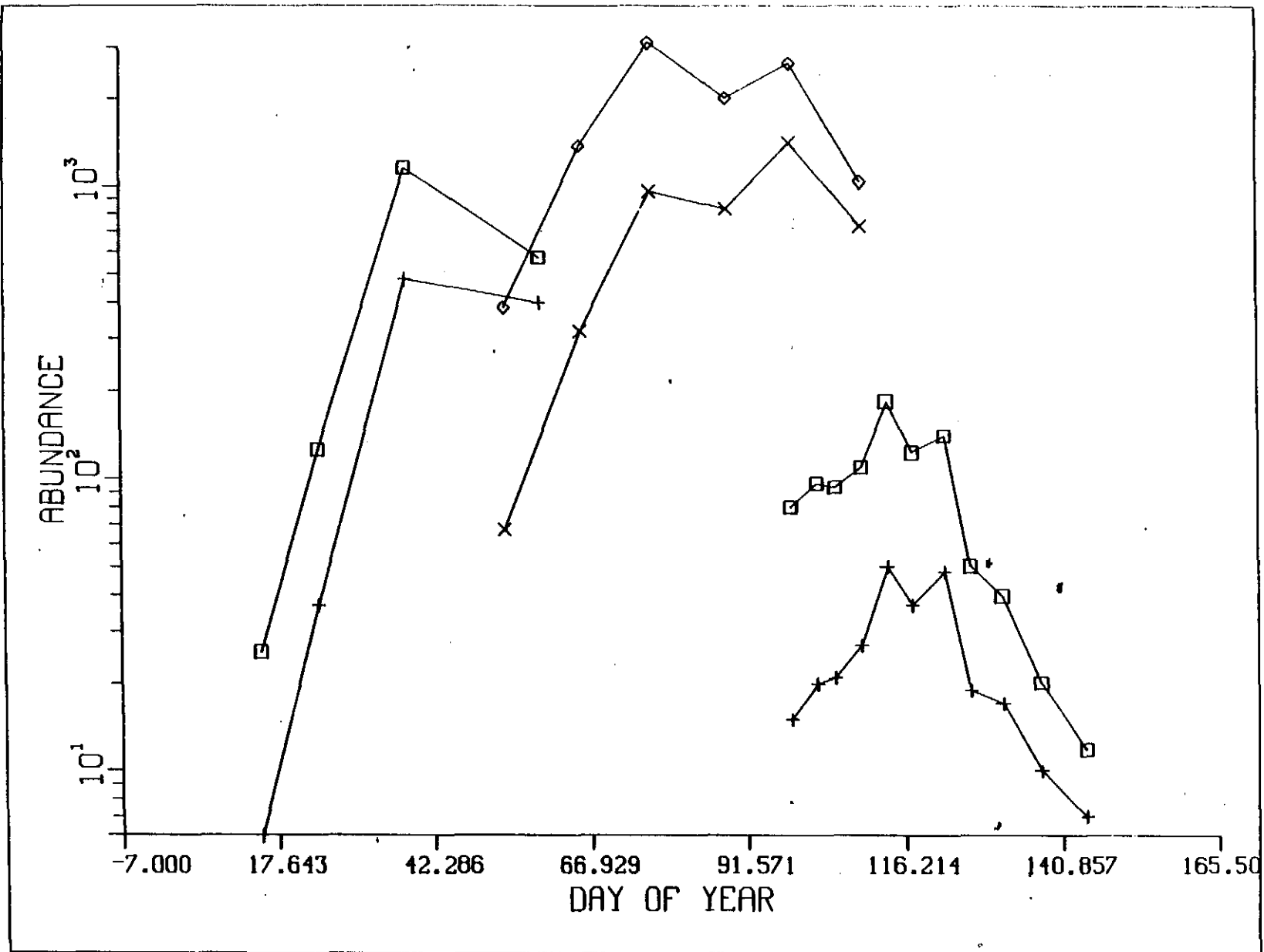


Figure 40. Length frequencies of Georges Bank haddock larvae for 1980 were converted to ages using average daily water temperatures during the life of the larva (X). The ages were back-calculated to numbers at spawning (□) using a 0.025 mortality rate.

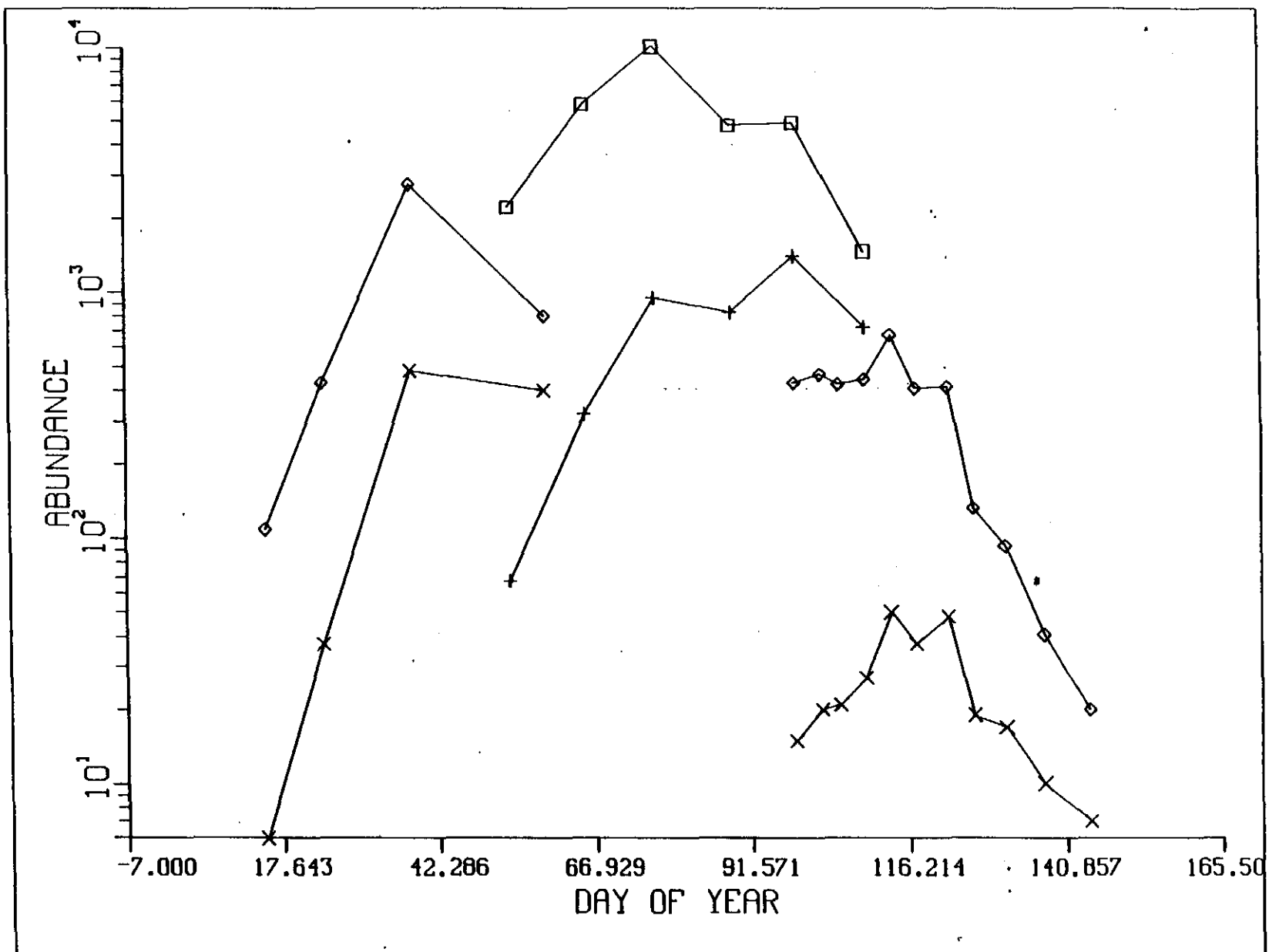


Figure 41. Length frequencies of Georges Bank haddock larvae for 1980 were converted to ages using average daily water temperatures during the life of the larva (×). The ages were back-calculated to numbers at spawning (□) using a 0.05 mortality rate.

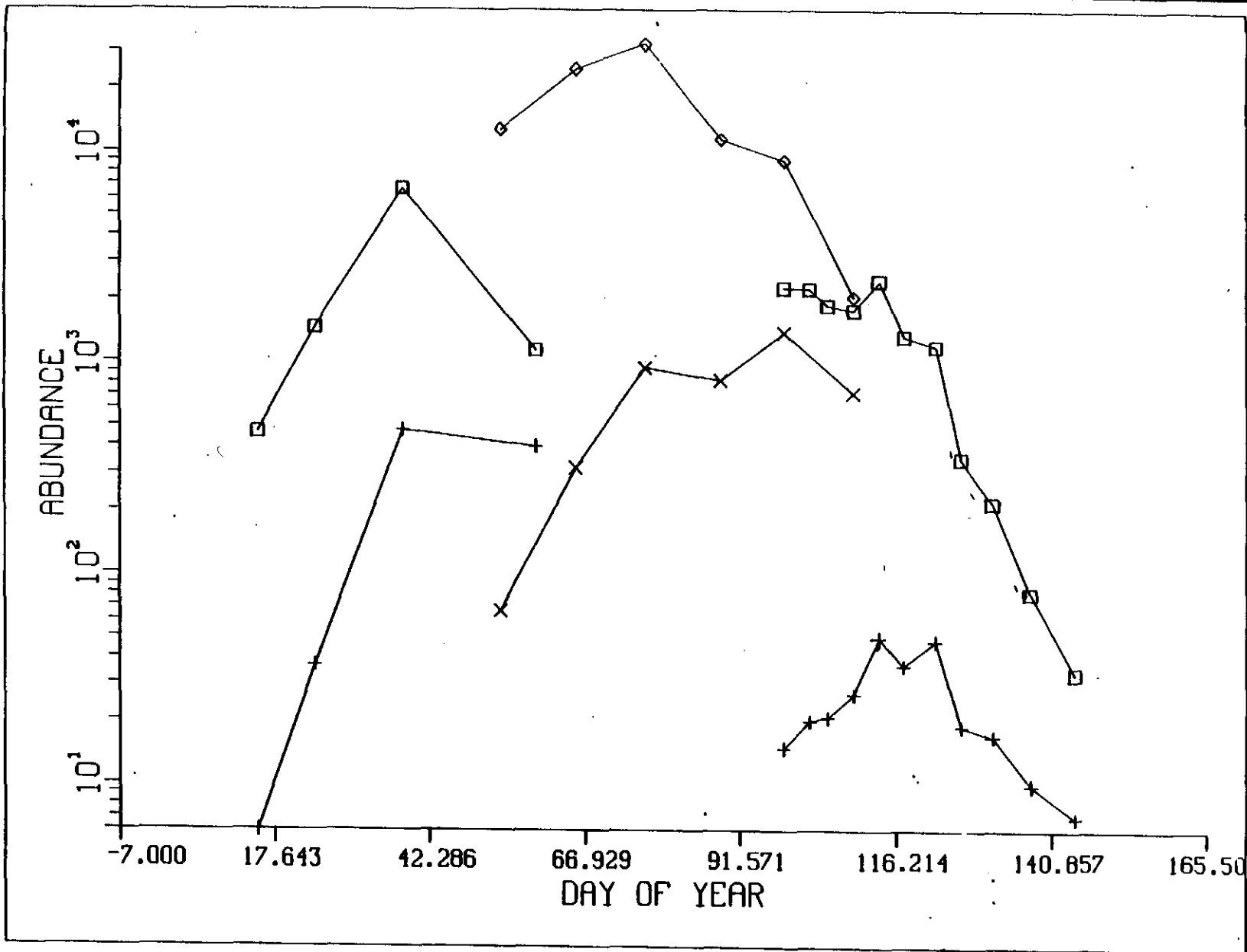


Figure 42. Length frequencies of Georges Bank haddock larvae for 1980 were converted to ages using average daily water temperatures during the life of the larva (X). The ages were back-calculated to numbers at spawning (\square) using a 0.075 mortality rate.

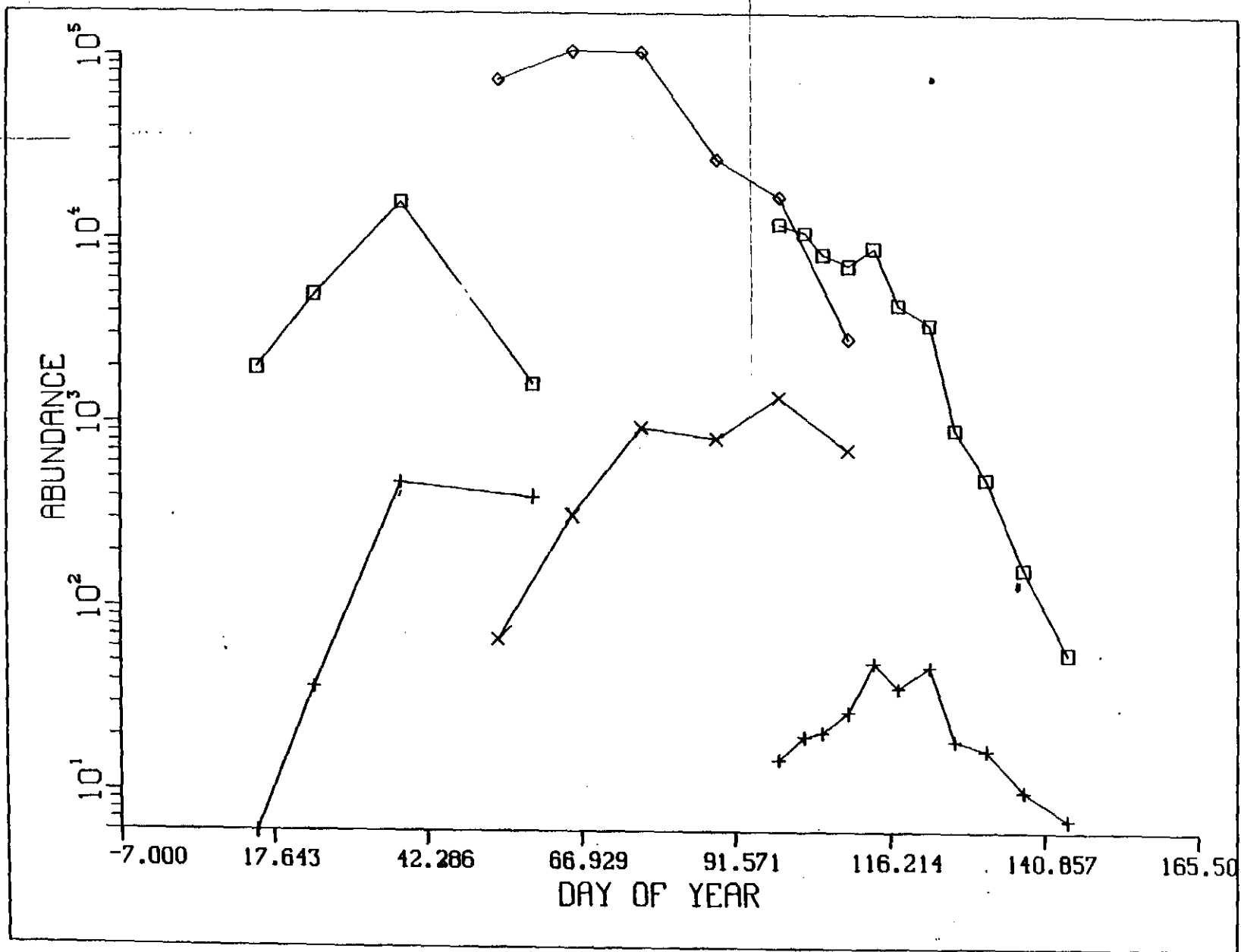


Figure 43. Length frequencies of Georges Bank haddock larvae for 1980 were converted to ages using average daily water temperatures during the life of the larva (X). The ages were back-calculated to numbers at spawning (\square) using a 0.10 mortality rate.

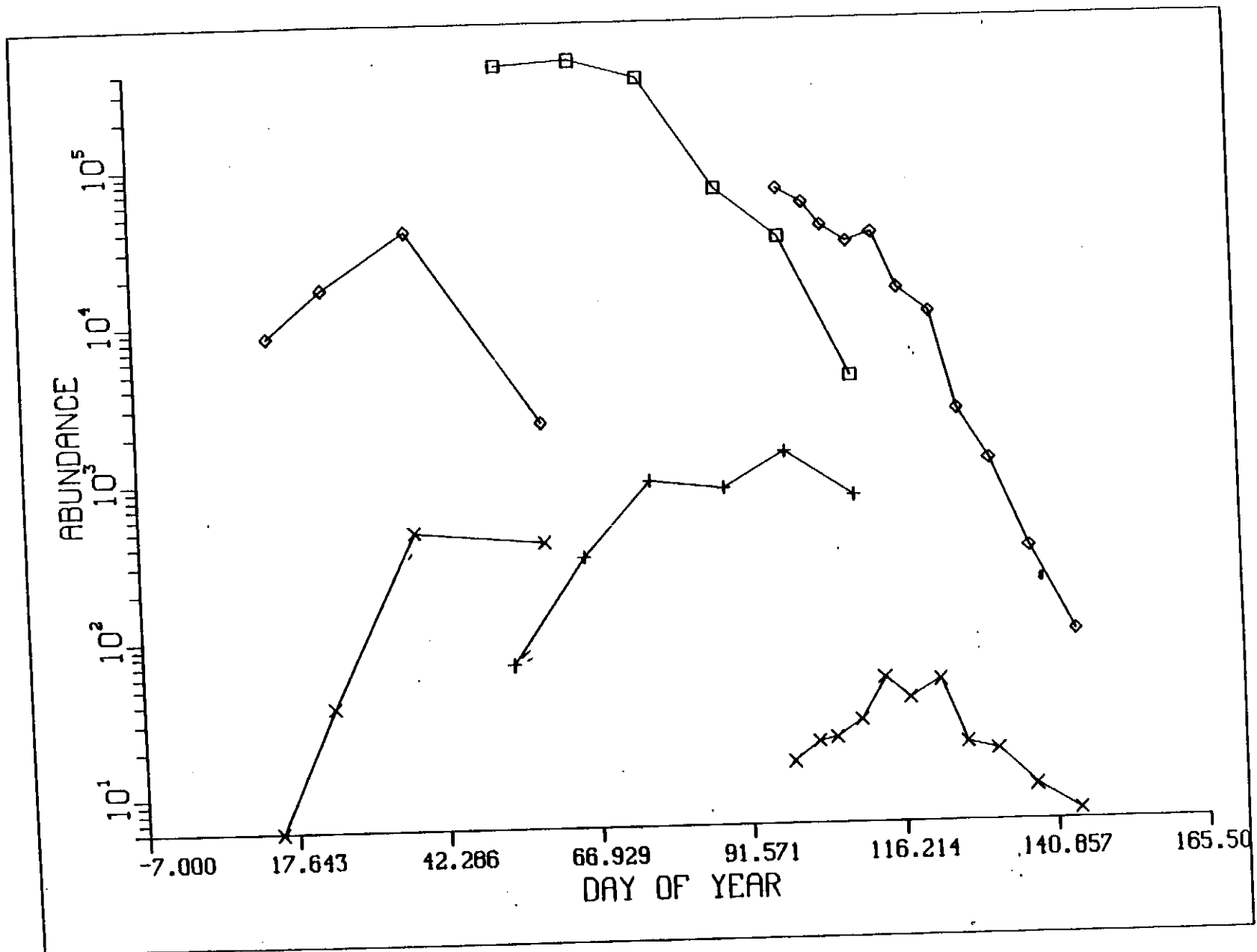


Figure 44. Length frequencies of Georges Bank haddock larvae for 1980 were converted to ages using average daily water temperatures during the life of the larva (X). The ages were back-calculated to numbers at spawning (\square) using a 0.125 mortality rate.

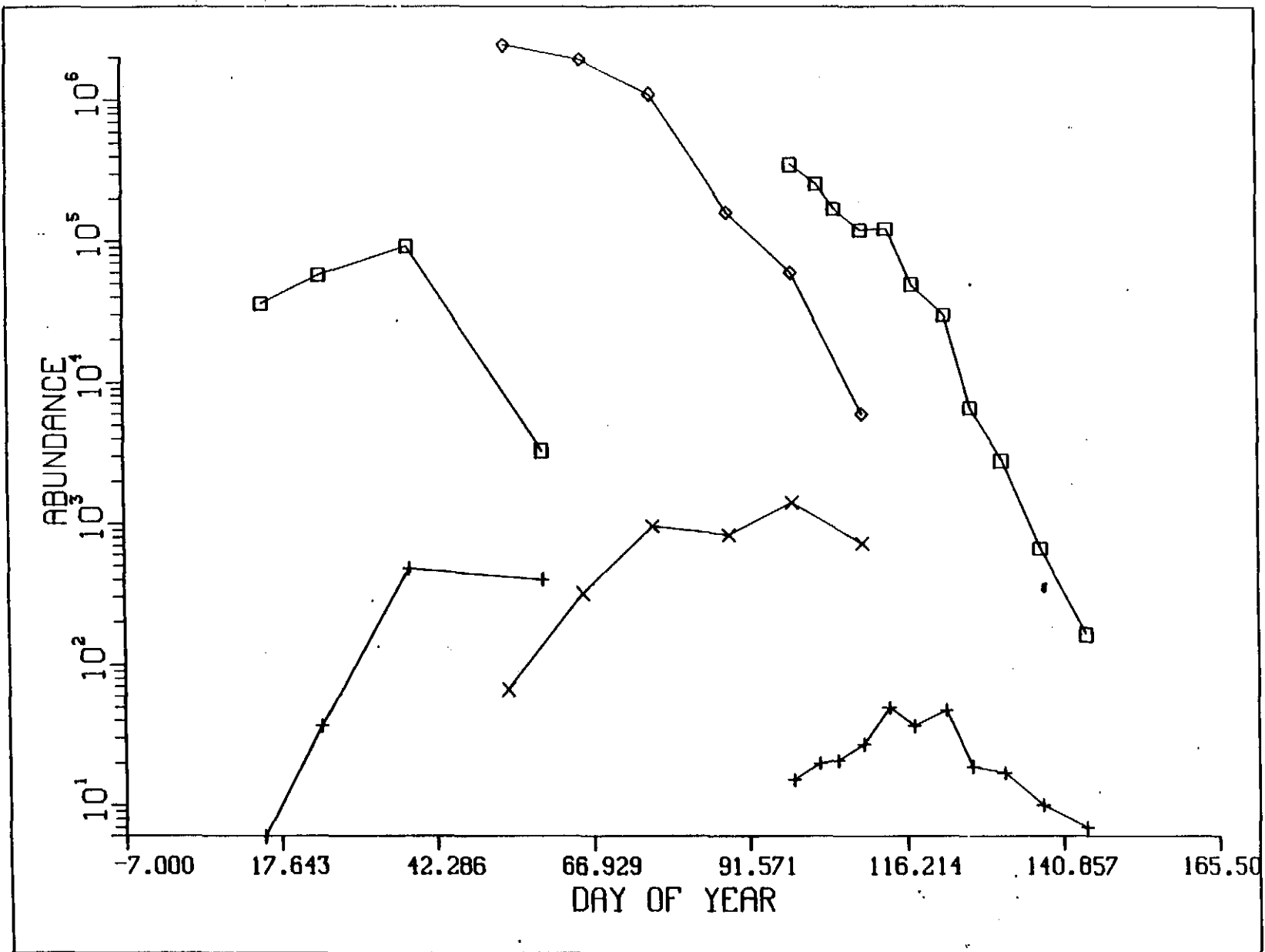


Figure 45. Length frequencies of Georges Bank haddock larvae for 1980 were converted to ages using average daily water temperatures during the life of the larva (X). The ages were back-calculated to numbers at spawning (□) using a 0.15 mortality rate.

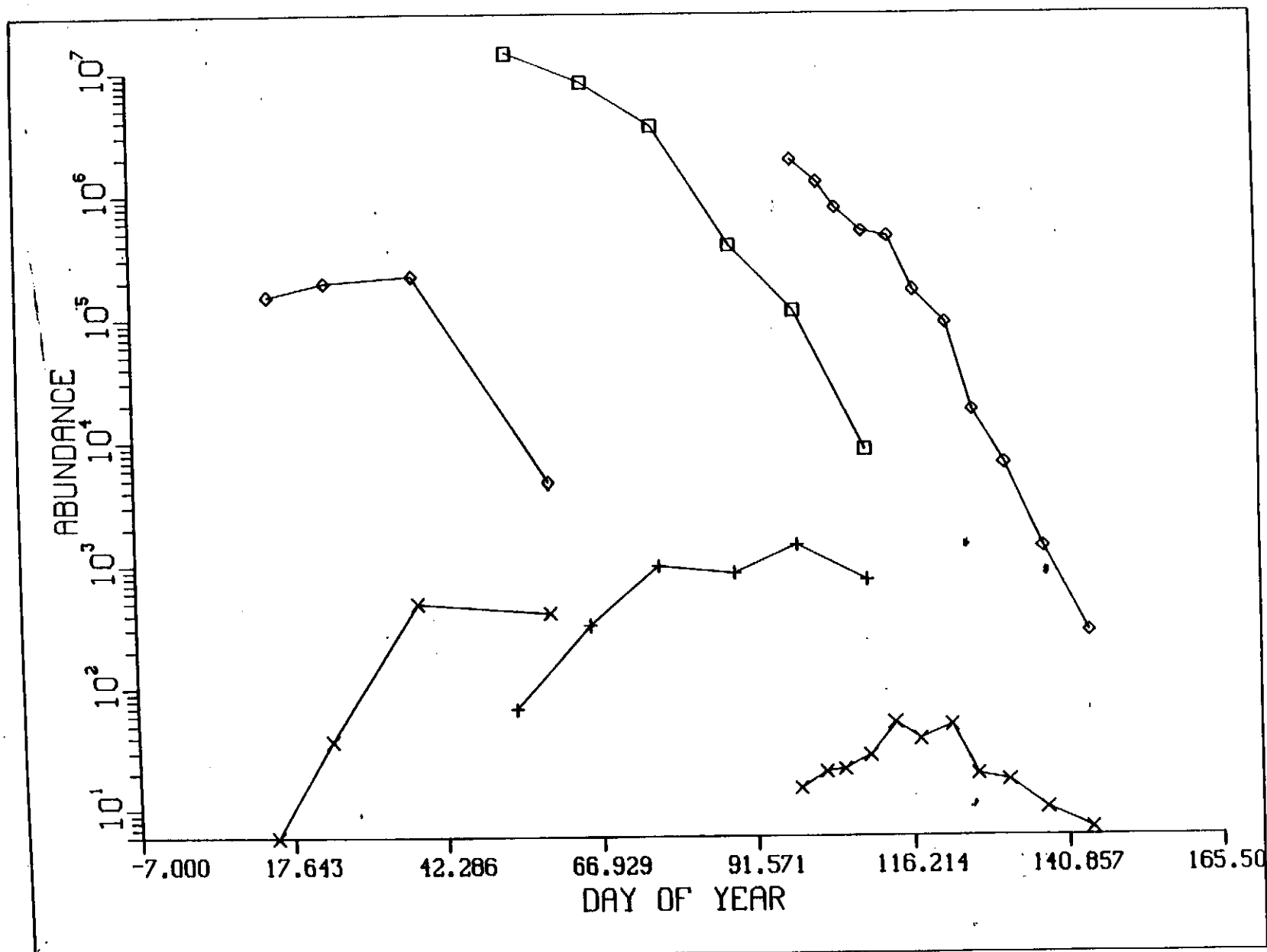


Figure 46. Length frequencies of Georges Bank haddock larvae for 1980 were converted to ages using average daily water temperatures during the life of the larva (X). The ages were back-calculated to numbers at spawning (\square) using a 0.175 mortality rate.

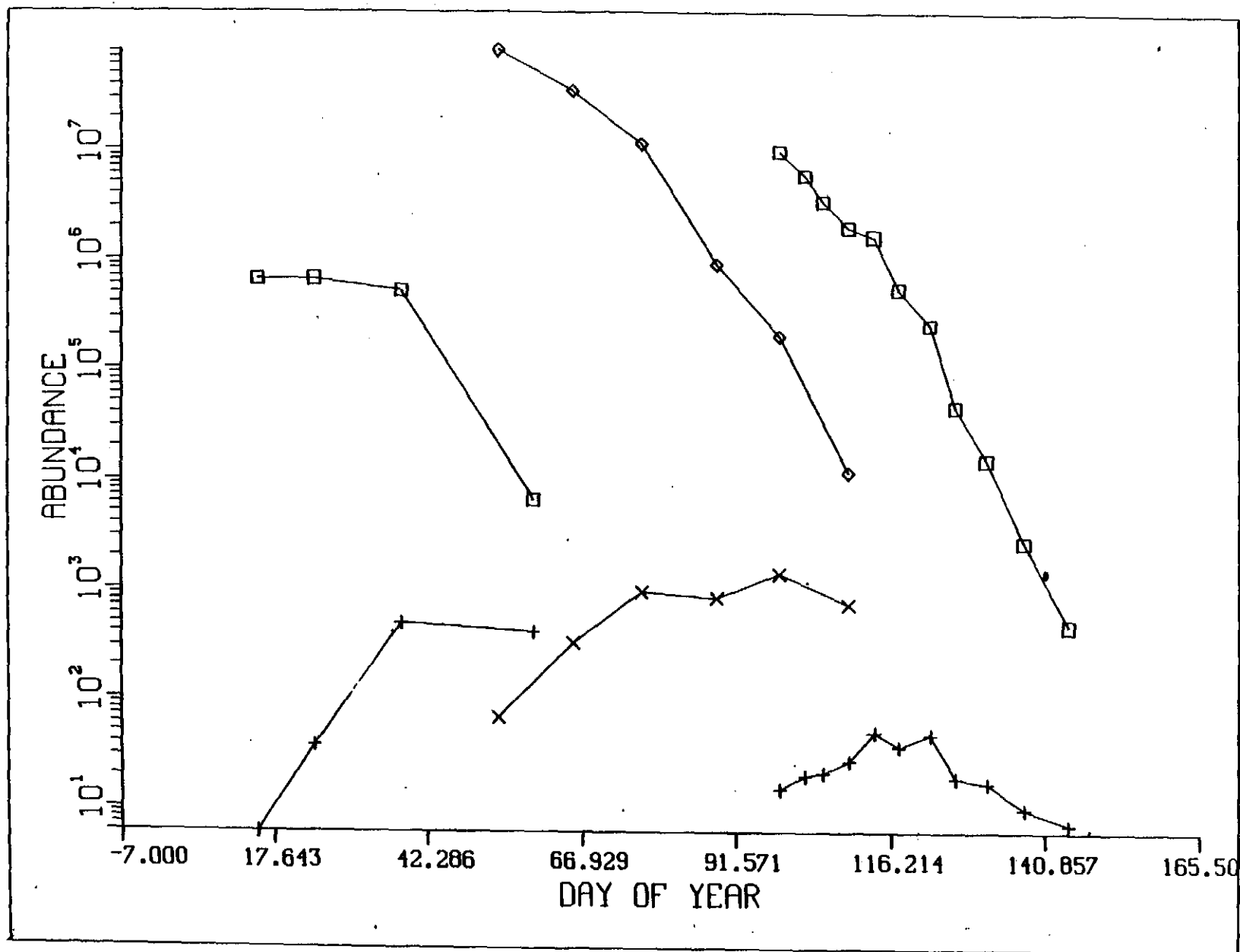


Figure 47. Length frequencies of Georges Bank haddock larvae for 1980 were converted to ages using average daily water temperatures during the life of the larva (X). The ages were back-calculated to numbers at spawning (\square) using a 0.20 mortality rate.

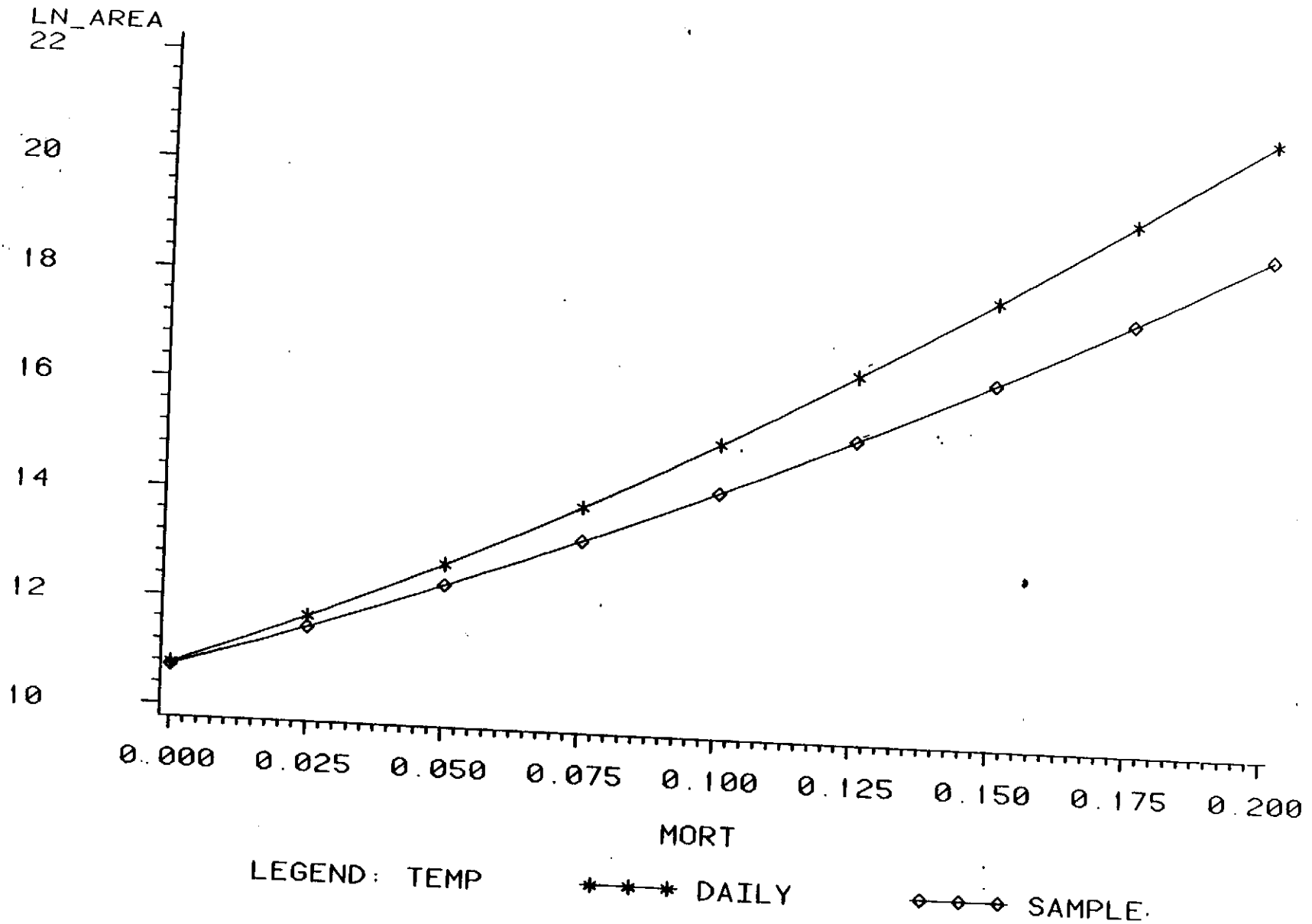


Figure 48. The relationship of the area of the spawning curve to the input mortality. Length frequencies of the 1980 Georges Bank haddock larvae were converted to ages by a single temperature for each survey and the by the daily temperature.